DISSERTATION

BEYOND THE CASE STUDY: CHARACTERIZING NATURAL FLOODPLAIN

HETEROGENEITY IN THE UNITED STATES

Submitted by

Emily Paige Iskin

Department of Geosciences

In partial fulfillment of the requirements

For the Degree of Doctor of Philosophy

Colorado State University

Fort Collins, Colorado

Spring 2023

Doctoral Committee:

    Advisor: Ellen Wohl

    Ryan Morrison
    Daniel McGrath
    Michael Ronayne

ABSTRACT

BEYOND THE CASE STUDY: CHARACTERIZING NATURAL FLOODPLAIN

HETEROGENEITY IN THE UNITED STATES

With human degradation of natural river corridors, the number of natural, functional floodplains is rapidly decreasing due to dams, diversions, artificial levees, draining, development, agriculture, and invasive species. At the same time, small- to large-scale interest in and implementation of river restoration is expanding, with floodplain restoration soon to take a starring role. To properly manage and restore processes to floodplains, we first need a broad understanding of what they look like and why. A key component of natural river-floodplain systems is heterogeneity, defined as the spatial variation of geomorphic and vegetation classes and patches across a floodplain. Heterogeneity of floodplains both reflects and influences the fluvial processes acting on floodplains and can help shape our understanding of the form and function of floodplains. To begin characterizing floodplain spatial heterogeneity, I present in this dissertation: 1) the development of a method to combine field measurements and remote sensing data products to calculate integrative landscape-scale metrics of floodplain spatial heterogeneity, and the demonstration of which metrics from landscape ecology are likely to be useful for identifying qualities of natural floodplains at four case study sites; 2) a sensitivity analysis to determine whether and how the values of the heterogeneity metrics change when spatial and spectral resolution of the input data are increased, and the extraction of underlying data from the classification results to determine whether using higher resolution data allows identification of the resulting unsupervised classes in relation to field and remote data at four case study sites; and

3) quantification of floodplain spatial heterogeneity, evaluation of whether statistically significant patterns are present, and interpretation of the statistical analyses with respect to the influence of channel lateral mobility and valley-floor space available using a complete dataset of 15 sites representing diverse floodplains across the continental United States. I found that "stacking" Sentinel-2A multispectral satellite imagery and digital elevation model topographic data allows for unsupervised classification of floodplains, and that metrics from landscape ecology can differentiate between different floodplain types. I also found via a sensitivity analysis that increasing the spatial resolution of the topographic data to finer than 10 m and including band ratios related to vegetation improves the classification results. Comparison of the field classes with the remote sensing classes allows for general interpretation of the results, but it is the heterogeneity within the broad classes that I expect is most important to these ecosystems. Lastly, through classification of 15 diverse river corridors across the United States, calculation of five heterogeneity metrics, and completion of a comparative analysis, I found that these natural floodplains have moderate aggregation of classes (median aggregation index = 58.8%), high evenness (median Shannon's evenness index = 0.934) and intermixing of classes (median interspersion and juxtaposition index = 74.9%), and a wide range of patch densities (range of patch density = 491–1866 patches/100 ha). I also found that the river corridor characteristics of drainage area, floodplain width ratio (space available), and elevation, precipitation, total sinuosity, large wood volume, planform, and flow regime (channel mobility) emerge as important variables to understanding floodplain heterogeneity.

1. CH 1: INTRODUCTION

Floodplains can be described as dynamic bioreactors (Wohl, 2021) that provide many ecosystem services in river corridors, including, as summarized by Petsch et al. (2022): soil formation, nutrient cycling (e.g. Harms et al., 2009; Appling et al., 2014; Wohl et al., 2018; Wohl and Knox, 2022), primary production, habitat provisioning (e.g. Bellmore and Baxter, 2014), water regulation, erosion control, water purification, waste treatment, disease regulation, climate regulation, and genetic resources. Importantly, each of these processes is closely tied to the three-dimensional spatial heterogeneity of the floodplain (Naiman et al., 2005; Appling et al., 2014; Helton et al., 2014), defined in this study as the spatial variation of geomorphic and vegetation classes and patches across a floodplain. Classes represent distinct types of floodplain habitats that blend geomorphic features and vegetation communities. Geomorphic features identified in the field include active channels, secondary channels with limited or no surface hydrologic connectivity, accretionary bars, backswamps, and natural levees. Vegetation communities include old-growth and younger conifer forest and deciduous forest, mesic wetlands, grasses, xeric vegetation, and beaver meadows (willow carrs). Floodplain heterogeneity results from erosion and deposition created by diverse fluvial processes (Nanson and Croke, 1992), as well as biotic processes such as beaver (*Castor* spp.) modifications (Larsen et al., 2021) in the northern hemisphere, vegetation dynamics (Naiman et al., 2005; Larsen and Harvey, 2010), and wildfire (Kleindl et al., 2015). Fundamentally, floodplain spatial heterogeneity responds to interactions among multiple controls (Figure 1.1) and both reflects and influences fluxes and storage of water, solutes, sediment, and large wood.
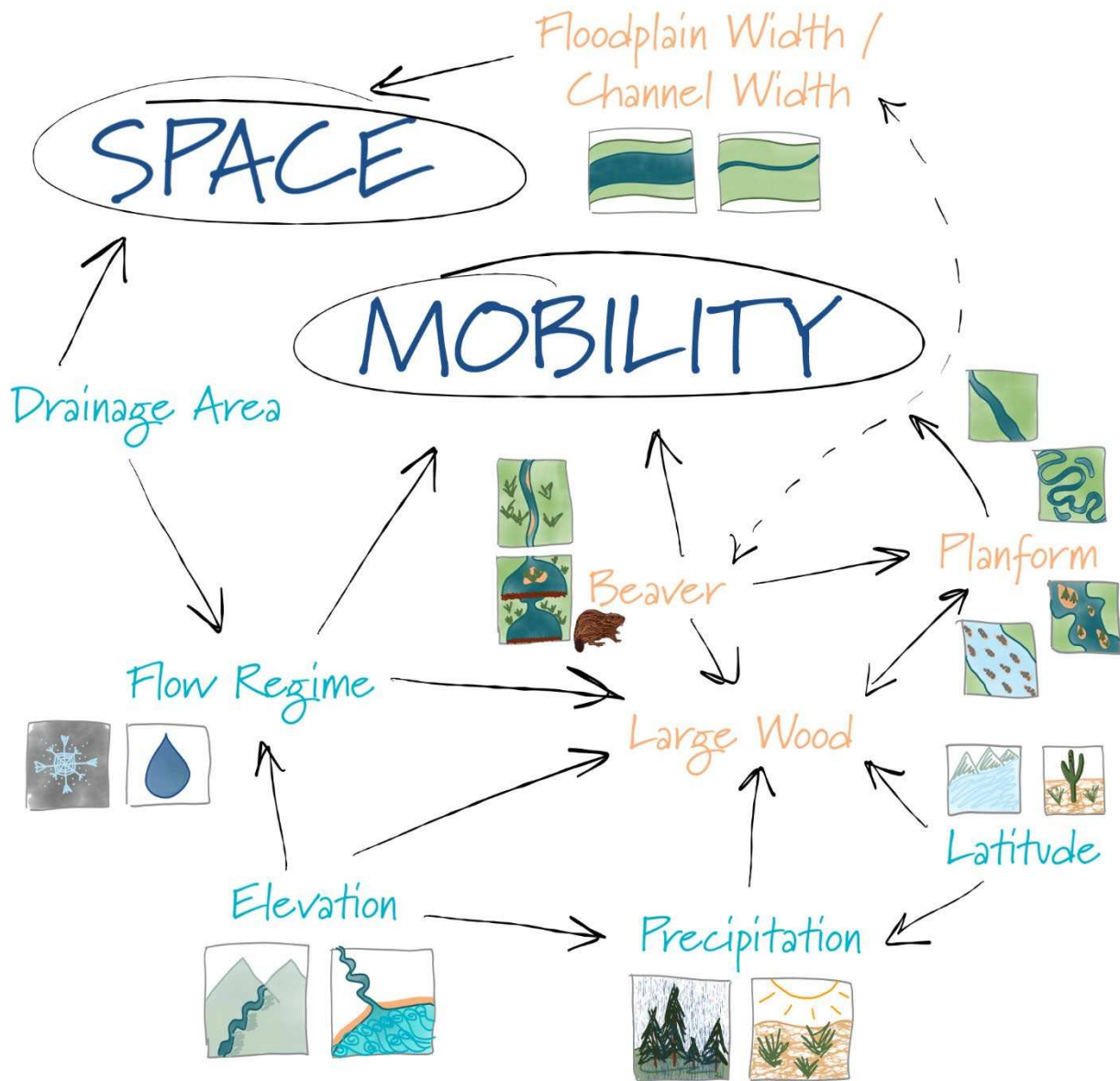
Figure 1.1. Conceptual model of controls of floodplain spatial heterogeneity. Main controls are shown in dark blue text and predictors are shown in turquoise and orange text. Turquoise predictors indicate drainage basin-level values and categories, and orange predictors indicate study site-level values and categories. Solid arrows connect predictor variables to the main controls they represent and to other predictor variables that they influence or are influenced by, and double-sided arrows connect predictor variables that interact reciprocally with each other. The dashed arrow connecting Beaver and Floodplain Width/Channel Width represents the habitat preference of beaver for wider floodplains, but also the fact that their presence and dam building can increase the regularly flooded width of the valley floor (e.g., Westbrook et al., 2011). The inset tiles illustrate contrasting values or levels for each variable.

At present, spatially heterogeneous and fully functional floodplains are disappearing due

to human modifications such as flow regulation (Thoms, 2003), land drainage, and artificial

levees (Knox et al., 2022). We know that managed river corridors have lower spatial heterogeneity and functionality (Samaritani et al., 2011; Kuiper et al., 2014; Schindler et al., 2016; Wohl and Iskin, 2019), further emphasizing the need to quantify heterogeneity in natural floodplains.

My approach to this urgent issue and the objectives of this dissertation are to 1) develop a method to quantify spatial floodplain heterogeneity using remote sensing principles and landscape ecology metrics; 2) refine the method by increasing many facets of data resolution and determine a suite of suitable metrics through a sensitivity analysis; and 3) apply the method to 15 diverse river systems around the United States, evaluate whether statistically significant patterns occur among these data, determine whether there are salient characteristics of river corridors that relate to multiple facets of heterogeneity, and interpret the statistical results in terms of the primary controls – channel lateral mobility and valley-floor space available – as well as the factors underlying mobility and space, such as flow regime and biota. The three primary chapters of this dissertation outline the specific workflow and tools I used to collect, process, and analyze the remotely sensed data to ensure repeatability of this work. The chapters provide insight into important considerations when conducting remote sensing of river systems, and present multiple statistical tools to investigate patterns. They also provide a framework for both classification and quantification of heterogeneity that should be applicable to floodplains anywhere, expanding the applicability of this work far beyond the United States. Each of the next three chapters is a self-contained unit that has been published (Chapter 2 in *River Research and Applications*), submitted to (Chapter 3 to *Journal of Hydrology*), or is in preparation for (Chapter 4 expected to *Water Resources Research*) a peer-reviewed journal.

1.1 References

Appling, A.P., Bernhardt, E.S., Stanford, J.A., 2014. Floodplain biogeochemical mosaics: A multidimensional view of alluvial soils. *JGR Biogeosciences* 119(8), 1538–1553. https://doi.org/10.1002/2013JG002543

Bellmore, J.R., Baxter, C. V., Martens, K., Connolly, P.J., 2013. The floodplain food web mosaic: A study of its importance to salmon and steelhead with implications for their recovery. *Ecological Applications* 23(1), 189–207. https://doi.org/10.1890/12-0806.1

Harms, T.K., Wentz, E.A., Grimm, N.B., 2009. Spatial heterogeneity of denitrification in semi-arid floodplains. *Ecosystems* 12, 129-143. https://doi.org/10.1007/s10021-008-9212-6

Helton, A.M., Poole, G.C., Payn, R.A., Izurieta, C., Stanford, J.A., 2014. Relative influences of the river channel, floodplain surface, and alluvial aquifer on simulated hydrologic residence time in a montane river floodplain. *Geomorphology* 205(15), 17–26. https://doi.org/10.1016/j.geomorph.2012.01.004

Kleindl, W.J., Rains, M.C., Marshall, L.A., Hauer, F.R., 2015. Fire and flood expand the floodplain shifting habitat mosaic concept. *Freshwater Science* 34(4), 1366–1382. https://doi.org/10.1086/684016

Knox, R.L., Wohl, E.E., Morrison, R.R., 2022. Levees don't protect, they disconnect: A critical review of how artificial levees impact floodplain functions. *Science of the Total Environment* 837, 155773. https://doi.org/10.1016/j.scitotenv.2022.155773

Kuiper, J.J., Janse, J.H., Teurlincx, S., Verhoeven, J.T.A., Alkemade, R., 2014. The impact of river regulation on the biodiversity intactness of floodplain wetlands. *Wetlands Ecology Management* 22, 647-658. https://doi.org/10.1007/s11273-014-9360-8

Larsen, A., Larsen, J.R., Lane, S.N., 2021. Dam builders and their works: Beaver influences on the structure and function of river corridor hydrology, geomorphology, biogeochemistry and ecosystems. *Earth-Science Reviews* 218, 103623. https://doi.org/10.1016/j.earscirev.2021.103623

Larsen, L.G., Harvey, J.W., 2010. How vegetation and sediment transport feedbacks drive landscape change in the Everglades and wetlands worldwide. *American Naturalist* 176(3), E66–E79. https://doi.org/10.1086/655215

Naiman, R.J., Bechtold, J.S., Drake, D.C., Latterell, J.J., O'Keefe, T.C., Balian, E. V., 2005. Origins, Patterns, and Importance of Heterogeneity in Riparian Systems, in: Lovett, G.M., Turner, M.G., Jones, C.G., Weathers, K.C. (Eds.), *Ecosystem Function in Heterogeneous Landscapes*. Springer Science + Business Media, Inc., New York, pp. 279–309. https://doi.org/10.1007/0-387-24091-8_14

Nanson, G.C., Croke, J.C., 1992. A genetic classification of floodplains. *Geomorphology* 4(6), 459–486. https://doi.org/10.1016/0169-555X(92)90039-Q

Petsch, D.K., Cioneck, V.d., Thomaz, S.M., dos Santos, N.C.L., 2022. Ecosystem services provided by river-floodplain ecosystem. *Hydrobiologia*. https://doi.org/10.1007/s10750-022-04916-7

Samaritani, E., Shrestha, J., Fournier, B., Frossard, E., Gillet, F., Guenat, C., Niklaus, P.A., Pasquale, N., Tockner, K., Mitchell, E.A.D., Luster, J., 2011. Heterogeneity of soil carbon pools and fluxes in a channelized and a restored floodplain section (Thur River, Switzerland). *Hydrology and Earth System Sciences* 15(6), 1757–1769. https://doi.org/10.5194/hess-15-1757-2011

Schindler, S., O'Neill, F.H., Biro, M., Damm, C., Gasso, V., Kanka, R., van der Sluis, T., Krug, A., Lauwaars, S.G., Sebesvari, Z., et al., 2016. Multifunctional floodplain management and biodiversity effects: a knowledge synthesis for six European countries. *Biodiversity and Conservation* 25, 1349-1382. https://doi.org/10.1007/s10531-016-1129-3

Thoms, M.C., 2003. Floodplain-river ecosystems: Lateral connections and the implications of human interference. *Geomorphology* 56(3-4), 335-349. https://doi.org/10.1016/S0169-555X(03)00160-0

Westbrook, C.J., Cooper, D.J., Baker, B.W., 2011. Beaver assisted river valley formation. *River Research and Applications* 27(2), 247–256. https://doi.org/10.1002/rra.1359

Wohl, E., 2021. An Integrative Conceptualization of Floodplain Storage. *Reviews of Geophysics* 59(2), e2020RG000724. https://doi.org/10.1029/2020rg000724

Wohl, E., Iskin, E., 2019. Patterns of Floodplain Spatial Heterogeneity in the Southern Rockies, USA. *Geophysical Research Letters* 46(11), 5864–5870. https://doi.org/10.1029/2019GL083140

Wohl, E., Knox, R., 2022. A first-order approximation of floodplain soil organic carbon stocks in a river network: The South Platte River, Colorado, USA as a case study. *Science of the Total Environment* 852, 158507. https://doi.org/10.1016/j.scitotenv.2022.158507

Wohl, E., Lininger, K.B., Scott, D.N., 2018. River beads as a conceptual framework for building carbon storage and resilience to extreme climate events into river management. *Biogeochemistry* 141, 365–383. https://doi.org/10.1007/s10533-017-0397-7

2. CH 2: METHODS & METRICS[1]

Summary

Floodplains provide numerous ecosystem services that depend on the spatial
heterogeneity, or patchiness, of the floodplain. Direct and indirect human alterations of rivers can
reduce floodplain heterogeneity and function, but relatively little is known of patterns of
floodplain heterogeneity in natural, fully functional floodplains. I quantify floodplain
heterogeneity at four sites in the United States with the objectives of (i) developing a method of
combining field measurements and remote sensing data products to calculate integrative
landscape-scale metrics of floodplain spatial heterogeneity and (ii) demonstrating which metrics
from landscape ecology are likely to be useful for identifying qualities of natural floodplains,
differentiating floodplains, and inferring processes, based on a case study of three prairie
floodplains and one beaver-modified floodplain in the continental United States. I developed a
new unsupervised classification workflow that combines field data, topography, and Sentinel-2A
imagery to create classified floodplains for all four field sites that could be used to calculate
heterogeneity metrics. I identified six heterogeneity metrics for characterizing natural floodplain
heterogeneity: aggregation index, interspersion and juxtaposition index, largest patch index,
patch density, percentage of like adjacencies, and Shannon's evenness index, and these metrics
capture both intermetric (variation in spatial heterogeneity between the floodplains) and
intrametric variation (variation in the patterns of the metrics). Results show that natural
floodplains have high evenness and interspersion and juxtaposition of classes, and I attribute this

---

to natural flow and sediment regimes driving channel migration, erosion, deposition, vegetation succession, and active beaver modifications. Colorado floodplains show higher aggregation and lower fragmentation than the Oklahoma floodplain. I attribute this to the greater incision and lower hydrologic variability at the Oklahoma site.

2.1 Introduction

Floodplain heterogeneity, defined here as the three-dimensional spatial variation of topography and vegetation communities, influences many aspects of river corridors. My objectives are to develop a method to calculate integrative landscape-scale metrics of floodplain spatial heterogeneity and demonstrate which metrics from landscape ecology are likely to be useful for identifying qualities of natural floodplains, differentiating floodplains, and inferring processes with a case study of four floodplains and one beaver-modified floodplain in the continental United States. In this introduction, I first review the drivers and implications of floodplain spatial heterogeneity in relation to ecosystem services provided by floodplains, then review the use of spatial heterogeneity metrics in landscape ecology, and finally discuss the objectives of this paper.

2.1.1 Floodplain Heterogeneity

Floodplains can be described as dynamic bioreactors (Wohl, 2021) that provide many ecosystem services in river corridors. Examples of floodplain ecosystem services include flood-peak attenuation, groundwater recharge and aquifer storage, hyporheic exchange, denitrification (Harms et al., 2009; Appling et al., 2014; Wohl et al., 2018), organic carbon sequestration (Wohl and Knox, 2022), habitat abundance and diversity, and biodiversity (Bellmore and Baxter, 2014). Each of these processes is closely tied to the three-dimensional spatial heterogeneity of the floodplain (Naiman et al., 2005; Appling et al., 2014; Helton et al., 2014). Floodplain

heterogeneity results from erosion and deposition created by diverse fluvial processes (Nanson and Croke, 1992), as well as biotic processes such as beaver (*Castor* spp.) modifications (Larsen et al., 2021) in the northern hemisphere, vegetation dynamics (Naiman et al., 2005; Larsen and Harvey, 2010), and wildfire (Kleindl et al., 2015). Floodplain erosion, deposition, and storage reflect fluctuating inputs of water (Junk et al., 1989; Tockner et al., 2000), sediment (Trimble, 1981; Lecce, 1997), and large wood (Collins et al., 2012) that drive channel movements (Amoros and Bornette, 2002; Choné and Biron, 2016) and overbank erosion and deposition. Floodplain heterogeneity also creates spatial heterogeneity in river corridor processes (Zeug and Winemiller, 2008; Doering et al., 2021), such as channel sinuosity and meander migration (Güneralp and Rhoads, 2011; Schwendel et al., 2015), channel planform (Polvi and Wohl, 2012), subsurface flow paths (Fuchs et al., 2009), sediment transport and storage (Westbrook et al., 2011; Baartman et al., 2013), contaminant transport and storage (Lowell et al., 2009; Ciszewski and Grygar, 2016), carbon storage (Samartini et al., 2011; Lininger et al., 2018), soil nutrients (Naiman et al., 2005; Appling et al., 2014), inundation patterns and associated vegetation establishment (Scott et al., 1996; Hughes, 1997; Friedman and Lee, 2002), and fish life cycles and food webs (Bellmore et al., 2013; Zeug and Winemiller, 2008; Stoffers et al., 2022). Fundamentally, floodplain spatial heterogeneity responds to interactions among multiple drivers and both reflects and influences fluxes and storage of water, solutes, sediment, and large wood (Figure 2.1).

Floodplain heterogeneity is dynamic in time in response to changes in drivers and interactions among response variables. At present, spatially heterogeneous and fully functional floodplains are rapidly disappearing due to human modifications such as flow regulation (Thoms, 2003), land drainage, and artificial levees (Knox et al., 2022). As loss of heterogeneity

creates loss of floodplain functionality (Samaritani et al., 2011; Kuiper et al., 2014; Schindler et al., 2016; Wohl and Iskin, 2019), floodplains are becoming a major focus of river restoration (Tockner et al., 2008; Wohl et al., 2021), emphasizing the need to quantitatively characterize heterogeneity in natural floodplains.
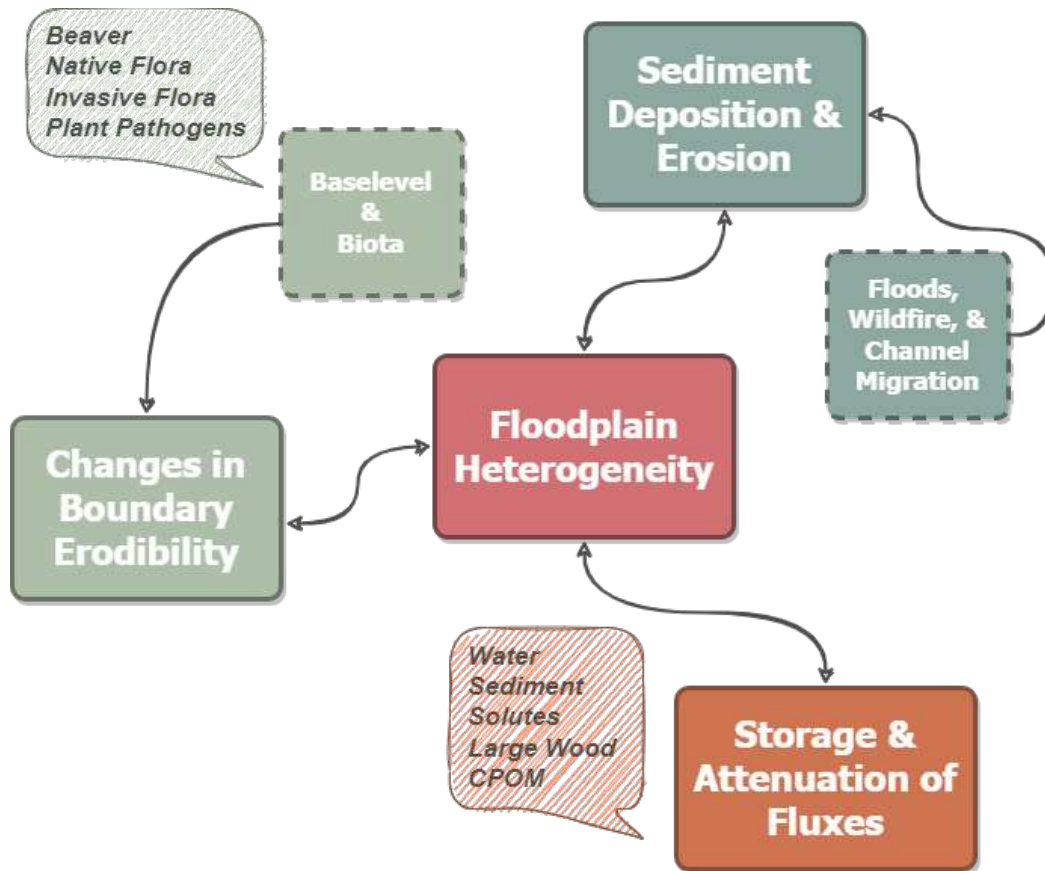
Figure 2.1. Conceptual diagram of the dynamic interactions of natural heterogeneous floodplains. Colors group the processes into three types and arrows indicate the directionality of influence. Solid text boxes surrounding floodplain heterogeneity indicate the three main physical factors that interact with floodplain heterogeneity. These arrows are double-sided as the interactions are dynamic and reciprocal. The dashed text boxes list some specific larger-scale processes that could result in changes in boundary erodibility and/or sediment deposition and erosion. The striped callouts list some specific biota and fluxes that interact with floodplains. CPOM is coarse particulate organic matter.

The three-dimensional spatial heterogeneity of the floodplain can be described as the patchiness of the floodplain (Ward et al., 1999; Beechie et al., 2006). Patches are discrete spatial units that differ from adjacent units. Recognition of channel and floodplain patches gave rise to the conceptual model of the shifting habitat mosaic in river corridors (Arscott et al., 2002;

Stanford et al., 2005) and Thoms et al. (2005) describe floodplains as dynamic mosaics of patches. Patches can be defined using diverse criteria, such as depositional history and associated differences in substrate and topography (e.g., levee versus backswamp), vegetation community, or soil moisture. Many of these characteristics correlate with one another, so the primary criteria used to define patches depend on the focus of the investigation (Scott et al., 2022). Patches can also be defined at diverse spatial scales, from sub-meter habitat patches for macroinvertebrates, for example, to individual floodplain wetlands covering tens to hundreds of square meters.

2.1.2 Metrics in Landscape Ecology

The field of landscape ecology deals with heterogeneity of surfaces across spatial and temporal scales, including landscape composition and configuration (With, 2019). Classic descriptions of landscapes are segmented into landscapes, classes, and patches ("patch-based", Figure 2.2), and the spatial metrics are consequently grouped by landscape-scale, class-scale, and patch-scale metrics. Although there are other types of analyses in landscape ecology beyond patch-based (Erős and Lowe, 2019; With, 2019), I have chosen to use patch-based, following Scott et al. (2022), landscape-scale metrics in this study to simplify the methods and to facilitate comparison between floodplains at the reach scale (here, a reach is a length of river corridor with consistent channel and valley geometry). More detailed analysis of specific classes could use class- or patch-scale metrics.

General metrics of heterogeneity include measures of richness, diversity, and evenness. Measures of richness relate to the number of different types of classes present in a landscape – many different class types would be a rich landscape (With, 2019). Measures of diversity relate to the number of classes and their relative abundance. Evenness is a normalized measure of diversity. Shannon's and Simpson's indices are commonly used diversity and evenness metrics

(With, 2019; Hesselbarth et al., 2021). Before the *landscapemetrics* package was developed for the R programming language by Hesselbarth et al. (2019), the FRAGSTATS program was used to calculate landscape metrics from different types of digital images (McGarigal and Marks, 1995).
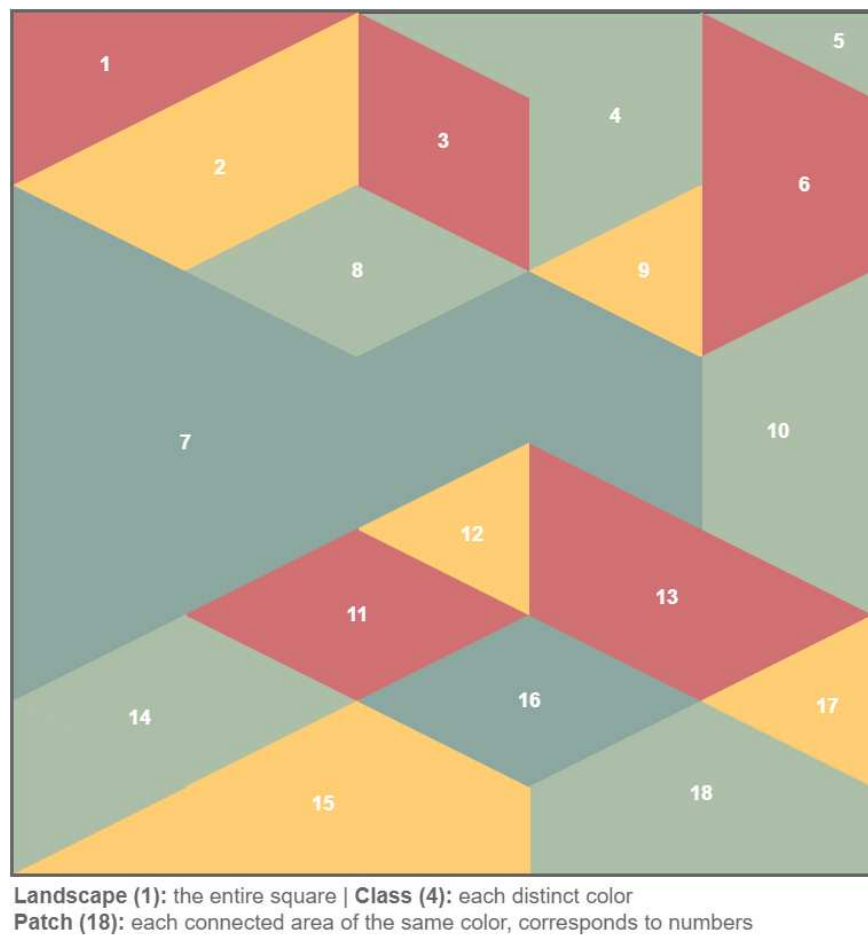
Figure 2.2. Example landscape illustrating the different spatial scales of patch-based landscape ecology. This landscape has four classes and 18 patches. Metrics could be calculated for a landscape like this and compared with analogous metrics for other landscapes. In this analysis, landscapes, or riverscapes, are the delineated floodplains, classes were defined in the field for each floodplain, and patch boundaries were delineated along lateral transects.

Heterogeneity, complexity, connectivity, diversity, and other terms are used to describe related facets of temporal and spatial variation characteristic of river corridors (Table 2.1). Different methods have been used to measure floodplain variations, typically with the intent of inferring underlying processes (Turner and Chapin III, 2005; Scott et al., 2022).

Table 2.1. Definitions of terms commonly used to describe the natural variation of river corridors

Term	Definition	References
Spatial heterogeneity	Spatially explicit structure commonly described in terms of spatial units (e.g., patches)	Cadenasso et al., 2006; Wohl, 2016
Complexity	Nonlinear dynamics, self-organization, and emergent properties	Werner and McNamara, 2007; Rhoads, 2013; Phillips, 2014
Connectivity	The degree to which matter and organisms can move among spatially defined units in a natural system	Fryirs, 2013; Bracken et al., 2013, 2015; Wohl, 2017; Wohl et al., 2019
Spatial diversity	Analogous to spatial heterogeneity	Feoli et al., 2013
Natural range of variability	The spatial and temporal bounds of variations in specified system parameters within a specified timespan, for systems relatively unaffected by people	Landres et al., 1999; Grondin et al., 2018
Historic range of variability	Analogous to the natural range of variability, but including systems or periods of time with human influence on the system; sometimes used synonymously with natural range of variability	Morgan et al., 1994; Fryirs et al., 2012

Multiple metrics are useful for distinguishing different aspects of floodplain heterogeneity, which varies across spatial scales and can be captured by different window sizes (Table 2.2). However, temporal metrics for heterogeneity are lacking. Table 2 suggests that previous ecological and geomorphic investigations of floodplains have focused primarily on surface variation, including topography and hydraulic habitat. Subsurface properties affect topography, hydrologic flow paths and associated biogeochemical reactions, and vegetation (Scott et al., 1996; Hughes, 1997; Friedman and Lee, 2002; Naiman et al., 2005; Güneralp and Rhoads, 2011; Appling et al., 2014; Helton et al., 2014; Schwendel et al., 2015), and therefore should be included in metrics of floodplain heterogeneity, but there is a disconnect between the extensive literature on floodplain sedimentology and stratigraphy (e.g., Allen, 1965; Slingerland and Smith, 2004) and the literature on floodplain spatial heterogeneity. And while many studies investigate riparian vegetation structure and health with a landscape ecology lens (Walford and Baker, 1995; van Coller et al., 2000; Bagstad et al., 2006; Aguiar et al., 2009, 2011; Fernandes et al., 2011), there is commonly a lack of explicit inclusion of vegetation in the development of

general floodplain heterogeneity metrics based on topography (Table 2.2). I start to address these gaps in the analyses presented here, which incorporate topography and vegetation. Subsequent analyses will include subsurface soil texture data collected in the field.

Table 2.2. Summary of previous studies of floodplain hydrological and geomorphic variation in the context of estimating spatial heterogeneity

Dimension	Metric	Data	Results	Reference
Floodplain complexity	Surface elevation measures	-	-	Wohl, 2016
Floodplain connectivity	Surface Hydrological Connectivity (temporal, longitudinal) Riverscape Diversity (spatial Shannon index with turbidity classes and channel length proportion as abundance)	Historical records, digitized maps, aerial photographs, field data	Surface Hydrological Connectivity reveals a threshold channel length of 15 km below which channel length increases and surface connectivity stays about constant. Riverscape Diversity increases with increasing river length.	Ward et al., 2002
Hydraulic habitat	Hydromorphological Index of Diversity, Entropy, and Modal Density (all spatial, over river networks)	Worldview II imagery, field calibration, hydraulic modeling	All three metrics varied when calculated over 130- and 430-m window sizes. Hydromorphological Index of Diversity and Entropy where able to identify a "heterogeneity hotspot"	Gostner et al., 2013; Hugue et al., 2016
Surface topography complexity	Four statistical metrics	Digital elevation models	All the metrics vary across spatial scales, and that the Standard Deviation of Surface Height and Standard Deviation of Total Surface Curvature showed surface elevation varies more for confined floodplains,	Scown et al., 2015a
	Four statistical metrics + four more		Thresholds of scale for patchiness emerged at a few different window sizes.	Scown et al., 2015b
	Floodplain Surface Complexity (from three measures of variability and two measures of spatial organization)		Floodplain width was related to Floodplain Surface Complexity at all spatial scales.	Scown et al., 2016
Floodplain heterogeneity	Number of patches per transect length	Field patch delineation	Decreasing drainage area, planform, and decreasing channel gradient are associated with increasing floodplain spatial heterogeneity. More complex planforms (anastomosing, meandering, and braided) have higher values of spatial heterogeneity.	Graf, 2006; Wohl and Iskin, 2019
Vegetation	Riparian Vegetation Index: multimetric index of biotic integrity	Plant field sampling	Metric was able to separate sites based on different criteria	Aguiar et al., 2009

2.1.3 Objectives

Although previous reviews suggest that landscape ecology methods are appropriate for river systems (Poole, 2002; Wiens, 2002) and have even coined the phrase "riverscape ecology"

to highlight the specific importance of longitudinal connectivity in river corridors compared to terrestrial landscapes (Erős and Lowe, 2019), no one has yet systematically applied heterogeneity metrics from landscape ecology to diverse natural floodplains and then related these metrics to drivers of fluvial processes. Previous studies have called for quantification of floodplain heterogeneity (Tockner et al., 2000; Wohl, 2021) and ecological conditions of large floodplain rivers (Erős et al., 2019).

My primary objectives are to (i) develop a method of combining field measurements and remote sensing data products to calculate integrative landscape-scale metrics of floodplain spatial heterogeneity and (ii) demonstrate which metrics from landscape ecology are likely to be useful for identifying qualities of natural floodplains, differentiating floodplains, and inferring processes with a case study of three prairie floodplains and one beaver-modified floodplain in the continental US. Although the proposed method only measures spatial heterogeneity, it could be repeated over time to measure temporal heterogeneity as well using repetitive capture of Earth images. I include a brief discussion of change through time at all sites as an indicator of how well the metrics calculated here might represent diverse timespans.

2.2 Study Area

This case study focuses on three prairie floodplains in the western and central United States, West Bijou Creek and East Plum Creek in Colorado and Sand Creek in Oklahoma, and one beaver meadow floodplain in the Rocky Mountains, Rough and Tumbling Creek in Colorado (Figure 2.3). The study reaches vary in most of their basic characteristics (Supplemental Table 2.1), especially Rough and Tumbling Creek's lithology, basin elevation, slope, channel planform, flow regime, and dominant vegetation.
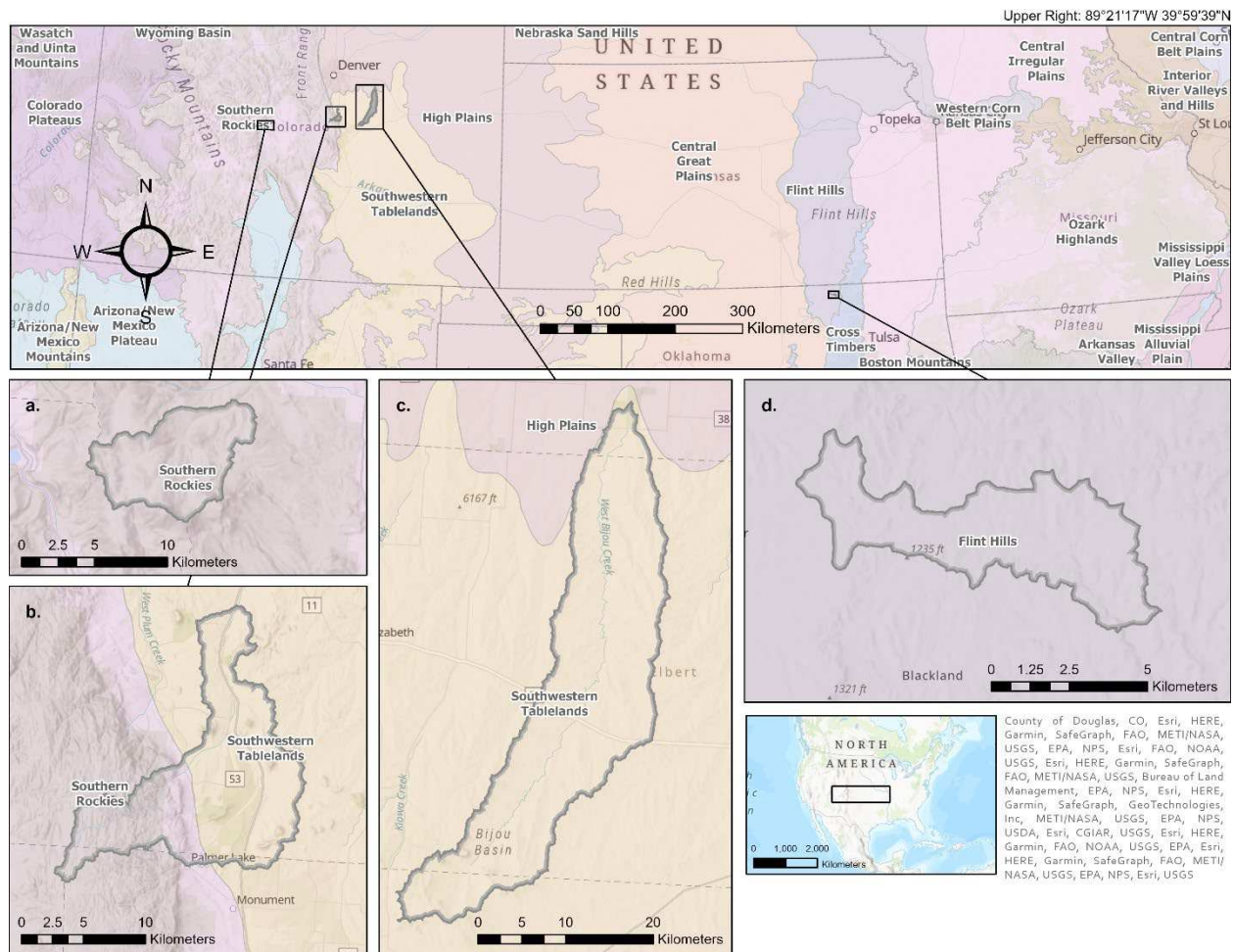
Figure 2.3. Location map of field sites: a) Rough and Tumbling Creek, Colorado (flow direction is east); b) East Plum Creek, Colorado (flow direction is north); c) West Bijou Creek, Colorado (flow direction is north); and d) Sand Creek, Oklahoma (flow direction is east). Map shows the drainage area boundaries upstream of the downstream-most point of each study reach. Level III Ecoregions are labeled. Drainage area shapefiles delineated and downloaded from USGS StreamStats in September 2021 and September 2022 (USGS, 2021, 2022a), and ecoregion shapefiles downloaded from the Environmental Protection Agency in December 2021 (U.S. EPA, 2013).

These field sites are conducive to measuring natural floodplain heterogeneity because they have minimal large-scale human impacts such as artificial levees, land drainage, flow regulation, or land cover changes. This can be observed as little-to-no change of land use category via the NLCD Land Cover Change Index (MRLC, 2022). This facilitates distinguishing natural floodplain characteristics in contrast to those modified by human activities (Graf, 2006; Tockner et al., 2008; Wohl and Iskin, 2019).

2.3 Methods

Data were collected through a combination of field measurements and compiling of remote imagery. The field measurements were conducted primarily to inform interpretation of remote imagery but are not essential to using the classification method described below. I specifically did not to pre-define floodplain classes ("field classes" and "field patches") as I did not want to limit the types of classes to what I saw during the pilot study (Wohl and Iskin, 2019). The pilot was conducted only on Colorado mountain stream floodplains, and I wanted the field classes in this study to reflect each unique site (Scott et al., 2022).

Floodplain patches were mapped along mostly linear transects perpendicular to the valley trend at each site. The purpose of this ground-based mapping was primarily to ground-truth patch boundaries delineated by classification ("ISO classes" and "ISO patches") with the field patches. Ground-based transects were spaced at approximately 10x the approximate active channel width where possible (10 transects at West Bijou and Sand Creeks, 3 at East Plum Creek because the length of the study area was limited by human alterations of the floodplain up- and downstream, and 1 at Rough and Tumbling Creek due to easily identified floodplain boundaries at the valley walls). Each transect spanned the active floodplain at each location. The edges of the active floodplain were determined visually using relative topography, vegetation types, water features, and evidence of flow observed in the field. Topographic features with vertical relief greater than 2 m above the surrounding floodplain were interpreted as terraces rather than floodplain on these relatively small creeks. Areas with known wetland and mesic plants, such as sedges, rushes, and cottonwoods (*Populus* spp.) generally indicated active floodplain. Surfaces with xeric upland vegetation, such as yucca (*Yucca* spp.) and conifers, generally indicated inactive floodplain. Presence of and relative age of cottonwoods reflect the history of floodplain dynamics via

channel migration, degradation, and aggregation (Everitt, 1968). Areas with evidence of flow, such as flowing or standing water, well-sorted gravel or larger sediment, directional accumulations of coarse particulate organic matter (CPOM) and wood, and highwater marks, were used as indicators of active floodplain, and indicated processes such as sediment and wood transport and storage (e.g., Wohl et al., 2016).

Field classes and field patches were differentiated visually based on depositional and erosional features, vegetation type and relative age, relative sediment grain size and moisture, and presence of large wood accumulations (Table 2.3). Depositional and erosional features included side channels, overflow surfaces, overgrown surfaces, and abandoned meanders. These features indicate processes such as channel migration and avulsion, side channel formation, wood transport and storage, sediment transport and deposition, and meander cutoff (e.g., Hooke, 1995; Collins et al., 2012). Vegetation type and age characteristics were defined at each field site rather than being predetermined, and included plant height, tree trunk diameter at breast height, coniferous vs. deciduous trees and shrubs, grasses, xeric or upland plants, wetland plants such as sedges and rushes, and visual assessment of "healthy" or "stressed" (wilting, dry, etc.) vegetation condition. Relative vegetation age, type, and health are indicators of recurrence of floodplain inundation and large flooding, depth to groundwater, and succession (e.g., Hughes, 1998; Karimi et al., 2021). Relative sediment grain size included simple visual differentiation (not explicitly measured) between sand, gravel, cobbles, and boulders. Grain size is an indicator of source material, flow competence, and stream power (e.g., Nicholas and Walling, 1997). Large wood features included small accumulations of sticks and CPOM and true logjams ($\geq$ 3 pieces of large wood $\geq$ 1 m long and $\geq$10 cm diameter). CPOM is an indicator of floodplain inundation and flow (Hein et al., 2003), whereas large wood and jams are indicators of processes such as wood

recruitment, transport, and storage (Pettit et al., 2005; Lininger et al., 2021). All of these features were used to define the field classes. Field patch edges were generally delineated as a single GPS point between two field classes, as most of the patch edges were smaller than the 3 m resolution of the GPS. The criteria used to delineate field classes and field patch boundaries are arbitrary and subjective in the sense that they are based on visual assessments and limited measurements rather than statistically defined categories but allow for simple and quick class designation. I endeavored to be consistent in the types of classes that I designated at each field site and to choose criteria that could be easily applied by other field investigators.

I differentiated ten classes at West Bijou Creek in July and October of 2020, six at East Plum Creek in September 2020, eight at Sand Creek in June 2021, and three at Rough and Tumbling Creek in August 2022, all after peak seasonal flows (Table 2.3). Dates of field data collection differ due to availability and access to the sites, but the overall goal was to collect field data after seasonal high flows, so that more of the floodplain was visible from the ground. Watershed boundaries, digital elevation data, and remote imagery were gathered to align with the field data. Overall, field observations were used to map the extent of the active floodplain in the study area and to refine the classification workflow, so the mismatch of timing between field data and remote sensing products should not significantly affect results.

Table 2.3. Field class descriptions.

River	Class No.	Description
West Bijou Creek	1	"Active" channel from Transect 1 East boundary
	2	Sand to fine gravel overflow channel with discontinuous grass and seedling willows; 10 cm of loose sand/pebbles, then indurated
	3	Stable, higher floodplain surface, flat, continuous grass cover, abundant cottonwoods with 10–25 cm DBH, many pinned jams, silt/clay drape
	4	Older, multi-stem cottonwoods with 50 cm DBH, higher/sloped surface, low terrace, no jams, continuous grass with cheat grass, prickly pear
	5	Overflow/secondary channel, analogous to Class 3
	6	Young cottonwoods, no jams, yucca - GRASS
	7	Defined secondary channel, not recently active, ~2 m elevation drop

	8	Sandy, very young cottonwoods, max 10–15 cm DBH, more undergrowth that is cottonwood sprouts, coarse sand bars
	9	Similar elevation to Class 6, cottonwoods, a lot of LW on the ground, slight vertical undulations of floodplain
	10	Young cottonwoods, no jams, yucca – TREES
Rough and Tumbling Creek	1	Grassy beaver meadow, undulating topography, bushy willow interspersed, at base of valley wall
	2	Active channel with beaver dams, gravel point bars, sand to cobble size clasts
	3	Potentilla bushes with little yellow flowers, yarrow, thinner/drier grass, small willows, gentle sloping surface, burrowing rodents
Sand Creek	1	Tall green undergrowth, long-leafed trees that vary from 10–40 cm DBH, sapling oak tree, varied depressions with gravel, many types of undergrowth
	2	Downward sloping terrace, silty mud, tall undergrowth
	3	Active channel
	4	Thigh-high grasses
	5	Overflow surface, wetland plants, siltation on leaves, beaver chew visible on wood
	6	Overgrown section of multi-thread channel, maple-like trees in channel, 3 m high water marks, some ponded water, large clam
	7	Head-high bushy plants, 1 m high water marks
	8	Overflow channel upstream of channel-spanning logjam, 1 m high water marks, coarse sand to small boulders
East Plum Creek	1	Sumac, dying willows, grass, horsetails, flat, terrace transition, prickly pear, not active
	2	Dense willows (not healthy), raspberries, sumac, gradual down slope
	3	Slight increase in elevation, grasses, sparse stressed willow, sparse cottonwoods 15–20 cm DBH
	4	Active channel with flowing water, point bar, willows, annuals, seeding cottonwoods
	5	Dense stressed willows, coarse gravel, undulating topography 3 m above active channel, old channels
	Wetland	Off-transect wetland area

Note: DBH stands for diameter at breast height, measured mostly by eye. Species identification was not exact – no field guide was used.

2.3.1 Objective I Analysis

I developed a new workflow for combining topography and multispectral images (Table 2.4) in an unsupervised spectral classification scheme to determine whether I could successfully quantify floodplain heterogeneity remotely (Figure 2.4). It should be noted that while I used two datasets in the workflow, almost any raster data could be used in this classification methodology. The steps shown in Figure 2.4 are described in detail below.
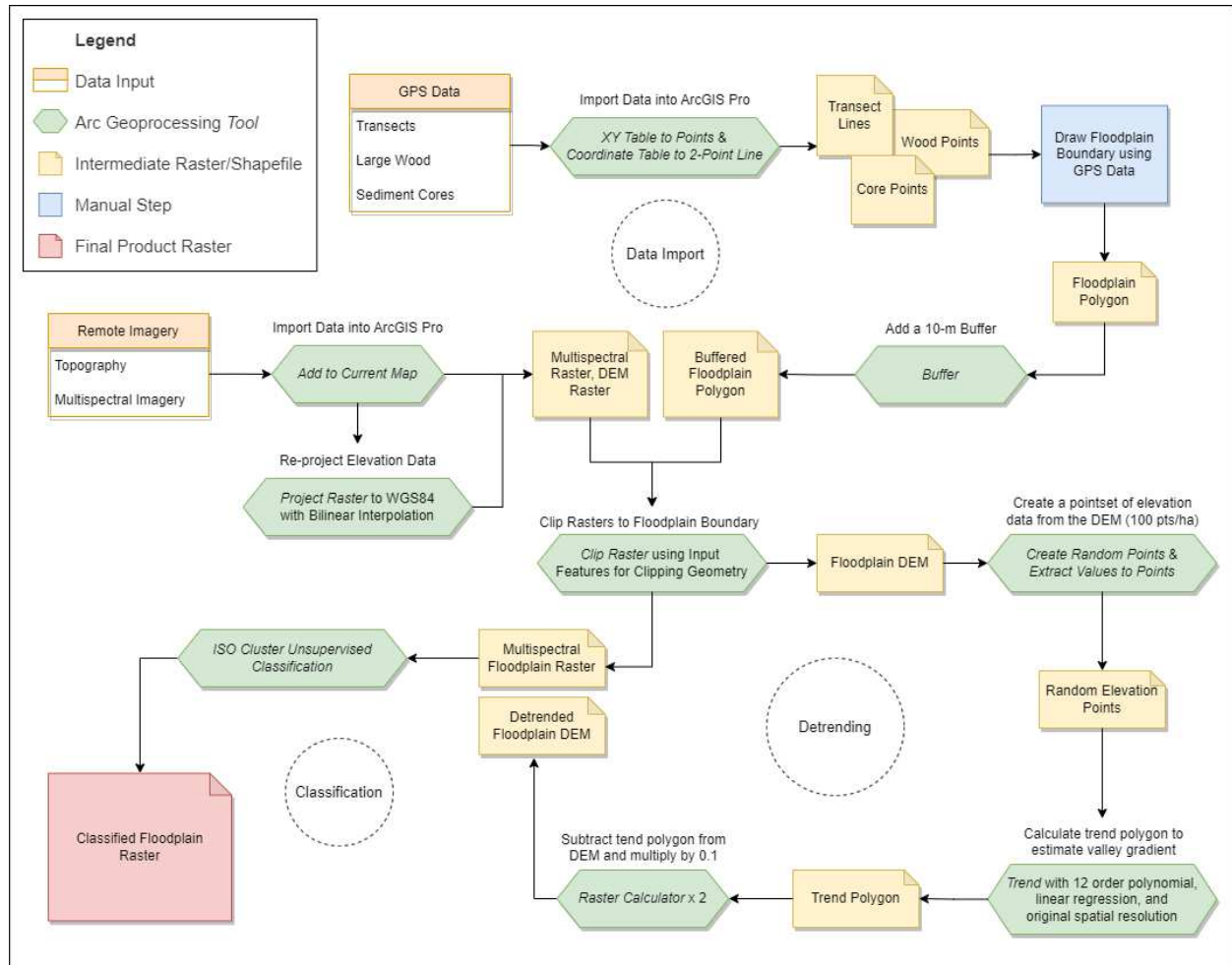
Figure 2.4. Flow chart of classification workflow completed in ArcGIS Pro (Esri, 2022a). Input data are shown in orange, specific ArcGIS tools in italicized green (specific options non-italicized), intermediate shapefiles and rasters in yellow, manual drawing step in blue, and final raster product in red.

The field data were imported into ArcGIS Pro (Esri, 2022a) using the *XY Table to Points* tool for the large wood and sediment core locations and the *Coordinate Table to 2-Point Line* tool (geodesic method) for the patch boundaries to represent the transects. Cloud-free mosaics were prepared from Sentinel-2A imagery (ESA, 2021) in Google Earth Engine (Gorelick et al., 2017; code links in Supplemental Information) and imported into ArcGIS Pro. Digital elevation models (DEMs) were downloaded from The National Map for each site (USGS, 2020).

17

Table 2.4. Data collected and used in this analysis.

Data	Details	Instrument	Resolution	Program Used	References
GPS Locations	Patch boundaries, large wood, and sediment cores	Garmin GPSMAP 66ST	± 3 m	-	-
Watershed Characteristics	Upstream drainage basin shapefiles and associated mean values, downloaded on 9/2021	-	Drainage basin scale	StreamStats	USGS, 2021, 2022a
Digital Elevation Models	NED n40w105 IMG 2018 NED n37w097 IMG 2019 NED n40w107 IMG 2022	Airborne Lidar	1/3 arc-second 1 x 1 degree 10 m	The National Map	Open Topography, 2021; USGS, 2022b, 2020, 2019, 2018
Cloud-free Mosaics	5% cloudy mean pixel values from 4/1/2020-10/31/2020 from GEE Image Collection "COPERNICUS/S2_SR"	Copernicus Sentinel-2A	10 m 12-bit radiometric 5-day temporal Bands 2, 3, 4, 8	Google Earth Engine	ESA, 2021; Gorelick et al., 2017; Sabins Jr. and Ellis, 2020

Active floodplain polygons were manually delineated using the field transects and DEM, and a 10-m geodesic buffer was added to account for field and/or user error. Because only one field transect was mapped at Rough and Tumbling Creek, I used the DEM, field transects, Google Maps imagery, and the Sentinel imagery to delineate this floodplain. The DEMs and Sentinel imagery were clipped to the floodplain polygons to be used in the classifications (Figure 2.5).
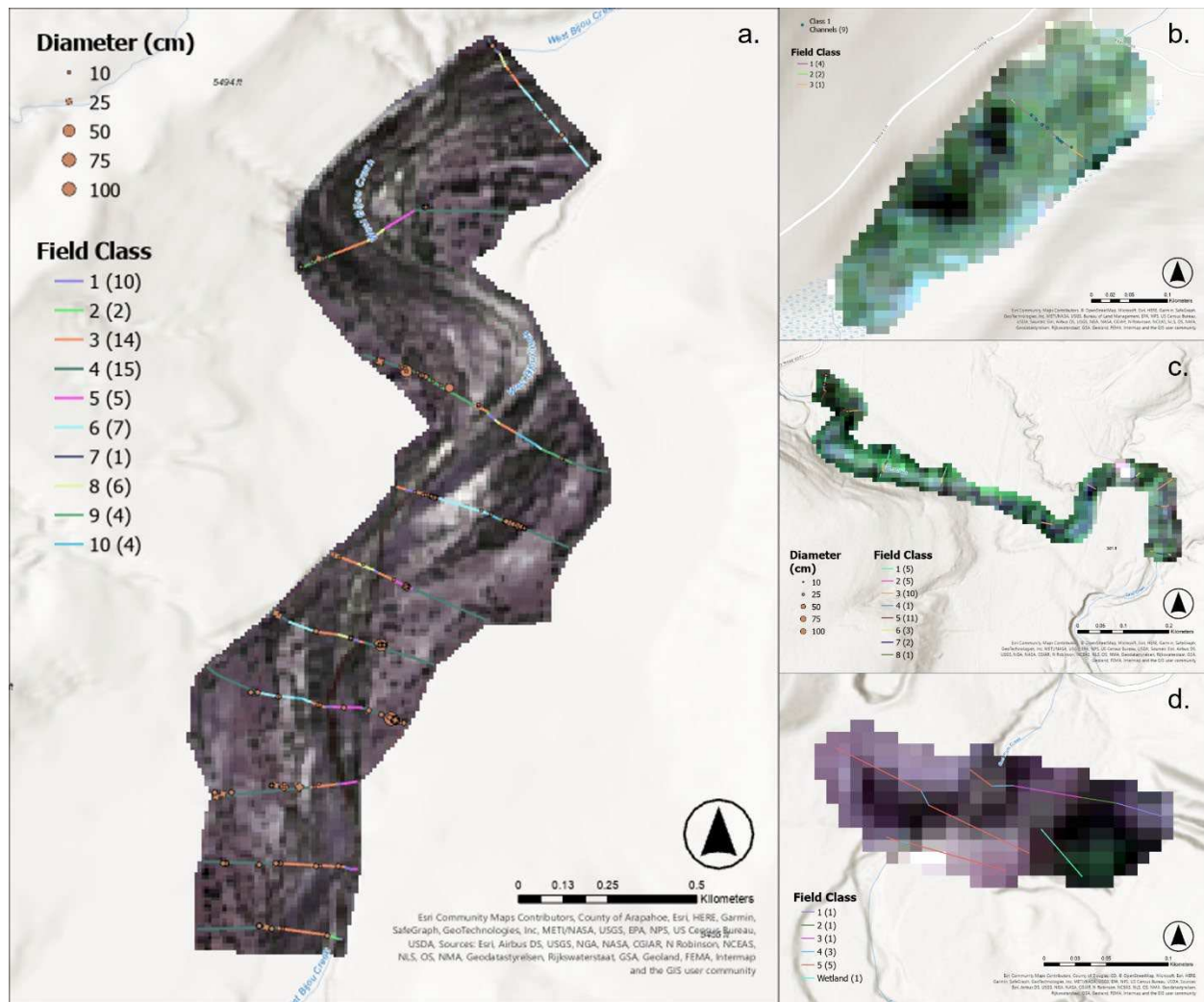
Figure 2.5. Sentinel-2A mosaics clipped to buffered floodplain boundaries, field classes, and large wood locations and (counts) for a) West Bijou Creek, Colorado, b) Rough and Tumbling Creek, Colorado (small channel locations in Class 1 also included), c) Sand Creek, Oklahoma, and d) East Plum Creek, Colorado.

The DEMs were processed further to emphasize the local elevation changes of floodplain features (side channels, terraces, etc.). To decrease the influence of the river corridor gradients, the DEM data were detrended. This involved (i) reprojecting the DEMs to WGS84 using bilinear interpolation (for continuous values; Esri 2022c), (ii) extracting elevation values from random points (number of points calculated from the floodplain area to give a point density of 100 pts/ha, numbers given in Supplemental Table 2.1), (iii) creating a linear trend polygon using a 12th order polynomial (the maximum for the tool and the highest complexity surface), and (iv) subtracting the trend from the DEM. The East Plum Creek DEM was not detrended because the study area

was small relative to the scale of the valley trend and detrending did not seem necessary. To decrease the dominance of the topographic data over the spectral data from the Sentinel imagery, a reducing factor of 0.1 was applied to the detrended DEMs (non-detrended DEM for East Plum Creek).

An unsupervised classification scheme was used to classify the floodplains (*ISO Cluster Unsupervised Classification* tool). The 4-band Sentinel imagery and the processed DEMs were used as the input rasters. In addition, the tool requires the user to input a number of classes, minimum class size in pixels (default: 20), and sample interval (default: 10) (Esri, 2022b). To balance analysis consistency with floodplain area diversity of the sites, I used the same pixel values for all classifications and adjusted the number of classes (Supplemental Table 2.2). Low numbers for minimum class size (4 pixels) and sample interval (2 pixels) were used so that classes would be identified for even the smallest floodplains (and to match the 2-to-1 ratio of the default values). Number of classes was set to 20 for the largest floodplain, 10 for the medium-sized floodplains, and 5 for the smallest (Supplemental Table 2.2). Final classified rasters were then projected into the appropriate UTM coordinates using a cell size of 10 and exported for statistical analysis (*Project Raster* tool with nearest neighbor resampling technique and *Copy Raster* tool to eliminate null values outside the floodplain boundaries).

2.3.2 Objective II Analysis

All post-classification analyses were conducted in R (R Core Team, 2022) using the *landscapemetrics* package (Hesselbarth et al., 2019). The package can calculate over 100 metrics and "reimplements the most common metrics from FRAGSTATS and new ones from the current literature on landscape metrics" (Hesselbarth et al., 2021, p. 23). The 11 landscape-scale metrics that are normalized, bounded, relative, scalable, and/or comparable were identified: aggregation

index, division index, interspersion and juxtaposition index, patch density, percentage of like adjacencies, largest patch index, disjunct core area density, patch richness density, Shannon's evenness index, and perimeter-area fractal dimension. Shannon's diversity (and therefore I infer Shannon's evenness) can show opposite trends to and is more sensitive to rare cover types than Simpson's diversity (and therefore I infer Simpson's evenness and Modified Simpson's evenness) (Nagendra, 2002) and is more appropriate for this analysis.

The final list of metrics calculated in this study is the overlap of the 11 comparable metrics and the 24 metrics analyzed by Huang et al. (2006) in their sensitivity analysis: aggregation index, interspersion and juxtaposition index, patch density, percentage of like adjacencies, largest patch index, and Shannon's evenness index (Table 2.5). When specified, metrics were calculated in 8 directions (Queen's case). Metric details and interpretations provided in Table 2.5.

Table 2.5. Normalized, bounded, relative, scalable, and/or comparable landscape-scale metrics from Huang et al. (2006); interpretations adapted from Hesselbarth et al. (2021) and With (2019).

Metric	Type	Interpretation	Range (units)
Aggregation Index	Aggregation	Aggregation of classes 0 = disaggregated classes 100 = aggregated classes	[0, 100] (%)
Interspersion and Juxtaposition Index	Aggregation	Patch intermixing index, low value indicates pairing of two class types 0 = certain class only next to another certain class 100 = certain class next to all other classes equally	(0, 100] (%)
Patch Density	Aggregation	Simple fragmentation, higher value as landscape gets patchier	$(0, 1 \times 10^6]$ (#/100 ha)
Percentage of Like Adjacencies	Aggregation	Aggregation within a class, likelihood that two adjacent cells are the same class 0 = no like adjacencies, complete disaggregation 100 = whole landscape is the same class	[0, 100] (%)
Largest Patch Index	Area and Edge	Simple area dominance of the single largest patch	(0, 100] (%)
Shannon's Evenness Index	Diversity	Measure of dominance of a class across the landscape, normalized Shannon's diversity, large values indicate equal distribution	[0, 1)

2.4 Results

I present the results of the classification workflow and the resulting heterogeneity metrics calculated.

2.4.1 Objective I Results

The resulting classified floodplains are shown Figure 2.6 and were used to calculate heterogeneity metrics. Although the choice of input values directly affects the resulting classification, the sensitivity of the metrics to changing inputs has been thoroughly documented (Huang et al., 2006). I acknowledge that the process of choosing input values for classification is somewhat arbitrary, and that this inherently reduces the reproducibility of the study. This is why documentation of values used is important when presenting results so that the classifications can be reproduced.
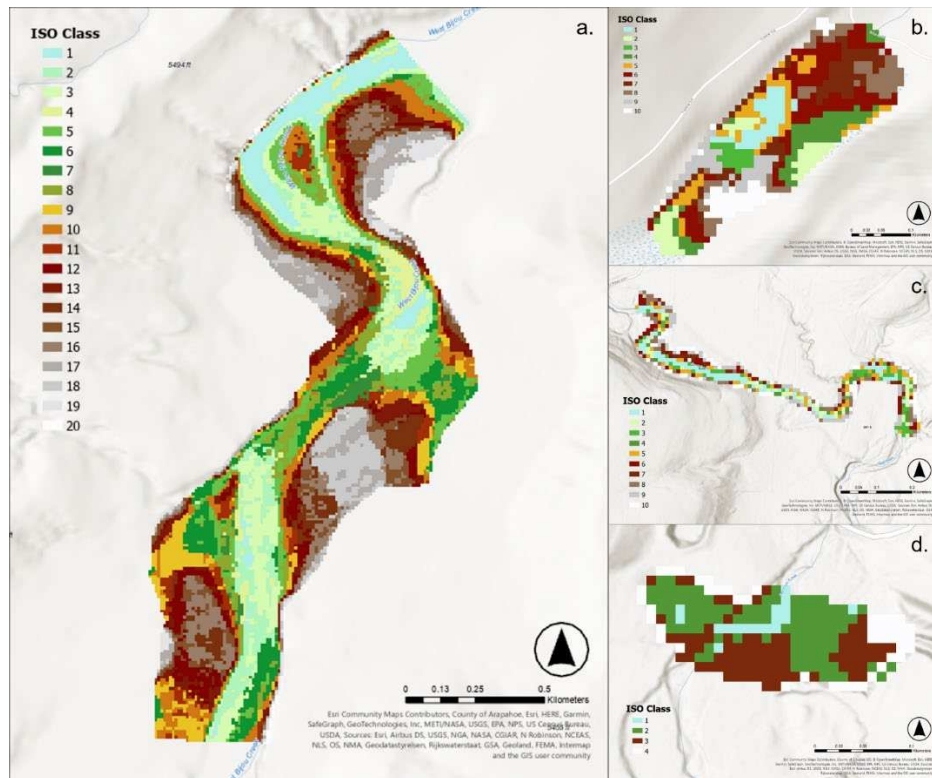
Figure 2.6. ISO cluster unsupervised classifications for a) West Bijou Creek, Colorado, b) Rough and Tumbling Creek, Colorado, c) Sand Creek, Oklahoma, and d) East Plum Creek, Colorado. The classification was completed using 4-band Sentinel-2A imagery and detrended, flattened DEMs. ISO Class numbers are separate from Field Class numbers.

22

2.4.2 Objective II Results

The classified rasters were imported into RStudio and the six heterogeneity metrics were calculated for each floodplain (Table 2.6 and Figure 2.7).

Table 2.6. Values of landscape heterogeneity metrics for the classified floodplain rasters.

Metric	West Bijou Creek	Rough and Tumbling Creek	Sand Creek	East Plum Creek
Aggregation Index (%)	64.1	65.5	28.5	64.9
Interspersion and Juxtaposition Index (%)	76.3	78.3	93.7	78.5
Largest Patch Index (%)	4.8	12.5	7.0	21.1
Patch Density (#/100 ha)	947	1154	4374	1186
Percentage of Like Adjacencies (%)	62.6	60.3	28.5	62.0
Shannon's Evenness Index	0.970	0.960	0.966	0.902
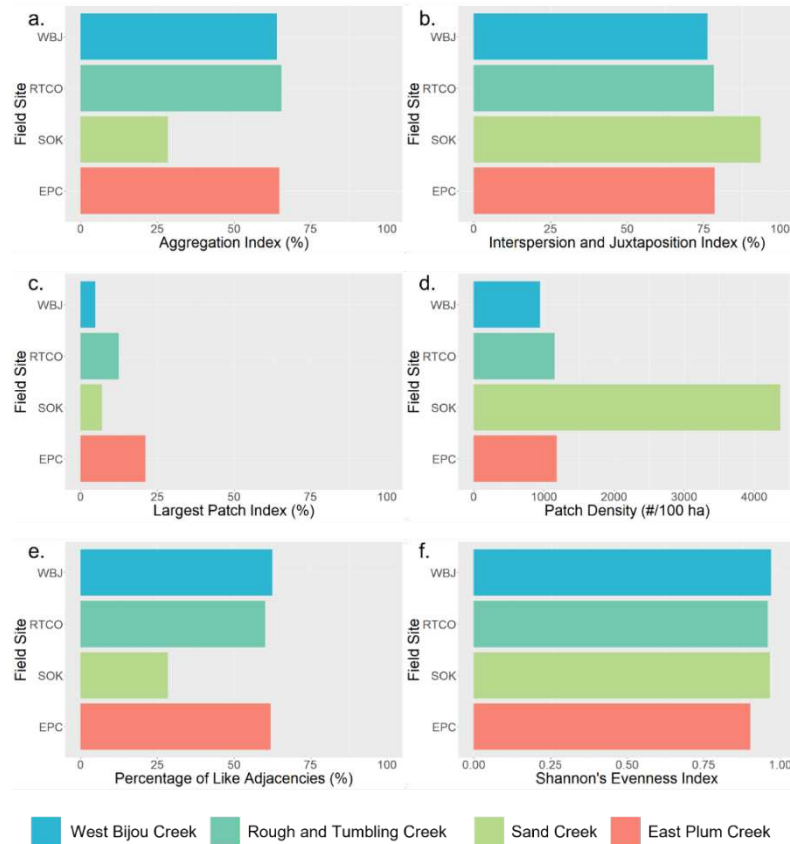
Figure 2.7. Bar plot visualizations of the levels of each metric for each floodplain: a) aggregation index, b) interspersion and juxtaposition index, c) largest patch index, d) patch density, e) percentage of like adjacencies, and f) Shannon's evenness index. In descending order of floodplain area, blue bars represent West Bijou Creek, Colorado (109 ha), turquoise represent Rough and Tumbling Creek, Colorado (5.6 ha), green represent Sand Creek, Oklahoma (5.5 ha), and coral represent East Plum Creek, Colorado (2.1 ha). Intermetric variation can be seen by looking at the values of a single metric for all three sites while intrametric variation ban be seen by looking at the similarities and differences between the levels of each site for all metrics (a–f).

For the purposes of the following results and discussion, I define a "high" level of a metric as a value falling in the top 25% of the range for that metric, a "moderate" level as a value falling in the middle 50%, and a "low" level as a value falling in the bottom 25% (ranges given in Table 2.5), except for patch density that is defined as ≥ 0. These designations are arbitrary and moderate is conservatively wide, as there are no published thresholds for these metrics as they relate to floodplain heterogeneity.

West Bijou, Rough and Tumbling, and East Plum Creeks all have moderate aggregation indices and percentage of like adjacencies, while Sand Creek has low values for both metrics. This indicates that the Colorado sites have moderately aggregated classes and moderate aggregation within the classes, while Sand Creek has class and within-class disaggregation (Figure 2.7a, e; Hesselbarth et al., 2021). All four floodplains have high interspersion and juxtaposition, indicating that there is not much preference for one class to occur next to another (Figure 2.7b; Hesselbarth et al., 2021). All four floodplains have low largest patch indices, indicating that the largest patch on each landscape is small compared to the entire landscape (Figure 2.7c; Hesselbarth et al., 2021). This is probably driven by the small input value of 4 pixels used for minimum class size in the classification workflow. I anticipate that largest patch index would be very sensitive to changes in this number so I held it constant for this analysis. All of the floodplains have high levels of Shannon's evenness (Figure 2.7f). This indicates that all the landscapes have abundant, evenly distributed classes (Hesselbarth et al., 2021). Patch density varies across the landscapes, with Sand Creek having the highest (near 4,400 patches/100 ha), Rough and Tumbling and East Plum Creeks having similar values near 1,200 patches/100 ha, and West Bijou Creek having the lowest near 950 patches/100 ha. This indicates that Sand Creek is more fragmented than the other floodplains. As these metrics exhibit different patterns

between sites (intermetric variation) and between metrics for all sites (intrametric variation;

Figure 2.7), I infer that I am capturing different facets of floodplain heterogeneity with this suite

of six metrics.

2.5 Discussion

In this section, I outline the advantages and disadvantages of the classification workflow

and discusses inferences regarding fluvial processes.

2.5.1 Objective I Discussion

There are a few important advantages to being able to calculate floodplain heterogeneity

from remote imagery. First, Sentinel-2 imagery is available for most of the United States and is

repeated every 5 days (starting in 2015; Sabins Jr. and Ellis, 2020). This allows for repeat

classification and comparison of spatial and temporal differences in heterogeneity. 3DEP

elevation data are also available for most the United States, allowing for stacking of these two

types of data for almost any floodplain. Moreover, other topographic and multispectral imagery

could be used in the workflow. In addition, there are many metrics available in the

landscapemetrics package that could be calculated with this workflow if a specific metric is of

interest.

Disadvantages of this workflow include mismatched resolutions when looking back in

time. For example, the Landsat program has gone through three generations of imaging systems,

starting in 1972 with a spatial resolution of 60 m and a spectral resolution of four bands, and now

has a spatial resolution of 30 m and a spectral resolution of 11 bands (Sabins Jr. and Ellis, 2020).

This evolution of just one satellite system illustrates that the resolution gets poorer farther back

in time, making it more difficult to compare results for a single location. When completing

classification, the user sets a number of classes for the tool to find. Sometimes if the value is set

too high, the tool finds fewer classes than if the number is set lower. For example, if the number of classes is set to 20, the classifier may find 5 classes, but if it is set to 8, it may find 8 classes. This was evident for the smaller floodplains in this study, causing me to lower the number of classes. Number of classes specified and actual number of classes found are given in Supplemental Table 2.2. Moreover, unsupervised classification means I do not inherently know what the resulting classes represent, such as landcover class or vegetation health. While this workflow only includes 4-band spectral data and 3 m elevation data, inclusion of more detailed data and comparison to field data could better illuminate the meaning of the classes. This will be the focus of work going forward.

Overall, a strength of this workflow is that it can be easily repeated for other locations. The main types of data needed are approximate boundaries of the floodplain of interest, and some idea of the spatial scale of floodplain patches. Although I was able to delineate the active floodplain and patches at the test field sites, this information is not necessary to get an order of magnitude estimate of floodplain heterogeneity. If the active floodplain boundary is not available, topographic data could be used to approximate the floodplain/valley bottom boundary, and remote data could be clipped to the topographic data. If field-delineated patches and classes are not available, descriptions, aerial imagery, or other studies could be used to estimate the approximate spatial scale of patches.

2.5.2 Objective II Discussion

I have identified six heterogeneity metrics to use for characterizing spatial floodplain heterogeneity: aggregation index, interspersion and juxtaposition index, largest patch index, patch density, percentage of like adjacencies, and Shannon's evenness index. The results indicate variation within each metric between sites (intermetric) and variation in patterns of the values for

all sites between metrics (intrametric). The intermetric variation, as shown by the levels of the

bars in each bar plot (Figure 2.7), indicates that there is variation in spatial heterogeneity

between the floodplains. The intrametric variation, as shown as patterns of the bars between bar

plots (Figure 2.7), indicates that there is variation in the patterns of the metrics. These metrics

provide six dimensions of spatial heterogeneity information and exhibit both intermetric and

intrametric variation, expanding the simple analysis of floodplain heterogeneity in Wohl and

Iskin (2019). This result aligns with the ideas from Forman and Gordon (1981) that both number

of patches and patch configuration in space may be important to landscape structure, and the

recommendations from Scott et al. (2022) to use both diversity and spatial configuration metrics

to characterize geomorphic heterogeneity.

The floodplains in Colorado exhibit moderate aggregation, high intermixing, low

dominance, lower fragmentation, and high evenness. The Oklahoma floodplain exhibits low

aggregation, high intermixing, low dominance, higher fragmentation, and high evenness. These

results suggest that high intermixing, low dominance, and high evenness may be characteristic of

natural floodplains, while differences in aggregation and fragmentation between Colorado and

Oklahoma may indicate differences in fluvial processes between these two regions. Natural

floodplains may exhibit high intermixing and evenness due to intact natural flow and sediment

regimes that result in overbank flooding, reworking of material, and establishment of

successional species.

The Colorado shortgrass prairie floodplains may exhibit higher aggregation and lower

fragmentation than the Oklahoma tallgrass prairie floodplain due to more dynamic hydrology,

less cohesive soils, and reduced channel incision, as observed in the field. Other investigators

have documented substantial shifts in channel planform and dynamics in the shortgrass prairie of

eastern Colorado over timespans of several decades, with repeated alternations between relatively narrow, sinuous, single-thread channel planform in a vegetated floodplain (the condition at the time of my measurements) and wide, braided channel planform in a floodplain stripped of vegetation following a large flood (Friedman and Lee, 2002). Although rivers in the mixed prairie and tallgrass prairie of Kansas and Oklahoma can exhibit alterations between narrow and wide planforms (Schumm and Lichty, 1963; Bergman and Sullivan, 1963), there was less evidence of this at Sand Creek due to thick layers of clay-rich, cohesive sediment present in the bed and banks and the dense vegetation both in and beside the river. Sand Creek is also in a more humid climate than the Colorado sites, which corresponds to higher baseflow and lower magnitude of flow variability relative to drier sites (Berghuijs et al., 2014). Greater flow variability tends to correlate with substantial temporal variations in channel planform and floodplain dimensions (e.g., Miller and Friedman, 2009; Hooke, 2016), which may explain the higher aggregation seen at the Colorado sites.

Resource preferences differ somewhat between cattle (*Bos* spp.) and bison (*Bison* spp.) (Allred et al., 2010), but it is unclear if their grazing affects landscapes differently (Towne et al., 2005). The observed heterogeneity metrics may reflect the influence on vegetation distribution of large ungulate grazing at the sites (bison at Sand Creek, and cows at West Bijou and East Plum Creeks). This could potentially account for some of the differences in aggregation and fragmentation between the Colorado and Oklahoma sites. The metrics qualitatively distinguish all of the Colorado sites from the Oklahoma sites, but do not distinguish the prairie and beaver meadow sites in Colorado. I infer that this reflects the dynamic and patchy nature of river corridors actively occupied by beaver, which continually modify existing dams and build new

dams, creating newly flooded areas and multiple ponds in gradual stages of infilling (Ives, 1942; Polvi and Wohl, 2012; Laurel and Wohl, 2019).

The sensitivity of these landscape metrics to changes in classification scheme have been documented by Huang et al. (2006). They found that all six of the metrics used in this study exhibited a "high" amount of total change as the number of classes specified in the classification was increased, and sensitivity of the metrics to increased classification differed between groups of metrics (Huang et al., 2006). Interspersion and juxtaposition (no consistent models, sensitivity window of 3–8 classes), patch density (flat line predictability, sensitivity window of 11–34 classes), and Shannon's evenness (flat line predictability, sensitivity window of 7–29 classes) all increased with increasing number of classes, while largest patch (declining power law predictability, sensitivity window of 3–13 classes), aggregation (declining logarithmic predictability, sensitivity window of 8–32 classes), and percentage of like adjacencies (declining logarithmic predictability, sensitivity window of 8–32 classes) decreased with increasing number of classes (Huang et al., 2006). I observe weak positive correlation between number of classes and both aggregation index (R = 0.08) and percentage of like adjacencies (R = 0.12); weak negative correlation between number of classes and both interspersion and juxtaposition (R = -0.22) and patch density (R = -0.16); strong positive correlation between number of classes and Shannon's evenness (R = 0.77); and strong negative correlation between number of classes and largest patch index (R = -0.86). I do not provide p-values because correlation values were calculated in Microsoft Excel. Huang et al. (2006) also found that the metrics I used exhibited "high", "moderate-high", or "moderate" differences between locations, expect for Shannon's evenness that exhibited "low" difference (Huang et al., 2006). This indicates that these metrics are useful for discerning landscape differences, as used in this study.

For this study, this means that, although the metrics are sensitive to changes in number of classes (and I classified with different numbers of classes), the direction and character of change are predictable for most cases (except interspersion and juxtaposition). Caution should be exercised when class numbers are low, for example, East Plum Creek, as the sensitivity windows identified by Huang et al. (2006) include the number of classes used in this study. Even if I exclude East Plum Creek from the analysis, I still see differentiation between Colorado and Oklahoma. Overall, I feel that using different numbers of classes is reasonable for this analysis, because I expect different rivers to differ in structure and class number, and I controlled for resolution differences by using the same type of remote imagery and same input values for class size and sample interval for all four landscapes.

This study is a detailed documentation of the methods used to classify floodplains using remotely sensed data and an analysis of heterogeneity metrics applied to river corridors. This is a small piece of a larger study that applies these methods with higher resolution and more detailed data across 10+ natural floodplains in the United States. The ultimate goal of this work is to relate levels of spatial heterogeneity to river corridor characteristics (biome, drainage area, flow regime, valley confinement, and channel planform), and then infer processes, through a rigorous statistical analysis.

2.6 Conclusion

Floodplain heterogeneity is an integral component of natural river corridors and influences the ecosystem functions of natural floodplains. The field of landscape ecology deals substantially with characterizing and quantifying spatial heterogeneity at multiple scales. Although some fluvial research has incorporated tenets of landscape ecology, I directly use metrics from this discipline to calculate the spatial heterogeneity of four natural floodplains.

I have developed an unsupervised classification workflow to classify natural floodplains. The workflow can be completed with any type of raster data, and inclusion of the field data enhances the analysis and interpretation but is not necessary. I calculated a suite of six heterogeneity metrics that show intra- and intermetric variation and capture different facets of floodplain heterogeneity: aggregation index, interspersion and juxtaposition index, largest patch index, patch density, percentage of like adjacencies, and Shannon's evenness index. It is useful to know that no single metric captures all the facets of floodplain heterogeneity. The metrics are sensitive to the choices made by the user during classification, and documenting these choices is essential to reproducibility. All of the metrics are normalized in some way and are highly sensitive to changes in location and are therefore very useful for comparing floodplains in space.

Results show that natural floodplains have high evenness and interspersion and juxtaposition of classes. I attribute this to natural flow and sediment regimes driving channel migration, erosion, deposition, vegetation succession, and active beaver modifications. The Colorado floodplains at West Bijou, East Plum, and Rough and Tumbling Creeks show higher aggregation and lower fragmentation than the Oklahoma floodplain at Sand Creek. I attribute this to the greater incision and lower hydrologic variability in Oklahoma. Future research will expand this method of quantifying floodplain spatial heterogeneity to include additional field sites with varying hydrological (drainage area, precipitation, and flow regimes), ecological (dominant species types, beaver vs. large wood dynamics), and geomorphological (channel planform) characteristics, and include high-resolution elevation data, near-surface soil texture data, large wood load data, and vegetation and moisture spectral indices to better parse out what the classes might indicate about fluvial processes and floodplain geomorphic history.

2.7 References

Aguiar, F.C., Fernandes, M.R., Ferreira, M.T., 2011. Riparian vegetation metrics as tools for guiding ecological restoration in riverscapes. *Knowledge & Management of Aquatic Ecosystems* 402(21). https://doi.org/10.1051/kmae/2011074

Aguiar, F.C., Ferreira, M.T., Albuquerque, A., Rodríguez-González, P., Segurado, P., 2009. Structural and functional responses of riparaian vegetation to human disturbance: performance and spatial scale-dependence. *Fundamental and Applied Limnology* 175(3), 249–267. https://doi.org/10.1127/1863-9135/2009/0175-0249

Allen, J.R.L., 1965. A review of the origin and characteristics of recent alluvial sediments. *Sedimentology* 5(2), 89-191. https://doi.org/10.1111/j.1365-3091.1965.tb01561.x

Allred, B.W., Fuhlendorf, S.D., Hamilton, R.G., 2010. The role of herbivores in Great Plains conservation: comparative ecology of bison and cattle. *Ecosphere* 2(3), 1–17. https://doi.org/10.1890/ES10-00152.1

Amoros, C., Bornette, G., 2002. Connectivity and biocomplexity in waterbodies of riverine floodplains. *Freshwater Biology* 47(4), 761-776. https://doi.org/10.1046/j.1365-2427.2002.00905.x

Appling, A.P., Bernhardt, E.S., Stanford, J.A., 2014. Floodplain biogeochemical mosaics: A multidimensional view of alluvial soils. *JGR Biogeosciences* 119(8), 1538–1553. https://doi.org/10.1002/2013JG002543

Arscott, D.B., Tockner, K., Van der Nat, D., Ward, J.V., 2002. Aquatic habitat dynamics along a braided alpine river ecosystem (Tagliamento River, Northeast Italy). *Ecosystems* 5, 802-814. https://doi.org/10.1002/esp.3434

Baartman, J.E.M., Masselink, R., Keesstra, S.D., Temme, A.J.A.M., 2013. Linking landscape morphological complexity and sediment connectivity. *Earth Surface Processes and Landforms* 38(12), 1457–1471. https://doi.org/10.1002/esp.3434

Bagstad, K.J., Lite, S.J., Stromberg, J.C., 2006. Vegetation, Soils, and Hydrogeomorphology of Riparian Patch Types of a Dryland River. *Western North American Naturalist* 66(1), 23–44. https://doi.org/10.3398/1527-0904(2006)66[23:VSAHOR]2.0.CO;2

Beechie, T.J., Liermann, M., Pollock, M.M., Baker, S., Davies, J. 2006. Channel pattern and river-floodplain dynamics in forested mountain river systems. *Geomorphology* 78(1-2), 124-141. https://doi.org/10.1016/j.geomorph.2006.01.030

Bellmore, J.R., Baxter, C. V., 2014. Effects of geomorphic process domains on river ecosystems: A comparison of floodplain and confined valley segments. *River Research and Applications* 30(5), 617–630. https://doi.org/10.1002/rra.2672

Bellmore, J.R., Baxter, C. V., Martens, K., Connolly, P.J., 2013. The floodplain food web mosaic: A study of its importance to salmon and steelhead with implications for their recovery. *Ecological Applications* 23(1), 189–207. https://doi.org/10.1890/12-0806.1

Bracken, L.J., Wainwright, J., Ali, G.A., Tetzlaff, D., Smith, M.W., Reaney, S.M., Roy, A.G., 2013. Concepts of hydrological connectivity: research approaches, pathways and future agendas. *Earth-Science Reviews* 119, 12-34. https://doi.org/10.1016/j.earscirev.2013.02.001

Bracken, L.J., Turnbull, L., Wainwright, J., Bogaart, P., 2015. Sediment connectivity: a framework for understanding sediment transfer at multiple scales. *Earth Surface Processes and Landforms* 40(2). 177-188. https://doi.org/10.1002/esp.3635

Cadenasso, M.L., Pickett, S.T.A., Grove, J.M., 2006. Dimensions of ecosystem complexity: heterogeneity, connectivity, and history. *Ecological Complexity* 3(1), 1-12. https://doi.org/10.1016/j.ecocom.2005.07.002

Choné, G., Biron, P.M., 2016. Assessing the Relationship Between River Mobility and Habitat. *River Research and Applications* 32(4), 528–539. https://doi.org/10.1002/rra.2896

Ciszewski, D., Grygar, T.M., 2016. A Review of Flood-Related Storage and Remobilization of Heavy Metal Pollutants in River Systems. *Water, Air, & Soil Pollution* 227(Article 239). https://doi.org/10.1007/s11270-016-2934-8

Collins, B.D., Montgomery, D.R., Fetherston, K.L., Abbe, T.B., 2012. The floodplain large-wood cycle hypothesis: a mechanism for the physical and biotic structuring of temperate forested alluvial valleys in the North Pacific coastal ecoregion. *Geomorphology* 139-140, 460-470. https://doi.org/10.1016/j.geomorph.2011.11.011

Doering, M., Freimann, R., Antenen, N., Roschi, A., Robinson, C.T., Rezzonico, F., Smits, T.H.M., Tonolla, D., 2021. Microbial communities in floodplain ecosystems in relation to altered flow regimes and experimental flooding. *Science of the Total Environment* 788, 147497. https://doi.org/10.1016/j.scitotenv.2021.147497

Erős, T., Kuehne, L., Dolezsai, A., Sommerwerk, N., Wolter, C., 2019. A systematic review of assessment and conservation management in large floodplain rivers – Actions postponed. *Ecological Indicators* 98, 453–461. https://doi.org/10.1016/j.ecolind.2018.11.026

Erős, T., Lowe, W.H., 2019. The Landscape Ecology of Rivers: from Patch-Based to Spatial Network Analyses. *Current Landscape Ecology Reports* 4, 103–112. https://doi.org/10.1007/s40823-019-00044-6

Esri, 2022a. ArcGIS Pro.

Esri, 2022b. Iso Cluster Unsupervised Classification (Spatial Analyst). *ArcGIS Pro 2.9 Help: Multivariate toolset*. https://pro.arcgis.com/en/pro-app/2.9/tool-reference/spatial-analyst/iso-cluster-unsupervised-classification.htm (accessed 10.12.22).

Esri, 2022c. Project Raster (Data Management). *ArcGIS Pro 3.0 Help: Raster toolset*. https://pro.arcgis.com/en/pro-app/latest/tool-reference/data-management/project-raster.htm (accessed 12.19.22).

European Space Agency (ESA), 2021. Level-2A. *Sentinel Online*. https://sentinel.esa.int/web/sentinel/user-guides/sentinel-2-msi/product-types/level-2a (accessed 11.19.21).

Everitt, B.L., 1968. Use of the cottonwood in an investigation of the recent history of a flood plain. *American Journal of Science* 266(6), 417-439. https://doi.org/10.2475/ajs.266.6.417

Feoli, E., Ganis, P., Ricotta, C., 2013. Measuring diversity of environmental systems. In, J.J. Ibanez, J.G. Bockheim, eds., Pedodiversity. CRC Press, Boca Raton, FL, 29-58.

Fernandes, M.R., Aguiar, F.C., Ferreira, M.T., 2011. Assessing riparian vegetation structure and the influence of land use using landscape metrics and geostatistical tools. *Landscape and Urban Planning* 99(2), 166–177. https://doi.org/10.1016/j.landurbplan.2010.11.001

Forman, R.T.T., Gordon, M., 1981. Patches and Structural Components for A Landscape Ecology. *BioScience* 31(10), 733–740. https://doi.org/10.2307/1308780

Friedman, J.M., Lee, V.J., 2002. Extreme floods, channel change, and riparian forests along ephemeral streams. *Ecological Monographs* 72(3), 409–425. https://doi.org/10.1890/0012-9615(2002)072[0409:EFCCAR]2.0.CO;2

Fryirs, K., 2013. (Dis)Connectivity in catchment sediment cascades: a fresh look at the sediment delivery problem. *Earth Surface Processes and Landforms* 38(1), 30-46. https://doi.org/10.1002/esp.3242

Fryirs, K., Brierley, G.J., Erskine, W.D., 2012. Use of ergodic reasoning to reconstruct the historical range of variability and evolutionary trajectory of rivers. *Earth Surface Processes and Landforms* 37(7), 763-773. https://doi.org/10.1002/esp.3210

Fuchs, J.W., Fox, G.A., Storm, D.E., Penn, C.J., Brown, G.O., 2009. Subsurface transport of phosphorus in riparian floodplains: influence of preferential flow paths. *Journal of Environmental Quality* 38(2), 473-484. https://doi.org/10.2134/jeq2008.0201

Gorelick, N., Hancher, M., Dixon, M., Ilyushchenko, S., Thau, D., Moore, R., 2017. Google Earth Engine: Planetary-scale geospatial analysis for everyone. *Remote Sensing of the Environment* 202, 18–27. https://doi.org/10.1016/j.rse.2017.06.031

Gostner, W., Alp, M., Schleiss, A.J., Robinson, C.T., 2013. The hydro-morphological index of diversity: a tool for describing habitat heterogeneity in river engineering projects. *Hydrobiologia* 712, 43–60. https://doi.org/10.1007/s10750-012-1288-5

Graf, W.L., 2006. Downstream hydrologic and geomorphic effects of large dams on American rivers. Geomorphology 79(3-4), 336–360. https://doi.org/10.1016/j.geomorph.2006.06.022

Grondin, P., Gauthier, S., Poirier, V., Tardiff, P., Boucher, Y., Bergeron, Y., 2018. Have some landscapes in the eastern Canadian boreal forest moved beyond their natural range of variability? *Forest Ecosystems* 5(Article 30). https://doi.org/10.1186/s40663-018-0148-9

Güneralp, İ., Rhoads, B.L., 2011. Influence of floodplain erosional heterogeneity on planform complexity of meandering rivers. *Geophysical Research Letters* 38(14), L14401. https://doi.org/10.1029/2011GL048134

Harms, T.K., Wentz, E.A., Grimm, N.B., 2009. Spatial heterogeneity of denitrification in semi-arid floodplains. *Ecosystems* 12, 129-143. https://doi.org/10.1007/s10021-008-9212-6

Hein, T., Baranyi, C., Herndl, G.J., Wanek, W., Schiemer, F. 2003. Allochthonous and autochthonous particulate organic matter in floodplains of the River Danube: the importance of hydrological connectivity. *Freshwater Biology* 48(2), 220-232. https://doi.org/10.1046/j.1365-2427.2003.00981.x

Helton, A.M., Poole, G.C., Payn, R.A., Izurieta, C., Stanford, J.A., 2014. Relative influences of the river channel, floodplain surface, and alluvial aquifer on simulated hydrologic residence time in a montane river floodplain. *Geomorphology* 205, 17–26. https://doi.org/10.1016/j.geomorph.2012.01.004

Hesselbarth, M.H.K., Sciaini, M., Nowosad, J., Hanss, S., Graham, L.J., Hollister, J., With, K.A., 2021. Package "landscapemetrics" Reference Manual.

Hesselbarth, M.H.K., Sciaini, M., With, K.A., Wiegand, K., Nowosad, J., 2019. landscapemetrics: an open-source R tool to calculate landscape metrics. *Ecography* 42(10), 1648–1657. https://doi.org/10.1111/ecog.04617

Hooke, J.M., 2016. Morphological impacts of flow events of varying magnitude on ephemeral channels in a semiarid region. *Geomorphology* 252, 128-143. https://doi.org/10.1016/j.geomorph.2015.07.014

Hooke, J.M., 1995. River channel adjustment to meander cutoffs on the River Bollin and River Dane, northwest England. *Geomorphology* 14(3), 235-253. https://doi.org/10.1016/0169-555X(95)00110-Q

Huang, C., Geiger, E.L., Kupfer, J.A., 2006. Sensitivity of landscape metrics to classification scheme. *International Journal of Remote Sensing* 27(14), 2927-2948. https://doi.org/10.1080/01431160600554330

Hughes, F.M.R., 1997. Floodplain biogeomorphology. *Progress in Physical Geography: Earth and Environment* 21(4), 501–529. https://doi.org/10.1177/030913339702100402

Hughes, F.M.R., 1998. The ecology of African floodplain forests in semi-arid and arid zones: a review. *Journal of Biogeography* 15(1), 127-140. https://doi.org/10.2307/2845053

Hugue, F., Lapointe, M., Eaton, B.C., Lepoutre, A., 2016. Satellite-based remote sensing of running water habitats at large riverscape scales: Tools to analyze habitat heterogeneity for river ecosystem management. *Geomorphology* 253, 353–369. https://doi.org/10.1016/j.geomorph.2015.10.025

Ives, R.L., 1942. The beaver-meadow complex. *Geomorphology* 5(3), 191– 203.

Junk, W.J., Bayley, P.B., Sparks, R.E., 1989. The flood pulse concept in river-floodplain systems. In, D.P. Dodge, ed., Proceedings of the International Large River Symposium. Canadian Special Publications in Fisheries and Aquatic Sciences 106, 110-127.

Karimi, S.S., Saintilan, N., Wen, L., Cox, J., Valavi, R. 2021. Influence of inundation characteristics on the distribution of dryland floodplain vegetation communities. *Ecological Indicators* 124, 107429. https://doi.org/10.1016/j.ecolind.2021.107429

Kleindl, W.J., Rains, M.C., Marshall, L.A., Hauer, F.R., 2015. Fire and flood expand the floodplain shifting habitat mosaic concept. *Freshwater Science* 34(4), 1366–1382. https://doi.org/10.1086/684016

Knox, R.L., Wohl, E.E., Morrison, R.R., 2022. Levees don't protect, they disconnect: A critical review of how artificial levees impact floodplain functions. *Science of the Total Environment* 837, 155773. https://doi.org/10.1016/j.scitotenv.2022.155773

Kuiper, J.J., Janse, J.H., Teurlincx, S., Verhoeven, J.T.A., Alkemade, R., 2014. The impact of river regulation on the biodiversity intactness of floodplain wetlands. *Wetlands Ecology Management* 22, 647-658. https://doi.org/10.1007/s11273-014-9360-8

Landres, P.B., Morgan, P., Swanson, F.J., 1999. Overview of the use of natural variability concepts in managing ecological systems. *Ecological Applications* 9(4), 1179-1188. https://doi.org/10.1890/1051-0761(1999)009[1179:OOTUON]2.0.CO;2

Larsen, A., Larsen, J.R., Lane, S.N., 2021. Dam builders and their works: Beaver influences on the structure and function of river corridor hydrology, geomorphology, biogeochemistry and ecosystems. *Earth-Science Reviews* 218, 103623. https://doi.org/10.1016/j.earscirev.2021.103623

Larsen, L.G., Harvey, J.W., 2010. How vegetation and sediment transport feedbacks drive landscape change in the Everglades and wetlands worldwide. *American Naturalist* 176(3), E66–E79. https://doi.org/10.1086/655215

Laurel, D., Wohl, E., 2019. The persistence of beaver-induced geomorphic heterogeneity and organic carbon stock in river corridors. *Earth Surface Processes and Landforms* 44(1), 342-353. https://doi.org/10.1002/esp.4486

Lecce, S.A., 1997. Spatial patterns of historical overbank sedimentation and floodplain evolution, Blue River, Wisconsin. *Geomorphology* 18(3-4), 265-277. https://doi.org/10.1016/S0169-555X(96)00030-X

Lininger, K.B., Wohl, E., Rose, J.R., 2018. Geomorphic Controls on Floodplain Soil Organic Carbon in the Yukon Flats, Interior Alaska, From Reach to River Basin Scales. *Water Resources Research* 54(3), 1934–1951. https://doi.org/10.1002/2017WR022042

Lininger, K.B., Scamardo, J.E., Guiney, M.R., 2021. Floodplain large wood and organic matter jam formation after a large flood: Investigating the influence of floodplain forest stand characteristics and river corridor morphology. *JGR Earth Surface* 126(6), e2020JF006011. https://doi.org/10.1029/2020JF006011

Lowell, J.L., Gordon, N., Engstrom, D., Stanford, J.A., Holben, W.E., Gannon, J.E., 2009. Habitat heterogeneity and associated microbial community structure in a small-scale floodplain hyporheic flow path. *Microbial Ecology* 58, 611-620. https://doi.org/10.1007/s00248-009-9525-9

McGarigal, K., Marks, B.J., 1995. FRAGSTATS: Spatial Pattern Analysis Program for Quantifying Landscape Structure, U.S. Forest Service General Technical Report PNW-GTR-351. Portland. https://doi.org/10.2737/PNW-GTR-351

Morgan, P., Aplet, G.H., Haufler, J.B., Humphries, H.C., Moore, M.M., Wilson, W.D., 1994. Historical Range of Variability: A Useful Tool for Evaluating Ecosystem Change. *Journal of Sustainable Forestry* 2(1-2), 87-111. https://doi.org/10.1300/J091v02n01_04

MRLC: Multi-Resolution Land Characteristics Consortium, 2022. NLCD Land Cover Change Index (CONUS). URL https://www.mrlc.gov/data/nlcd-land-cover-change-index-conus (accessed 10.12.22).

Nagendra, H., 2002. Opposite trends in response for the Shannon and Simpson indices of landscape diversity. *Applied Geography* 22(2), 175–186. https://doi.org/10.1016/S0143-6228(02)00002-4

Naiman, R.J., Bechtold, J.S., Drake, D.C., Latterell, J.J., O'Keefe, T.C., Balian, E. V., 2005. Origins, Patterns, and Importance of Heterogeneity in Riparian Systems, in: Lovett, G.M., Turner, M.G., Jones, C.G., Weathers, K.C. (Eds.), *Ecosystem Function in Heterogeneous Landscapes*. Springer Science + Business Media, Inc., New York, pp. 279–309. https://doi.org/10.1007/0-387-24091-8_14

Nanson, G.C., Croke, J.C., 1992. A genetic classification of floodplains. *Geomorphology* 4(6), 459–486. https://doi.org/10.1016/0169-555X(92)90039-Q

Nicholas, A.P., Walling, D.E., 1997. Investigating spatial patterns of medium-term overbank sedimentation on floodplains: a combined numerical modelling and radiocaesium-based approach. *Geomorphology* 19(1-2), 133-150. https://doi.org/10.1016/S0169-555X(96)00043-8

Open Topography, 2021. USGS 1/3 arc-second Digital Elevation Model. https://doi.org/10.5069/G98K778D

Pettit, N.E., Naiman, R.J., Rogers, K.H., Little, J.E., 2005. Post-flooding distribution and characteristics of large woody debris piles along the semi-arid Sabie River, South Africa. *River Research and Applications* 21(1), 27-38. https://doi.org/10.1002/rra.812

Phillips, J.D., 2014. State transitions in geomorphic responses to environmental change. *Geomorphology* 204, 208–216. https://doi.org/10.1016/j.geomorph.2013.08.005

Polvi, L.E., Wohl, E., 2012. The beaver meadow complex revisited – the role of beavers in post-glacial floodplain development. *Earth Surface Processes and Landforms* 37(3), 332–46. https://doi.org/10.1002/esp.2261

Poole, G.C., 2002. Fluvial landscape ecology: Addressing uniqueness within the river discontinuum. *Freshwater Biology* 47(4), 641–660. https://doi.org/10.1046/j.1365-2427.2002.00922.x

R Core Team, 2022. R: A language and environment for statistical computing.

Rhoads, B.L. 2013. Process in geomorphology. In, A.R. Orme, D. Sacks, eds., Treatise on Geomorphology, v. 1 The Foundations of Geomorphology. Academic Press, San Diego, CA, 190-204.

Sabins Jr., F.F., Ellis, J.M., 2020. Remote Sensing: Principles, Interpretation, and Applications, 4th ed. Waveland Press, Inc., Long Grove.

Samaritani, E., Shrestha, J., Fournier, B., Frossard, E., Gillet, F., Guenat, C., Niklaus, P.A., Pasquale, N., Tockner, K., Mitchell, E.A.D., Luster, J., 2011. Heterogeneity of soil carbon pools and fluxes in a channelized and a restored floodplain section (Thur River, Switzerland). *Hydrology and Earth System Sciences* 15, 1757–1769. https://doi.org/10.5194/hess-15-1757-2011

Schindler, S., O'Neill, F. H., Biró, M., Damm, C., Gasso, V., Kanka, R., van der Sluis, T., Krug, A., Lauwaars, S. G., Sebesvari, Z., Pusch, M., Baranovsky, B., Ehlert, T., Neukirchen, B., Martin, J. R., Euller, K., Mauerhofer, V., Wrbka, T., 2016. Multifunctional floodplain management and biodiversity effects: A knowledge synthesis for six European countries. *Biodiversity and Conservation*, 25, 1349–1382. https://doi.org/10.1007/s10531-016-1129-3

Schumm, S.A., Lichty, R.W., 1963. Channel widening and flood-plain construction along Cimarron River in southwestern Kansas. *USGS Professional Paper 352-D*. https://doi.org/10.3133/pp352D

Schwendel, A.C., Nicholas, A.P., Aalto, R.E., Sambrook Smith, G.H., Buckley, S., 2015. Interaction between meander dynamics and floodplain heterogeneity in a large tropical sand-bed river: The Rio Beni, Bolivian Amazon. *Earth Surface Processes and Landforms* 40(15), 2026–2040. https://doi.org/10.1002/esp.3777

Scott, M.L., Friedman, J.M., Auble, G.T., 1996. Fluvial process and the establishment of bottomland trees. *Geomorphology* 14(4), 327–339. https://doi.org/10.1016/0169-555X(95)00046-8

Scott, D.N., Shahverdian, S., Flitcroft, R., Wohl, E., 2022. Geomorphic heterogeneity as a framework for assessing river corridor processes and characteristics. *River Research and Applications* 38(10), 1893–1901. https://doi.org/10.1002/rra.4036

Scown, M.W., Thoms, M.C., De Jager, N.R., 2016. An index of floodplain surface complexity. *Hydrology and Earth System Sciences* 20, 431–441. https://doi.org/10.5194/hess-20-431-2016

Scown, M.W., Thoms, M.C., De Jager, N.R., 2015a. Floodplain complexity and surface metrics: Influences of scale and geomorphology. *Geomorphology* 245, 102–116. https://doi.org/10.1016/j.geomorph.2015.05.024

Scown, M.W., Thoms, M.C., De Jager, N.R., 2015b. Measuring floodplain spatial patterns using continuous surface metrics at multiple scales. *Geomorphology* 245, 87–101. https://doi.org/10.1016/j.geomorph.2015.05.026

Slingerland, R., Smith, N.D., 2004. River avulsions and their deposits. *Annual Reviews of Earth and Planetary Sciences* 32, 257-285. https://doi.org/10.1146/annurev.earth.32.101802.120201

Stanford, J.A., Lorang, M.S., Hauer, F.R. 2005. The shifting habitat mosaic of river ecosystems. *Internationale Vereinigung für Theoretische und Angewandte Limnologie: Verhandlungen* 29, 123-136. https://doi.org/10.1080/03680770.2005.11901979

Stoffers, T., Buijse, A.D., Verreth, J.A.J., Nagelkerke, L.A.J., 2022. Environmental requirements and heterogeneity of rheophilic fish nursery habitats in European lowland rivers: Current insights and future challenges. *Fish and Fisheries*. 23(1), 162–182. https://doi.org/10.1111/faf.12606

Thoms, M.C., 2003. Floodplain-river ecosystems: Lateral connections and the implications of human interference. *Geomorphology* 56(3-4), 335-349. https://doi.org/10.1016/S0169-555X(03)00160-0

Thoms, M.C., Southwell, M., McGinness, H.M., 2005. Floodplain-river ecosystems: Fragmentation and water resources development. *Geomorphology* 71(1-2), 126-138. https://doi.org/10.1016/j.geomorph.2004.10.011

Tockner, K., Bunn, S.E., Gordon, C., Naiman, R.J., Quinn, G.P., Stanford, J.A., 2008. Flood plains: critically threatened ecosystems, in: Polunin, N.V.C. (Ed.), *Aquatic Ecosystems: Trends and Global Prospects*. Cambridge University Press, Cambridge, pp. 45–62. https://doi.org/10.1017/CBO9780511751790.006

Tockner, K., Malard, F., Ward, J. V., 2000. An extension of the flood pulse concept. *Hydrological Processes* Special Issue: Linking Hydrology and Ecology, *Hydrological Processes* 14(16-17), 2861–2883. https://doi.org/10.1002/1099-1085(200011/12)14:16/17<2861::AID-HYP124>3.0.CO;2-F

Towne, E.G., Hartnett, D.C., Cochran, R.C., 2005. Vegetation trends in tallgrass prairie from bison and cattle grazing. *Ecological Applications* 15(15), 1550-1559. https://doi.org/10.1890/04-1958

Trimble, S.W., 1981. Changes in sediment storage in the Coon Creek basin, Driftless Area, Wisconsin, 1853 to 1975. *Science* 214(4517), 181-183. https://doi.org/10.1126/science.214.4517.181

Turner, Monica G., Chapin III, F.S., 2005. Causes and Consequences of Spatial Heterogeneity in Ecosystem Function, in: Lovett, G.M., Turner, M.G., Jones, C.G., Weathers, K.C. (Eds.), *Ecosystem Function in Heterogeneous Landscapes*. Springer Science + Business Media, Inc., New York, pp. 9–30. https://doi.org/10.1007/0-387-24091-8_2

U.S. Environmental Protection Agency (EPA), 2013. Level III Ecoregions of the Conterminous United States shapefile.

U.S. Geological Survey (USGS), 2022a. StreamStats, ver 4.10.1. https://streamstats.usgs.gov/ss/

U.S. Geological Survey, 2021 (USGS). StreamStats, ver 4.6.2. https://streamstats.usgs.gov/ss/

U.S. Geological Survey (USGS), 2020. The National Map Download Client. https://apps.nationalmap.gov/downloader/

U.S. Geological Survey (USGS). 2022b. USGS NED 1/3 arc-second n40w107 1 x 1 degree IMG 2022.

U.S. Geological Survey (USGS), 2019. USGS NED 1/3 arc-second n37w097 1 x 1 degree IMG 2019.

U.S. Geological Survey (USGS), 2018. USGS NED 1/3 arc-second n40w105 1 x 1 degree IMG 2018.

van Coller, A.L., Rogers, K.H., Heritage, G.L., 2000. Riparian vegetation-environment relationships: complimentarity of gradients versus patch hierarchy approaches. *Journal of Vegetation Science* 11(3), 337–350. https://doi.org/10.2307/3236626

Walford, G.M., Baker, W.L., 1995. Classification of the Riparian Vegetation Along a 6-km Reach of the Animas River, Southwestern Colorado. *The Great Basin Naturalist* 55(4), 287–303.

Ward, J.V., Tockner K., Schiemer, F. 1999. Biodiversity of floodplain river ecosystems: ecotones and connectivity. *Regulated Rivers: Research and Management* 15(1-3), 125-139. https://doi.org/10.1002/(SICI)1099-1646(199901/06)15:1/3<125::AID-RRR523>3.0.CO;2-E

Ward, J. V., Malard, F., Tockner, K., 2002. Landscape ecology: A framework for integrating pattern and process in river corridors. *Landscape Ecology* 17, 35–45. https://doi.org/10.1023/A:1015277626224

Werner, B.T., McNamara, D.E. 2007. Dynamics of coupled human-landscape systems. *Geomorphology* 91(3-4), 393-407. https://doi.org/10.1016/j.geomorph.2007.04.020

Westbrook, C.J., Cooper, D.J., Baker, B.W., 2011. Beaver assisted river valley formation. *River Research and Applications* 27(2), 247–256. https://doi.org/10.1002/rra.1359

Wiens, J.A., 2002. Riverine landscapes: Taking landscape ecology into the water. *Freshwater Biology* 47(4), 501–515. https://doi.org/10.1046/j.1365-2427.2002.00887.x

With, K.A. 2019. *Essentials of Landscape Ecology*. Oxford University Press: Oxford.

Wohl, E., 2021. An Integrative Conceptualization of Floodplain Storage. *Reviews of Geophysics* 59(2), e2020RG000724. https://doi.org/10.1029/2020rg000724

Wohl, E., 2016. Spatial heterogeneity as a component of river geomorphic complexity. *Progress in Physical Geography: Earth and Environment* 40(4), 598–615. https://doi.org/10.1177/0309133316658615

Wohl, E., 2017. Connectivity in rivers. *Progress in Physical Geography: Earth and Environment* 41(3), 345-362. https://doi.org/10.1177/0309133317714972

Wohl, E., Mersel, M.K., Allen, A.O., Fritz, K.M., Kichefski, S.L., Lichvar, R.W., Nadeau, T.L., Topping, B.J., Trier, P.H., Vanderbilt, F.B. 2016. Synthesizing the scientific foundation for ordinary high water mark delineation in fluvial systems. US Army Corps of Engineers Engineer Research and Development Center, ERDC/CRREL SR-16-5, Washington, DC.

Wohl, E., Brierley, G., Cadol, D., Coulthard, T.J., Covino, T., Fryirs, K.A., et al., 2019. Connectivity as an emergent property of geomorphic systems. *Earth Surface Processes and Landforms* 44(1), 4-26. https://doi.org/10.1002/esp.4434

Wohl, E., Castro, J., Cluer, B., Merritts, D., Powers, P., Staab, B., Thorne, C., 2021. Rediscovering, Reevaluating, and Restoring Lost River-Wetland Corridors. *Frontiers in Earth Science* 9. https://doi.org/10.3389/feart.2021.653623

Wohl, E., Iskin, E., 2019. Patterns of Floodplain Spatial Heterogeneity in the Southern Rockies, USA. *Geophysical Research Letters* 46(11), 5864–5870. https://doi.org/10.1029/2019GL083140

Wohl, E., Lininger, K.B., Scott, D.N., 2018. River beads as a conceptual framework for building carbon storage and resilience to extreme climate events into river management. *Biogeochemistry* 141, 365–383. https://doi.org/10.1007/s10533-017-0397-7

Wohl, E., Knox, R., 2022. A first-order approximation of floodplain soil organic carbon stocks in a river network: The South Platte River, Colorado, USA as a case study. *Science of the Total Environment* 852, 158507. https://doi.org/10.1016/j.scitotenv.2022.158507

Zeug, S.C., Winemiller, K.O., 2008. Relationships between hydrology, spatial heterogeneity, and fish recruitment dynamics in a temperate floodplain river. *River Research and Applications* 24(1), 90–102. https://doi.org/10.1002/rra.1061

3. CH 3: DETAIL & DIFFERENTIATION[2]

Summary

Spatial heterogeneity of floodplains is pervasive across floodplain form and affects associated floodplain functions. Natural floodplains and their functions are disappearing due primarily to human activities in river corridors. Quantification of heterogeneity at floodplains is needed to establish natural variability and inform floodplain restoration. I expanded on a previous unsupervised classification workflow that combines field data, remote sensing, and landscape ecology for three rivers in the U.S. Pacific Northwest and one river in the southeastern U.S. to conduct a sensitivity analysis on the spatial and spectral resolution of the data used. The results indicate that natural floodplains in the Pacific Northwest and coastal Southeast have moderate to high evenness, moderate to high intermixing, and moderate aggregation; and similar aggregation and evenness as rivers in Colorado and Oklahoma, U.S., but lower intermixing. I attribute lower intermixing at the Altamaha River, Georgia to slower rates of lateral channel migration, and lower intermixing at the Hoh River to the different hydrologic and sediment regimes and less stable braided planform. The results show that the larger rivers (arbitrarily floodplain area > 50 ha) in this study (Altamaha, Hoh, and Sol Duc Rivers) have similar spatial heterogeneity as beaver-modified and shortgrass prairie rivers in Colorado, while the more inland and smaller river (Lookout Creek) has similar spatial heterogeneity to the tallgrass prairie site (Sand Creek). From the results of the sensitivity analysis, I suggest using the highest spatial resolution topographic data available, using aerial imagery/mosaics from the same sensor, and

---

[2]Submitted as Iskin and Wohl, In Review. Sensitivity Analysis of Spatial and Spectral Resolution in Quantifying Floodplain Heterogeneity, *Journal of Hydrology*.

removing largest patch index from the suite of comparable indices. I find that field classifications, relative topography, and normalized difference vegetation index (NDVI) are useful for interpreting results from the unsupervised classification workflow. The metrics show that there are similarities and differences between rivers in Washington, Oregon, Colorado, Oklahoma, and Georgia, and that discernable trends may arise from a meta study comparing heterogeneity from more rivers across the country.

3.1 Introduction

Nearly every aspect of a floodplain – surface and subsurface water storage and movement; sediment grain-size distribution and associated porosity and permeability; soil chemistry; topography; vegetation communities; large wood abundance and distribution; microclimates; and channel migration – exhibit distinct levels of heterogeneity, and interactions among them influence floodplain functions (Appling et al., 2014; Harms et al., 2009; Naiman et al., 2005). With the disappearance of naturally functioning floodplains, managed river corridors have lower spatial heterogeneity and functionality (Kuiper et al., 2014; Samaritani et al., 2011; Schindler et al., 2016; Wohl and Iskin, 2019) and regulated river channels have lower channel spatial heterogeneity (Graf, 2006). We urgently need to quantitatively analyze spatial heterogeneity of natural floodplains to determine whether characteristic levels or types of heterogeneity are present in relation to potential controls such as flow, sediment regime, or biome. This more detailed understanding can then be used to inform future river corridor restoration.

My overriding research goal is to quantify natural floodplain heterogeneity in diverse river corridors. In this context, I define natural floodplains as occurring along rivers with minimal flow regulation, channel engineering, and contemporary or historical land cover

alterations in the floodplain. I first review the studies that provide the basis for the work presented here and then discuss the objectives of this paper.

3.1.1 Previous Work

This study builds on my previous analyses of floodplain heterogeneity. Wohl and Iskin (2019) calculate a simple measure of floodplain heterogeneity by dividing the number of patches along a transect by the transect length for a number of sites. They find that unmanaged floodplains have greater heterogeneity than managed floodplains (Wohl and Iskin, 2019). Iskin and Wohl (2023) expand their methods by focusing on a subset of four sites, develop a remote sensing and classification workflow, and calculate a suite of heterogeneity metrics from landscape ecology. This suite, chosen to maximize comparability between sites, consists of aggregation index (aggregation of classes), interspersion and juxtaposition index (patch/class intermixing, pairing of one class with another), largest patch index (simple dominance of largest patch), patch density (simple fragmentation), percentage of like adjacencies (within class aggregation – are cells of a class next to cells of the same class), and Shannon's evenness index (class dominance, normalized diversity) (Hesselbarth et al., 2021; With, 2019). These six indicators show intermetric (differences in spatial heterogeneity between the floodplains) and intrametric (differences in the patterns of the metrics) variation for four floodplains (Iskin and Wohl, 2023). Their results indicate that natural floodplains have high evenness and interspersion and juxtaposition of classes, and that a suite of six metrics distinguish between floodplains in Colorado and Oklahoma along small to moderate prairie rivers and a site modified by beaver (*Castor canadensis*). Iskin and Wohl (2023) attribute the differences in heterogeneity metrics to differences in fluvial processes.

In this study, I expand on the results of Iskin and Wohl (2023) by using the same methods to conduct a sensitivity analysis at four new sites and increasing the detail of the datasets with ≤ 3 m topography, 10-band Sentinel imagery, and vegetation band indices. Others have shown that the addition of ancillary data can improve the performance of classification schema (le Hégarat-Mascle et al., 1997; Lu and Weng, 2007). The addition of more detailed data allows me to examine how the values of the heterogeneity metrics change with increased spatial and spectral resolution, and to geomorphically and ecologically interpret the resulting classes from the unsupervised classification.

3.1.2 Objectives

By repeating the workflow from Iskin and Wohl (2023) at four new sites, I am able to compare results across diverse regions within the contiguous United States. My objectives are to i) conduct a sensitivity analysis to determine whether and how the values of the six heterogeneity metrics used in the earlier analysis change when I increase spatial (≤ 3 m lidar topography) and spectral resolution (10-band imagery) of the input data, and ii) extract the underlying data from the classification results and determine whether using higher resolution data allows identification of the resulting unsupervised classes in relation to relative topography, soil texture, and vegetation health and moisture content. This analysis concludes with comparing fluvial spatial heterogeneity across the United States from the Colorado and Oklahoma sites from Iskin and Wohl (2023) and the Washington, Oregon, and Georgia sites in this study.

3.2 Study Area

This study focuses on natural floodplains in the Pacific Northwest region of the United States (Lookout Creek in Oregon, and the Sol Duc and Hoh Rivers in Washington) and the

Altamaha River of the Southeastern region in coastal Georgia (Figure 3.1). Supplemental Table

3.1 provides background information on the study regions, drainage basins, and study reaches.
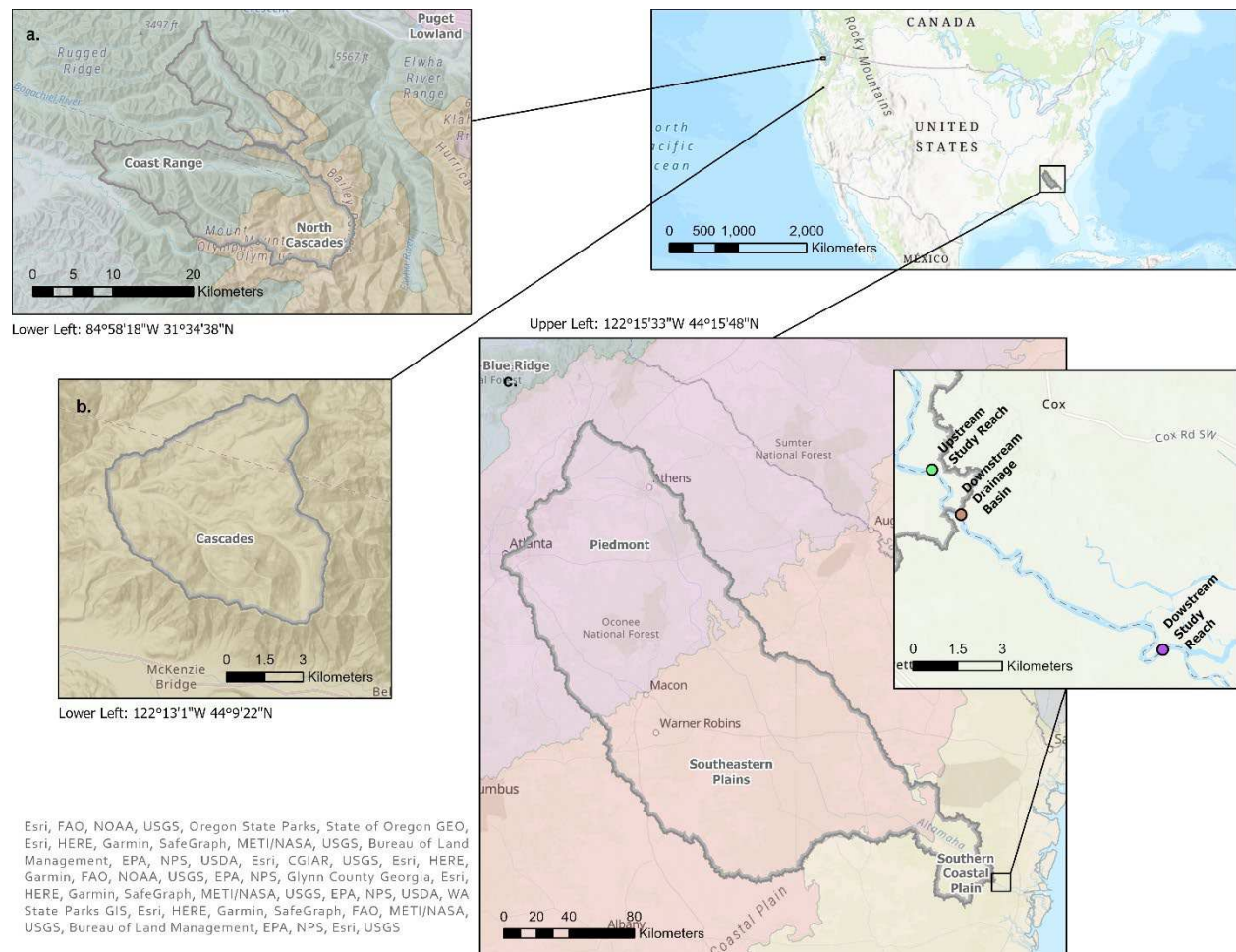
Figure 3.1. Location map of field sites: a) Sol Duc River (top) and Hoh River (bottom), Washington (flow direction is west) and b) Lookout Creek, Oregon (flow direction is southwest), and c) Altamaha River, Georgia (flow direction is southeast). Map shows the drainage area boundaries upstream of the downstream-most point of each study reach. The drainage basin for the Altamaha River includes 2.4 km of the study reach and excludes 11.2 km of the study reach (downstream) due to limitations in StreamStats and proximity to coastline (shown in the callout). Level III Ecoregions are labeled. Drainage area shapefiles delineated and downloaded from USGS StreamStats in November 2022 (USGS, 2022c) and January 2023 (USGS, 2023a), and ecoregion shapefiles downloaded from the Environmental Protection Agency in December 2021 (EPA, 2013).

3.3 Methods

Data were collected through a combination of field measurements and compiling of

remote imagery. Although field data is not required for the implementation of the workflow

(Iskin and Wohl, 2023), it is useful for ground truthing patches and interpreting the unsupervised

classification. Floodplain patches and classes were mapped in the field using the same techniques

as Iskin and Wohl (2023). I differentiated 10 classes at the Sol Duc River in July 2021, 13 at the

Hoh River in July 2021, and 13 at Lookout Creek in July 2022, all after peak spring flows. I

differentiated 7 classes at the Altamaha River in October 2021 during unexpected high flows.

Because of this, the Altamaha River study reach boundaries were chosen during data analysis as

between a bounding road on the upstream end and just above a distributary section on the

downstream end. Qualitative field descriptions of the class types are provided in Table 3.1.

Table 3.1. Field class descriptions.

River	Class No.	Description
Altamaha River, GA	0	Standing water with a little current, trees, some shrubs
	1	Small to 60 cm DBH conifers and deciduous trees, some undergrowth, but not dense; prolific leaf litter, bamboo, sparse palmettos, some vines. Sandy soil, pine needles, undulating topography with linear features
	2	Inundated, more palmetto, small to 60 cm DBH deciduous trees, no conifers in water, loam, silt, clay
	3	0.5 m vertical features, abundant palmettos, bamboo/small to 80 cm DBH trees, looks like wet recently (dark leaves and duff), linear features, viny, moss, no pine needles
	4	Similar to Class 3, but denser undergrowth, holly, palmettos, pine needles, same linear features as Class 3, bamboo
	5	Dry, pine needles, sandy, dense undergrowth, large palmettos, woody shrubs, a lot of conifers, 10–50 cm DBH, maples
	6	Small dense trees, interspersed old growth/large trees, dense leaf duff and pine needles, shrubs with big waxy leaves
Hoh River, WA	1	3 m high sediment deposit, fine sand to large cobbles, some bushy vegetation and dried grasses, old braid surface
	2	≤ to 10 cm DBH alders closely spaced, viny groundcover and moist soil
	3	40 cm DBH alders, 40–120 cm DBH conifers, bracken fern, abundant low groundcover, natural levee surface
	4	Undulating topo, 20–40 cm DBH alders, abundant bracken fern
	5	Waist high grasses, dry surface, drained abandoned channel?
	6	Horsetails, grasses, reeds, wetland
	7	Fine sand, < 10 year old willows and alders, marginal logjam in river, 1 m above water level HWMs, fluvially deposited, unconsolidated
	8	Snags and downed wood, 60–200 cm DBH, bracken fern, deer fern, alders and conifers, young maples, ground topo dominated by root wads and their holes
	9	Overgrown channel with running water, horsetails, downed wood, small maple
	10	0.5 m deep and 4 m wide side channel, bracken fern, no water or mud
	11	20–60 cm DBH maples, abundant grass cover, bracken fern interspersed in grasses, undulating topo
	12	Up to 30 cm DBH alders, viny groundcover, between 2 side channels
	13	Muddy/silty overflow surface, on the channel side of a 1 m high cutbank (in the river), beaver chew

Sol Duc River, WA	1	Fluvial surface, 2–3 m above water surface, covered with moss, ferns, widely spaced conifers, 30–250 cm DBH, bracken ferns, abundant downed wood, undulating topo under 1 m
	2	Sloping moss covered surface, closely spaced conifers, 6–15 cm DBH, small cobbles to boulders, some HWMs, terrace?
	3	Active channel
	4	Shallower slope than Class 2 from water level, small cobbles to boulders, <10 cm DBH alders, maples?, large leafy ground cover, maple up to 10 cm DBH, bracken ferns
	5	Overflow channel, evidence of recent competent flow, sparse moss on rocks, unconsolidated sediment, sand to large cobbles
	6	Off transect wetland/abandoned beaver pond: abundant vegetation, fern, large leafy ground cover, nurse logs, 20 cm DBH alders, sedges and rushes, side channel with flow in it, hellebore
	7	Ferns, devil's club, overgrown side channel, 0.5 m lower than previous patch, hellebore
	8	Small–40 cm DBH abundant maples, abundant bracken ferns, nurse logs, small–30 cm DBH conifers, cobbles and boulders hiding under duff, undulating topo/linear features
	9	Abandoned side channel, overgrown ferns/grasses/maples, maple saplings, sand to cobble sized clasts
	10	3+ distinct channels, 20 cm DBH conifers, 40 cm DBH maples, 10–30 cm DBH alders, bracken fern, abundant groundcover including grasses, overflow surface including 2+ distinct channels, channels are ≤ to 1 m wide and have small cobbles to large boulders, log jam present
Lookout Creek, OR	1	Active channel, ~2 m below Class 2, cobbles to boulders
	2	Debris flow/boulder bar, large gravel to boulder size clasts visible in bank cut, dense young veg, fir trees, viny maple, sword ferns, cedars, 2–20 cm DBH alders, beaver chew
	3	Backwater channel behind berm, multiple fern types, 3 m below top of Class 2, young viny maple, 8–30 cm DBH alder, standing water, sediment and coarse particulate organic matter build up, large nurse logs
	4	Backwater channel, 0.5 m above Class 3, abundant fern, abundant horsetail, deciduous plants, 10–30 cm DBH maple, undulating topo, gravel bars
	5	Abundant clover, downed wood, spaced out sword ferns, 10–100 cm DBH cedars/maple/fir
	6	Grassy side channel, 3 m wide, dry
	7	Cobble to boulder bar, mossy, dry, lower edges have dense viny maple, creek edge has dense willow
	8	Active side channel, 1.5 m wide, sand to boulders, leafy ground cover on banks, grassy banks, 1 m HWMs
	9	Overgrown side channel, thick layer of duff, 20–40 cm DBH fir and maple, clover
	10	Overflow cobble bank, dense willow, gentle slope from water surface, 50 cm HWMs
	11	Sandy riverbank between active channel and mossy terrace, 25 cm HWMs
	12	Overgrown surface, 5–15 cm DBH alder, groundcover, no flow (?)
	13	Active anastomosing island, beaver chew, very dense veg with willow, boulders underfoot, small side channels, viny maple

Note: DBH stands for diameter at breast height, measured mostly by eye. Species identification was not exact and not field guide was used.

Hand-driven soil cores were collected at each floodplain along the preestablished

transects. Two cores per class were collected at three approximate depths where possible (0–30,

30–60, and 60–90 cm). In some cases, I could not physically core to the full 90 cm depth because

of resistant layers such as cobbles and boulders. Core location, depth, and relative moisture (dry, moist, saturated) were noted in the field. Soil cores were subsequently sent to Ward Laboratories, Inc. for soil texture analysis. For the Hoh River, 48 of 52 soil samples were suitable for lab analysis (Figure 3.2a), 24 of 25 submitted samples were suitable for analysis for the Sol Duc River (Figure 3.2b), and 19 of 36 soil samples were suitable for analysis for Lookout Creek (Figure 3.2c). No soil cores were collected at the Altamaha River due to flooded conditions and air-travel restrictions for transporting soil. The soil data are used to interpret the resulting classes in Section 4.2.
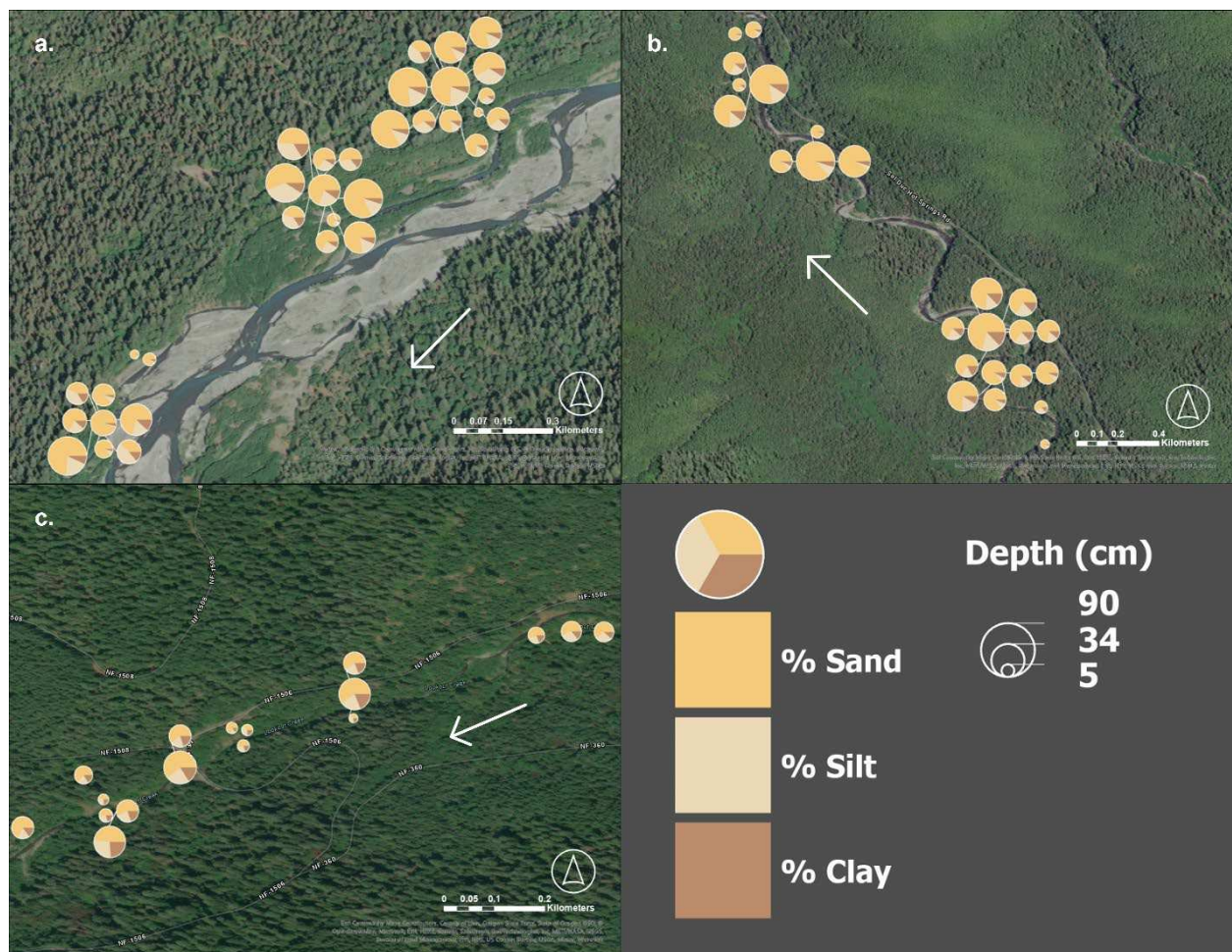
Figure 3.2. Fractional soil components for the a) Hoh River, Washington, b) Sol Duc River, Washington, and c) Lookout Creek, Oregon. Pie chart colors indicate soil components and size indicates core depth below the surface. White arrows indicate flow direction.

51

3.3.1 Objective I Analysis

This analysis is conducted in two parts for the four natural floodplains (Figure 3.3): (1) repeat the workflow developed by Iskin and Wohl (2023) (Classification 1) and (2) repeat the workflow with additional datasets to evaluate how the results compare (Classification 2). Data sets used are provided in Table 3.2.
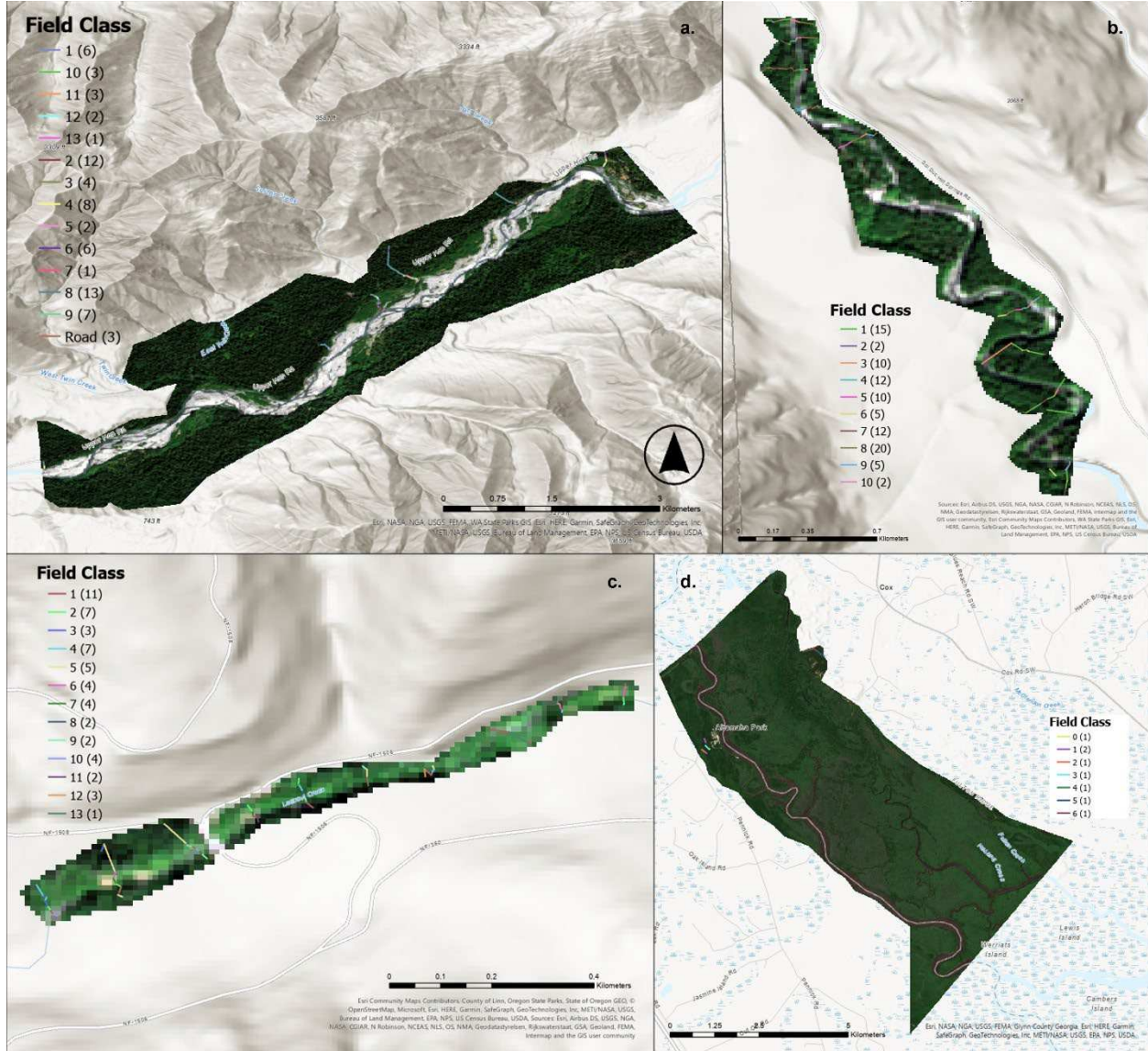
Figure 3.3. Sentinel-2A mosaics clipped to buffered floodplain boundaries and field classes and (counts) for a) Hoh River, Washington, b) Sol Duc River, Washington, c) Lookout Creek, Oregon, and d) Altamaha River, Georgia. Floodplain boundaries delineated based on field observation and data (transect, large wood, and sediment core locations), Sentinel remote satellite imagery, and elevation datasets.

Table 3.2. Data collected and used in this analysis.

Data	Details	Instrument	Resolution	Program Used	References
GPS Locations	Patch boundaries, large wood, and sediment cores	Garmin GPSMAP 66ST	± 3 m	-	-
Watershed Characteristics	Upstream drainage basin shapefiles and associated mean values, downloaded 11/2022 (HWA, SDWA, LOR) and 1/2023 (AGA)	-	Drainage basin scale	StreamStats	USGS, 2022c, 2023a
Digital Elevation Models	Tile N48W124 5/5/2022 (HWA, SDWA) Tile N48W125 1/9/2020 (HWA, SDWA) Tile N49W124 1/9/2020 (HWA, SDWA) Tile N45W123 4/26/2022 (LOR) Tile N32W082 7/25/2022 (AGA)	Airborne Lidar	1/3 arc-second 1 x 1 degree 10 m	The National Map	Open Topography, 2021; USGS, 2023b
High-Resolution Digital Terrain Models*	Hoh River 2013 DEM 4, 5 Sol Duc River 2014 DEM 47, 57 McKenzie River 2016 DEM mosaic Not available for AGA	Airborne Lidar	0.91 m (HWA and LOR) 3 m (SDWA) 32-bit radiometric	WA DNR Lidar Portal and The National Map	Allison and Martinez, 2013; Division of Geology and Earth Resources, 2022; Gleason and McWethy, 2014; USGS, 2016
Cloud-free Mosaics*	GEE Image Collection "COPERNICUS/S2_SR" 2% cloudy mean pixels from 5/1/2022-9/30/2022 (HWA, SDWA, LOR) 0.5% cloudy mean pixels from 4/1/2022-9/30/2022 (AGA)	Copernicus Sentinel-2A	10 m: Bands 2, 3, 4, 8 20 m: Bands 5, 6, 7, 8a, 11, 12 12-bit radiometric 5-day temporal	Google Earth Engine	ESA, 2021; Google Developers, 2022; Gorelick et al., 2017; Sabins Jr. and Ellis, 2020
Soil Data*	Soil texture data provided in % sand, % silt, and % clay (HWA, SDWA, LOR) Not available for AGA	JMC Soil Samplers 15 in Wet Sampling Tube (2.2 cm diameter)	± 3 m horizontal (GPS) ~30 cm maximum vertical (corer size)	-	-
*Note: The cloudy percentage was decreased for the Altamaha River due to increased cloud cover in the Southeast, and the date range was expanded by one month to account for the lower cloudy percentage. No high-resolution elevation data was available for the Altamaha River, so USGS 3DEP data was used in Classification 2, and no soil cores were collected.					
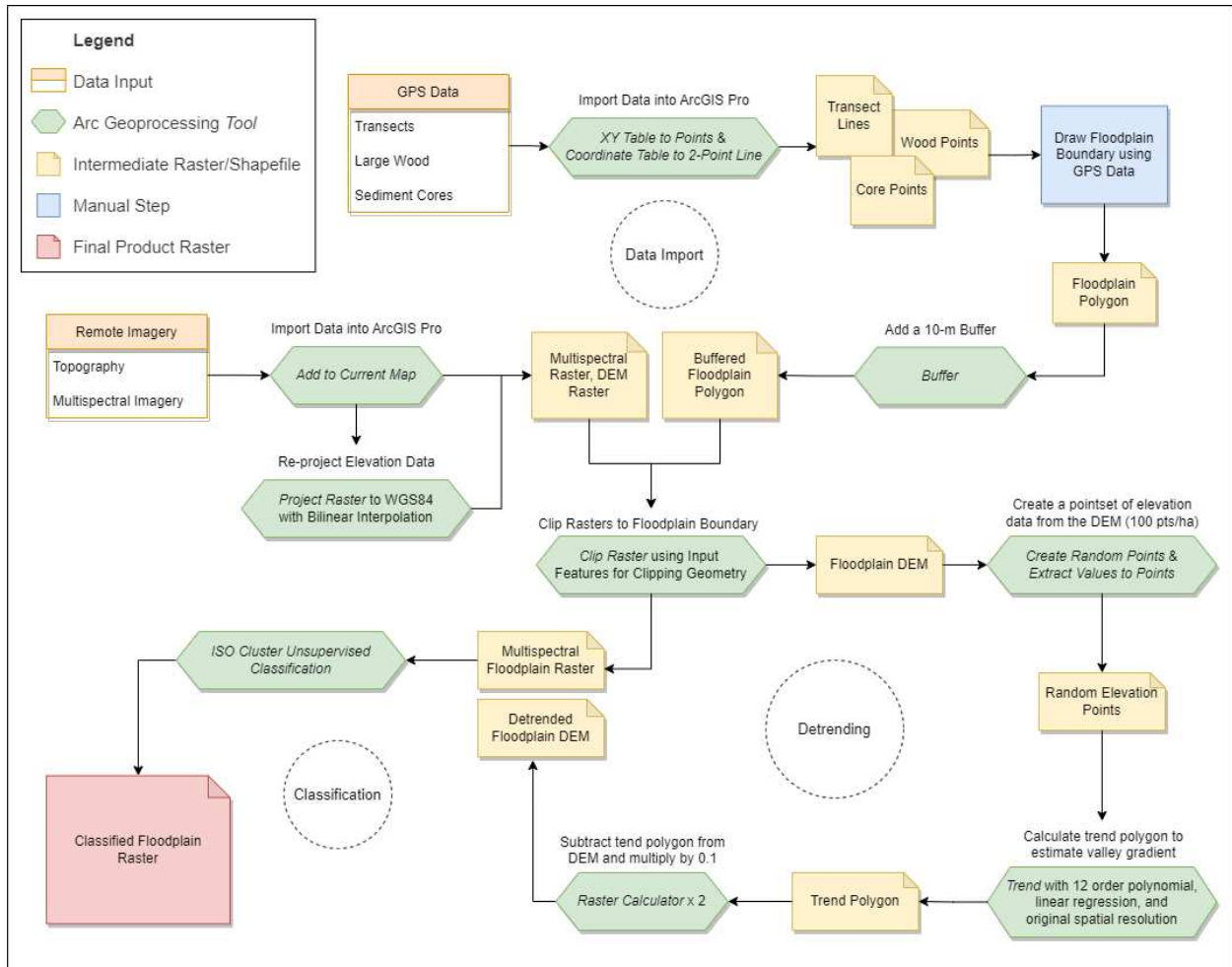
Figure 3.4. Flow chart of classification workflow completed in ArcGIS Pro (Esri, 2023) from Iskin and Wohl (2023). Input data are shown in orange, specific ArcGIS tools in italicized green (specific options non-italicized), intermediate shapefiles and rasters in yellow, manual drawing step in blue, and final raster product in red.

Classification 1 repeats the methods from Iskin and Wohl (2023) for the Altamaha River, Hoh River, Sol Duc River, and Lookout Creek (Figure 3.4). Data used are the 10 m DEMs (mosaicked for the Hoh and Sol Duc Rivers due to overlapping tiles) and 4-band Sentinel mosaics (RGB and IR, created using the *Make Raster Layer* tool) (Table 3.2). Classification 2 repeats the methods from Iskin and Wohl (2023) for the same four sites, but with different input data. Data used are the ≤ 3 m DEMs where available, 10-band Sentinel mosaics (all 10 and 20 m bands available, created using the *Make Raster Layer* tool) (Table 3.3), and two band ratio rasters: normalized difference vegetation index (NDVI) and normalized difference moisture

index (NDMI) (Table 3.4). Lidar tiles for the Hoh and Sol Duc Rivers (Table 3.2) were

mosaicked separately due to the difference in spatial resolution using the *Mosaic to New Raster*

tool before clipping to the respective floodplain boundaries. High-resolution DEMs were

detrended using the same methods as for Classification 1 but with higher spatial resolution. The

band ratio rasters were made by using the *Indices* tool from the ArcGIS Pro Imagery tab (Table

3.4). Separate rasters were created for each index by indicating which bands in the multispectral

image corresponded to the bands needed in the ratio formulas (near infrared and red for NDVI,

and near infrared and short-wave infrared for NDMI) (GISGeography, 2022b).

Table 3.3. Sentiel-2A bands used in this analysis (Google Developers, 2022).

Band	Description	Spatial Resolution (m)	Wavelength (nm)
2	Blue	10	496.6
3	Green	10	560
4	Red	10	664.5
5	Red Edge 1	20	703.9
6	Red Edge 2	20	740.2
7	Red Edge 3	20	782.5
8	Near Infrared	10	835.1
8a	Red Edge 4	20	864.8
11	Shortwave Infrared 1	20	1613.7
12	Shortwave Infrared 2	20	2202.4

Table 3.4. Data layers created from the cloud-free mosaics using ArcGIS Pro.

Data	Band Ratio	Spatial Resolution	Interpretation	References
NDVI	$\dfrac{B8 - B4}{B8 + B4}$	10 m	Range [-1, 1], indicator of vegetation greenness, health, and/or density; higher values indicate healthier/greener/denser vegetation	EOS Data Analytics, 2019; GISGeography, 2022a, 2022b; Google Developers, 2022; USGS, 2018, 2022a, 2022b
NDMI	$\dfrac{B8a - B11}{B8a + B11}$	20 m	Range [-1, 1], indicator of vegetation moisture content; higher values indicate vegetation with more water	

The *ISO Cluster Unsupervised Classification* ArcGIS Pro tool was run using a minimum

class size of four pixels and sample interval of two pixels for both classifications and all rivers.

The maximum number of classes to find was set to 30 for the large Altamaha and Hoh Rivers, 20 for the mid-sized Sol Duc River, and 10 for the small Lookout Creek for both classifications. This was done to balance the tool finding more classes than I saw in the field without causing the tool to find too few classes. To demonstrate for Classification 1, when the maximum number of classes for Lookout Creek is set to 20, the tool finds 1 class, but when it is set to 10, it finds 10 classes. The tool seems to differentiate fewer classes if the maximum number of classes is set too high. The suite of six heterogeneity metrics – aggregation index, interspersion and juxtaposition index, largest patch index, patch density, percentage of like adjacencies, and Shannon's evenness index – from Iskin and Wohl (2023) were calculated in R (R Core Team, 2023) for the four floodplains with the results from Classifications 1 and 2. Resulting metrics were compared qualitatively using the same high-moderate-low scale from Iskin and Wohl (2023). Classified rasters were projected to the appropriate UTM zone using a cell size of 10 m (*Project Raster* tool) and exported for analysis in R (*Copy Raster* tool).

3.3.2 Objective II Analysis

To interpret the classes from the unsupervised method for Classification 2, detrended-flattened elevation, NDVI, NDMI, and ISO Class values were extracted from the rasters to random points using the *Extract Multi Values to Points* tool (the same random points used to detrend the elevation data that have a point density of 100 pts/ha). The elevation data were "un-flattened" by dividing the values by 0.1 so that they were more representative of real elevations and therefore more interpretable. Field data were incorporated by joining the Field Class and soil core features with the extracted point data using the *Spatial Join* tool with the "One to Many" option selected, within geodesic distance specified, and not keeping all target features. Field Class was joined to the random points if they were within 3 m and cores were joined if they were

within 10 m. A greater distance was used for the core data because there were fewer core data than Field Class data. This process creates a few extracted/joined tables for each site, and those were exported to Excel for analysis. Pivot tables were used to calculate the average detrended elevation, NDVI, and NDMI for each ISO Class for each river. The nearest Field Class and soil core data were compared manually to the ISO Classes because one ISO Class point might be within 3 m of more than one Field Class line and/or within 10 m of more than one soil core point. ISO Classes were then interpreted based on elevation, NDVI, nearest field classes, nearest soil textures and moistures, and visual inspection in ArcGIS Pro and Google Earth.

3.4 Results

I present the results of Classification 1 and 2, the heterogeneity metric values, comparisons of the classifications and metrics, and identify the classes based on field and Classification 2 data.

3.4.1   Objective I Results

Resulting rasters from Classification 1 and 2 for all field sites are shown in Figure 3.5 and Figure 3.6, respectively. Visual inspection shows that the results from Classification 2 seem more detailed than those from Classification 1.
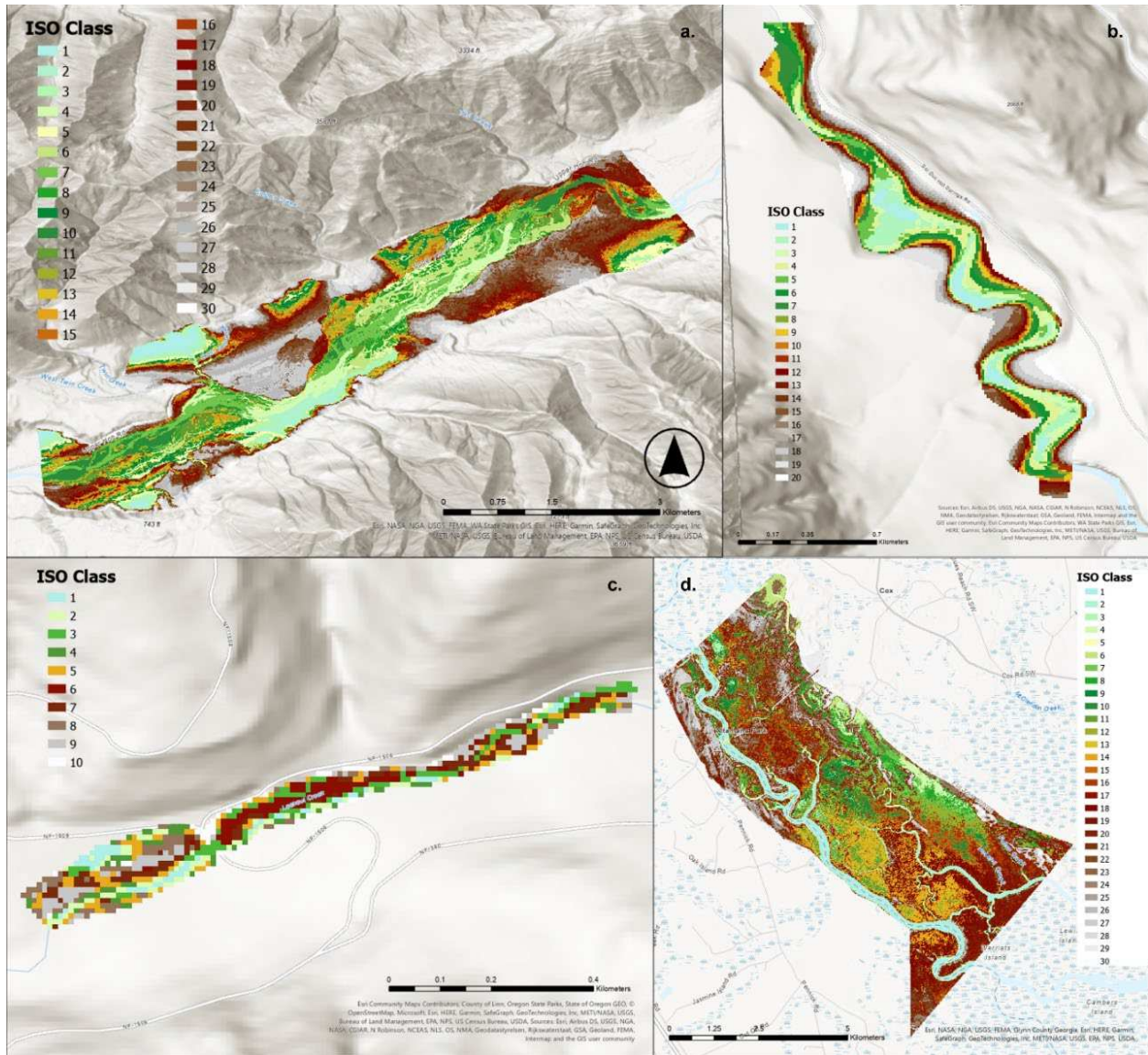
Figure 3.5. ISO cluster unsupervised classifications for a) Hoh River, Washington, b) Sol Duc River, Washington, c) Lookout Creek, Oregon, and d) Altamaha River, Georgia. The classification was completed using 4-band Sentinel-2A imagery and detrended, flattened DEMs. ISO Class numbers are separate from Field Class numbers.

58
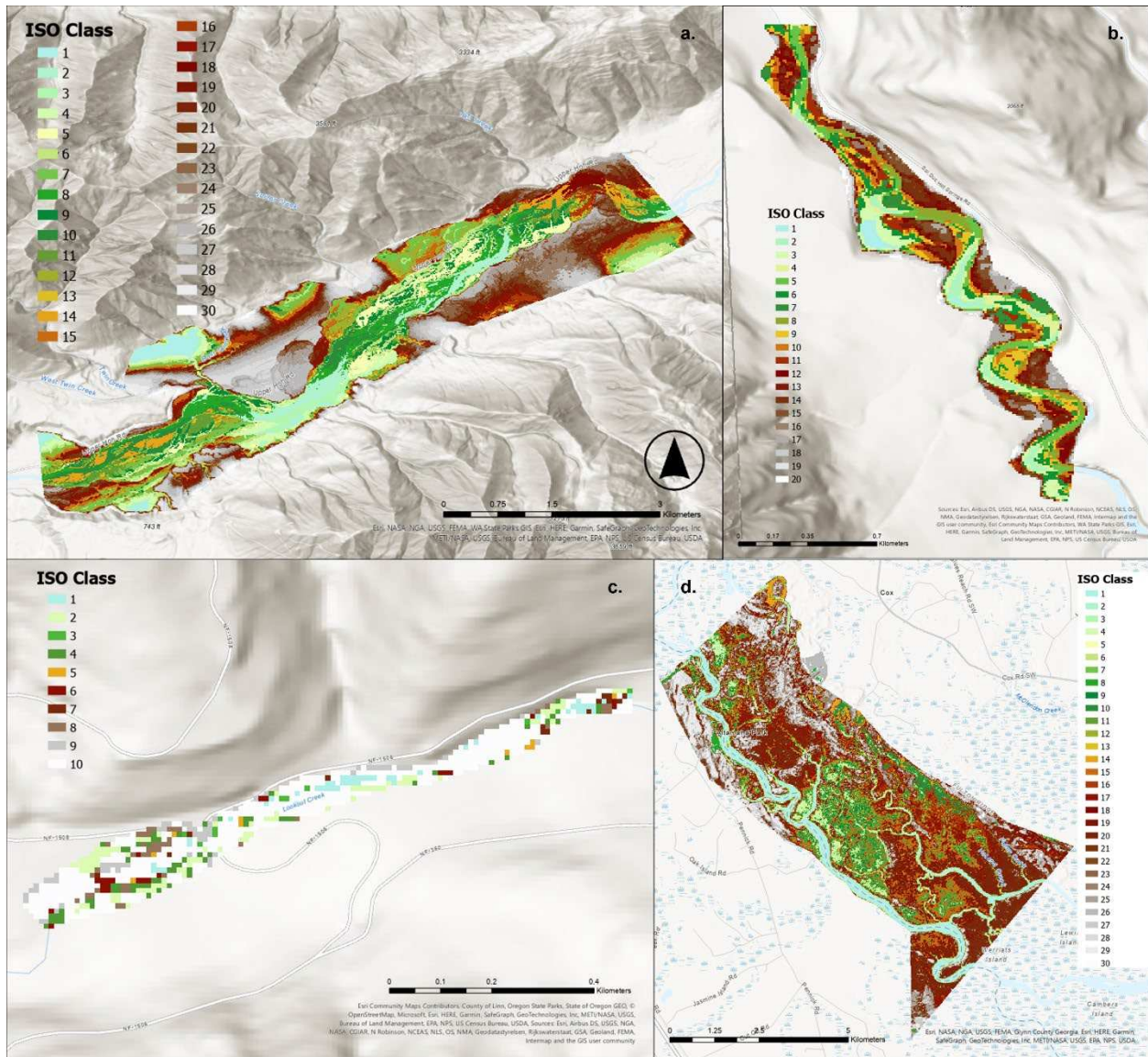
Figure 3.6. ISO cluster unsupervised classifications for a) Hoh River, Washington, b) Sol Duc River, Washington, c) Lookout Creek, Oregon, and d) Altamaha River, Georgia. The classification was completed using 10-band Sentinel-2A imagery, detrended, flattened high resolution lidar where available, NDVI, and NDMI. ISO Class numbers are separate from Field Class numbers.

The heterogeneity metrics calculated for the four rivers for both classifications are given in Table 3.5 and visualized in Figure 3.7. Percent difference was calculated between the values using Equation 3.1 and given in the Table 3.6.

Table 3.5. Values of landscape heterogeneity metrics for Classification 1 and 2.

Classification	Metric	Altamaha River	Hoh River	Sol Duc River	Lookout Creek
1	Aggregation Index (%)	56.2	62.3	53.5	39.5
	Interspersion and Juxtaposition Index (%)	73.8	73.8	76.3	88.8
	Largest Patch Index (%)	6.4	1.7	3.3	8.7
	Patch Density (#/100 ha)	1355.2	1043.7	1576.7	2662.7
	Percentage of Like Adjacencies (%)	55.9	61.6	52.2	38.5
	Shannon's Evenness Index	0.946	0.980	0.979	0.982
2	Aggregation Index (%)	58.8	66.0	50.8	57.4
	Interspersion and Juxtaposition Index (%)	73.3	71.6	79.9	74.9
	Largest Patch Index (%)	4.2	1.6	2.0	26.1
	Patch Density (#/100 ha)	1213.0	855.3	1866.4	1697.5
	Percentage of Like Adjacencies (%)	58.5	65.3	49.5	58.6
	Shannon's Evenness Index	0.934	0.973	0.967	0.639
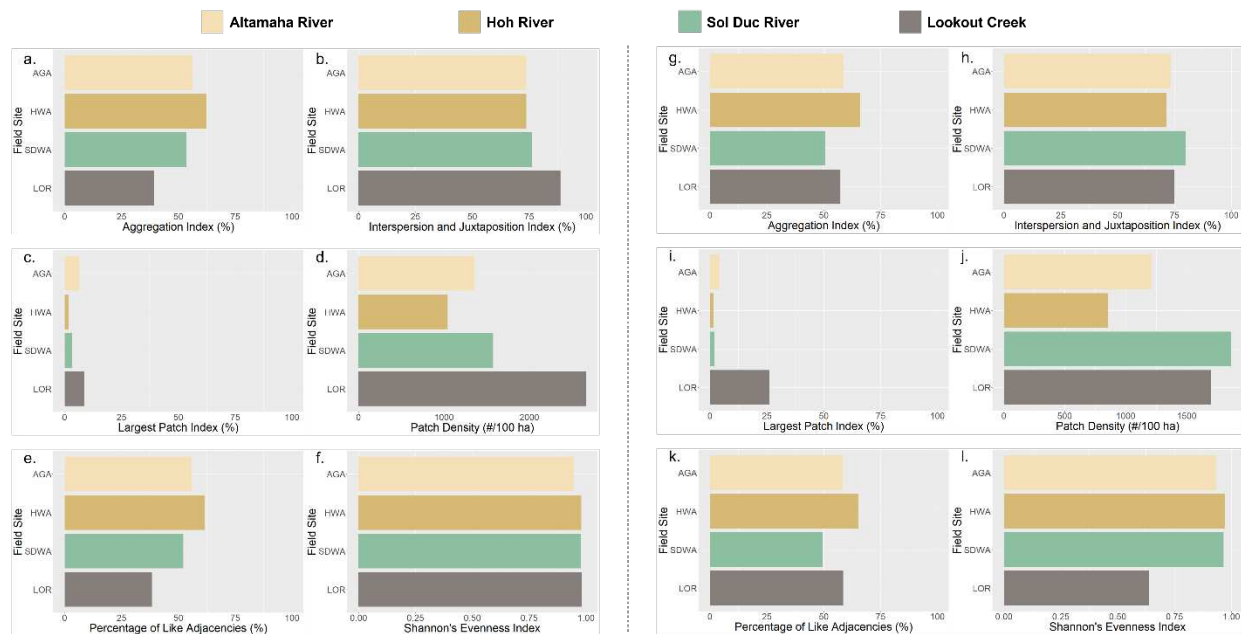
Figure 3.7. Bar plot visualizations of the levels of each metric for each floodplain for Classification 1 (a–f) and Classification 2 (g–l). In descending order of floodplain area, cream bars represent the Altamaha River, Georgia (3705.3), gold bars represent the Hoh River, Washington (987.8 ha), green bars represent the Sol Duc River, Washington (58.1 ha), and grey bars represent Lookout Creek, Oregon (6.9 ha).

I used the same qualitative high-moderate-low scale as Iskin and Wohl (2023), in which high is assigned to metric values in the top 75% of their range, moderate to values in the middle 50% of their range, and low to values in the bottom 25% of their range. All four sites exhibit moderate aggregation (Figure 3.7a,g) and moderate percentage of like adjacencies (Figure 3.7e,k) for both Classifications 1 and 2. The Altamaha, Hoh, and Sol Duc Rivers all exhibit low

largest patch index (Figure 3.7c,i) and high Shannon's evenness (Figure 3.7f,l) for both

classifications. The Hoh and Altamaha Rivers exhibit moderate interspersion and juxtaposition

(Figure 3.7b,h), whereas the Sol Duc River exhibits high interspersion and juxtaposition (Figure

3.7b,h) for both classifications. Lookout Creek exhibits high interspersion and juxtaposition

(Figure 3.7b), low largest patch index (Figure 3.7c), and high Shannon's evenness for

Classification 1 (Figure 3.7f), but moderate interspersion and juxtaposition (Figure 3.7h),

moderate largest patch index (Figure 3.7i), and moderate Shannon's evenness for Classification 2

(Figure 3.7l). Lookout Creek is the only river whose metrics change qualitatively between

Classification 1 and 2, with a decrease from high interspersion and evenness to moderate and an

increase from low to moderate largest patch. Table 3.6 shows the percent difference between

Classification 1 and 2 for each river and each metric (Eq. 3.1). Largest patch index and patch

density have the highest mean and median percent differences of the metrics, whereas

interspersion and juxtaposition has the smallest mean and median percent differences. Lookout

Creek has the highest percent differences for all metrics, whereas the other three rivers have

generally similar and lower percent differences.

$$Percent\ Difference = \left(\frac{|Class\ 1\ Metric - Class\ 2\ Metric|}{\frac{Class\ 1\ Metric + Class\ 2\ Metric}{2}} \right) \times 100 \hfill (3.1)$$

Table 3.6. Percent difference between Classification 1 and 2.

Metric	Altamaha River	Hoh River	Sol Duc River	Lookout Creek	Median	Mean
Aggregation Index (%)	4.5%	5.7%	5.2%	37.0%	5.5%	13.1%
Interspersion and Juxtaposition Index (%)	0.7%	3.1%	4.6%	17.0%	3.8%	6.3%
Largest Patch Index (%)	42.1%	3.6%	49.0%	99.7%	45.5%	48.6%
Patch Density (%)	11%	20%	17%	44%	18.3%	23.0%
Percentage of Like Adjacencies (%)	4.6%	5.7%	5.3%	41.5%	5.5%	14.3%
Shannon's Evenness Index (%)	1.26%	0.75%	1.26%	42.26%	1.3%	11.4%
Note: Colors indicate level of absolute value change, where red is a change of 75%, yellow is a change of 25%, and green is a change of 0%.						

These results indicate that these natural rivers have moderately aggregated classes and moderate aggregation within the classes; moderate to high intermixing; low to moderate dominance of the largest patch; and moderately to highly abundant, evenly distributed classes (Hesselbarth et al., 2021). These results also show that rivers of the Pacific Northwest and Southeast have similar aggregation and evenness as rivers in Colorado and Oklahoma, but lower intermixing (Iskin and Wohl, 2023). They also show that natural rivers on the Olympic Peninsula (Hoh and Sol Duc Rivers) and in the Southeast (Altamaha River) have similar spatial heterogeneity as beaver-modified and shortgrass prairie rivers in Colorado, while the more inland Lookout Creek of Oregon has similar spatial heterogeneity to Sand Creek in the tallgrass prairie of Oklahoma (Iskin and Wohl, 2023).

3.4.2 Objective II Results

Interpreting unsupervised classification results can be difficult without additional knowledge of the study locations. I use both the data from Classification 2 and field data to interpret the results. Extracted class-average detrended and un-flattened elevation, NDVI, NDMI, and nearest soil texture, moisture, and Field Class are given in Supplemental Tables 3.2–5. I started to group ISO Classes that had high positive class-average elevations and used general thresholds and ranges of NDVI values from the U.S. Geological Survey (2018) and visual inspection to further group ISO Classes. Nearest soil textures and moisture and nearest Field Classes were used to validate the groupings and provide geomorphic units and vegetation ages and species types. Figure 3.8 visualizes the lumped ISO Classes from Supplemental Tables 3.2–5.
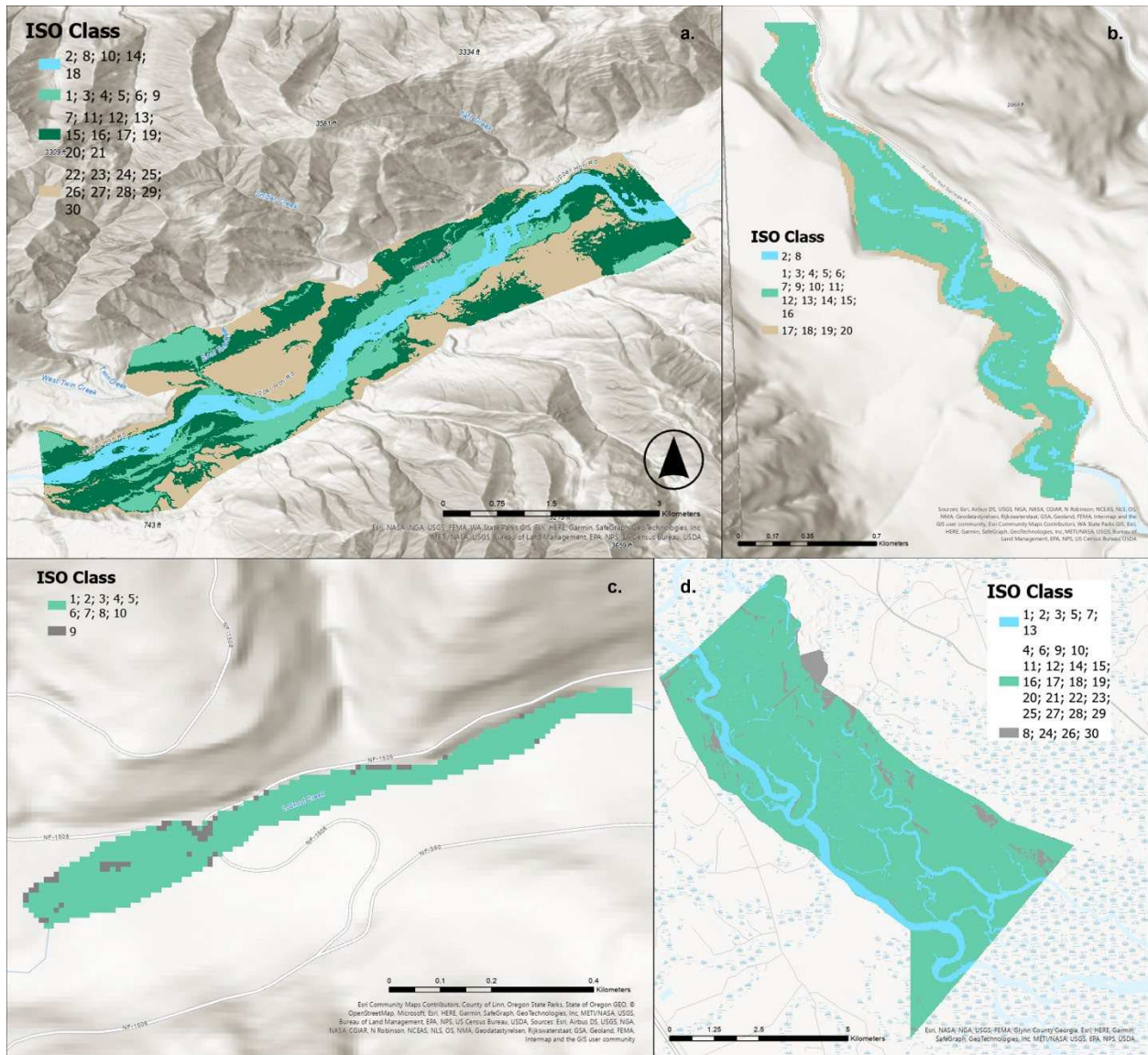
Figure 3.8. Grouped ISO Classes based on underlying data for a) Hoh River, Washington, b) Sol Duc River, Washington, and c) Lookout Creek, Oregon. ISO Class numbers are not the same as Field Class numbers.

In Figure 3.8a, blue represents the bare sediment, water, and/or sparsely vegetated midchannel islands in and around the active channel; light green represents the active floodplain with channel features, wetlands, younger forest and groundcover, and varying vegetation health/density; dark green represents old growth forest floor/inactive floodplain with nurse logs and varying vegetation health/density of mosses, fern (including *Polystichum* and *Athyrium* spp.), alder (*Alnus* spp.), conifer (including *Picea*, *Pseudotsuga*, and *Thuja* spp.), maple (*Acer*

spp.) (NPS, 2015, 2020); and beige represents uplands and inactive floodplain with varying vegetation health/density. In Figure 3.8b, blue represents the active channel; light green represents the active floodplain, and/or vegetation overhanging channel, with side channels, overflow surfaces, nurse logs, and varying vegetation health/density, including mosses, alder, maple, herbaceous groundcover, fern, conifer, and grasses; and beige represents higher elevation surfaces and/or uplands with conifer forest, including vertical cliffs above the channel. In Figure 3.8c, light green represents the active channel and floodplain with midchannel island, boulder bars, backwater channels, side channels and varying vegetation health/density, including fir, viny maple, fern, cedar, alders, horsetail (*Equisetum* spp.), grasses, and evidence of beaver chew (HJ Andrews Experimental Forest, n.d.); and grey represents the bridge, road, steep banks and/or boundaries next to channel and floodplain. In Figure 3.8d, blue represents the active channel, tributaries, side channels, and/or standing water; light green represents the Active floodplain with inundated areas and areas of exposed sediment, varying vegetation health/density, including evergreen and deciduous trees (including *Pinus*, *Quercus*, *Taxodium*, and *Ulmus* spp.), bamboo, palmetto (*Serenoa* spp.), moss, vines, leaf litter, holly (*Ilex* spp.), and maples (*Acer* spp.) (Luber, 2002); and grey represents structures, roads, other manmade surfaces, and/or active floodplain with similar spectral properties.

3.5 Discussion

This discussion addresses the differences between Classifications 1 and 2, the benefits and drawbacks of each dataset, the metric values compared to each other and regionally, and the geomorphic interpretations of the results.

3.5.1 Objective I Discussion

Although interspersion differs qualitatively between sites, aggregation, largest patch, and evenness do not differ between sites or classifications for the Altamaha, Hoh, and Sol Duc Rivers. This indicates that perhaps the metrics are more influenced by actual properties of the floodplains and less by the data used. This is encouraging, especially as there was a mismatch in resolution between the Hoh River and Lookout DEMs (0.91 m), the Sol Duc River DEM (3 m), and the Altamaha River DEM (10 m) for Classification 2. This indicates that using the highest available resolution for elevation data is recommended. This is exemplified in the results for the Sol Duc River (Figure 3.5b vs. Figure 3.6b). I find that the increased spatial resolution is most important for the smallest rivers, as each pixel covers a greater percentage of the floodplain for smaller rivers and therefore less granularity is possible per pixel than for larger rivers. For broad comparison studies, I suggest using aerial imagery with the same spectral resolution for all sites and the highest available resolution of topographic data. National Agriculture Image Program (NAIP) imagery could be used if the user wants higher spatial resolution at the expense of lower spectral and temporal resolution. The heterogeneity metrics differ qualitatively for Lookout Creek between Classification 1 and 2. This could be because the floodplain is small and adjustment to pixel values alters the results dramatically. With this in mind, I propose that using the same spectral data when comparing classifications between sites is more important than which spectral data are used to maintain the same spectral resolution, spectral ranges, and post-processing methods for deriving surface reflectance. For example, when comparing rivers like Lookout Creek and Altamaha River, it is more important to use the aerial imagery with the same spectral bands and use the highest spatial resolution data available.

Moving forward with similar analyses of additional sites, I suggest the removal of largest patch index from the suite of heterogeneity metrics because it is highly dependent on the input values of classification and has variable and sometimes large percent change across the rivers (99.7% for Lookout Creek). The smaller suite of five metrics I suggest moving forward with are aggregation index, interspersion and juxtaposition, patch density, percentage of like adjacencies, and Shannon's evenness index.

Overall, the results suggest that natural floodplains in the Pacific Northwest and coastal Southeast have moderate to high evenness, moderate to high intermixing, and moderate aggregation; and similar aggregation and evenness as rivers in Colorado and Oklahoma, but lower intermixing (Iskin and Wohl, 2023). The results show that the larger rivers (arbitrarily floodplain area > 50 ha) in this study (Altamaha, Hoh, and Sol Duc Rivers) have similar spatial heterogeneity as beaver-modified and shortgrass prairie rivers in Colorado, while the more inland and smaller river (Lookout Creek) has similar spatial heterogeneity to the tallgrass prairie site (Sand Creek) (Iskin and Wohl, 2023).

I calculated the ratio of average floodplain width to average channel width in ArcGIS Pro from six hand drawn, approximately evenly spaced cross sections at each river using the Sentinel imagery, floodplain boundaries, and field delineations. I find that the ratio of floodplain width to channel width is 19.3 for the Altamaha River, 7.0 for the Hoh and Sol Duc Rivers, and 3.2 for Lookout Creek. I attribute the lower interspersion at the Altamaha River compared to the Sol Duc River, and West Bijou, East Plum, and Rough and Tumbling Creeks to slower rates of lateral channel migration or avulsion across the much broader floodplains (Konrad, 2012). The Hoh River has lower interspersion than the Sol Duc River despite the same average floodplain to channel width ratio. I attribute this to the different hydrologic and sediment regimes on either

side of the Olympic Mountains. The Hoh River valley is considered a temperate rainforest (NPS, 2020), is glacially fed, and receives almost twice as much precipitation (Supplemental Table 3.1). The Sol Duc River valley is considered a lowland forest (NPS, 2015) and is lake-fed. These differences in precipitation and source flow could result in different sediment regimes (Wada et al., 2011) and the presence of braided planform in the Hoh River and not at the Sol Duc River. The more dynamic planform of the braided Hoh River (Sambrook Smith et al., 2006) could result in the higher pairing of certain classes (lower interspersion) by more punctuated/less gradual channel movement across the floodplain (Schumm, 1985). I attribute the high evenness at the Altamaha, Hoh, and Sol Duc Rivers to the natural flow, sediment, and wood regimes, as did Iskin and Wohl (2023) in the earlier analysis of West Bijou, East Plum, and Rough and Tumbling Creeks. I attribute the similarities of aggregation and intermixing between Lookout Creek (Classification 1) and Sand Creek to lateral confinement of the channels and low ratio of average floodplain width to average channel width at Lookout Creek.

3.5.2 Objective II Discussion

Extraction of the underlying data was useful for interpreting the ISO Classes from the unsupervised classifications. I find that class-averaged NDVI is good at differentiating vegetation from non-vegetation, and is therefore very useful for interpreting classes. Although NDMI seems to follow the same trend as NDVI, NDMI data are harder to interpret but seem to help in the classification step, so I left them in. I find that increasing the spatial resolution of the elevation data makes the classifications more visually interpretable. I also find that the field data are crucial for differentiating between different types of floodplain classes. I was able to differentiate between younger active floodplain and older floodplain for the Hoh River (Figure 3.8a) because of the field classifications, but I could not further differentiate the active floodplain

for the Altamaha River (Figure 3.8d) because I could not collect detailed field classifications due to unexpected inundation in October 2021. Although I was able to group ISO Classes into geomorphic units, the groups gloss over the inherent heterogeneity of the individual classes. The groups are visually interesting and generally interpretable, but I propose that it is the heterogeneity within the groups that is vital to floodplain functioning. For example, the grouped light green younger active floodplain at the Hoh River (Figure 3.8) includes side channels, but the individual channels where fluvial processes such as transporting water, sediment, organic matter and providing habitat occur are not actually visible. The classifications give us more insight to the structure and function of the floodplains than do the groupings.

3.6 Conclusion

I repeated a previously developed unsupervised classification workflow for three rivers in the U.S. Pacific Northwest and one river in the Southeast, and compared the results based on data used and metrics calculated. The results indicate that natural floodplains in the Pacific Northwest and coastal Southeast have moderate to high evenness, moderate to high intermixing, and moderate aggregation; and similar aggregation and evenness as rivers in Colorado and Oklahoma, but lower intermixing. I attribute lower intermixing at the Altamaha River to slower rates of lateral channel migration, and lower intermixing at the Hoh River to the different hydrologic and sediment regimes and less stable braided planform. The results show that the larger rivers (arbitrarily floodplain area > 50 ha) in this study (Altamaha, Hoh, and Sol Duc Rivers) have similar spatial heterogeneity as beaver-modified and shortgrass prairie rivers in Colorado, while the more inland and smaller river (Lookout Creek) has similar spatial heterogeneity to the tallgrass prairie site (Sand Creek).

These results also indicate that using the highest resolution topographic data available and the same spectral resolution aerial imagery is the best path forward when comparing results between sites. The metrics show that there are similarities and differences between rivers in Washington, Oregon, Colorado, Oklahoma, and Georgia, and that discernable trends may arise from a meta study comparing heterogeneity from more rivers across the country.

3.7 References

Allison, S., Martinez, D., 2013. Hoh River LiDAR-Delivery 2 Technical Data Report.

Appling, A.P., Bernhardt, E.S., Stanford, J.A., 2014. Floodplain biogeochemical mosaics: A multidimensional view of alluvial soils. *Journal of Geophysical Research: Biogeosciences* 119(8), 1538–1553. https://doi.org/10.1002/2013JG002543

Division of Geology and Earth Resources, 2022. Washington Lidar Portal. *Washington State Department of Natural Resources*. https://lidarportal.dnr.wa.gov/

EOS Data Analytics, Inc. (2019, August 30). NDVI FAQ: All You Need To Know About Index. https://eos.com/blog/ndvi-faq-all-you-need-to-know-about-ndvi/

Esri, 2023. ArcGIS Pro, ver 3.0.3. https://www.esri.com/en-us/arcgis/products/arcgis-pro/overview

European Space Agency (ESA), 2021. Level-2A. *Sentinel Online*. https://sentinel.esa.int/web/sentinel/user-guides/sentinel-2-msi/product-types/level-2a

GISGeography. (2022a, May 30). What is NDVI (Normalized Difference Vegetation Index)? https://gisgeography.com/ndvi-normalized-difference-vegetation-index/

GISGeography. (2022b, June 4). Sentinel 2 Bands and Combinations. https://gisgeography.com/sentinel-2-bands-combinations/

Gleason, A., and McWethy, G., 2014. Lidar Project Quality Assurance Report. https://www.dnr.wa.gov/geology

Google Developers, 2022. Sentinel-2 MSI: MultiSpectral Instrument, Level-2A. *Earth Engine Data Catalog*. https://developers.google.com/earth-engine/datasets/catalog/COPERNICUS_S2_SR#bands

Gorelick, N., Hancher, M., Dixon, M., Ilyushchenko, S., Thau, D., Moore, R., 2017. Google Earth Engine: Planetary-scale geospatial analysis for everyone. *Remote Sensing of Environment* 202, 18–27. https://doi.org/10.1016/j.rse.2017.06.031

Graf, W.L., 2006. Downstream hydrologic and geomorphic effects of large dams on American rivers. *Geomorphology* 79(3–4), 336–360. https://doi.org/10.1016/j.geomorph.2006.06.022

Harms, T.K., Wentz, E.A., and Grimm, N.B., 2009. Spatial heterogeneity of denitrification in semi-arid floodplains. *Ecosystems* 12, 129–143. https://doi.org/10.1007/s10021-008-9212-6

Hesselbarth, M.H.K., Sciaini, M., Nowosad, J., Hanss, S., Graham, L.J., Hollister, J., With, K.A., 2021. Package "landscapemetrics" Reference Manual. https://cran.r-project.org/web/packages/landscapemetrics/

HJ Andrews Experimental Forest, n.d. Vascular Plant List.

Iskin, E.P., Wohl, E., 2023. Quantifying floodplain heterogeneity with field observation, remote sensing, and landscape ecology: Methods and metrics. *River Research and Applications*, 1–19. https://doi.org/10.1002/rra.4109

Konrad, C.P., 2012. Reoccupation of floodplains by rivers and its relation to the age structure of floodplain vegetation. *Journal of Geophysical Research: Biogeosciences* 117(G4). https://doi.org/10.1029/2011JG001906

Kuiper, J.J., Janse, J.H., Teurlincx, S., Verhoeven, J.T.A., Alkemade, R., 2014. The impact of river regulation on the biodiversity intactness of floodplain wetlands. *Wetlands Ecology and Management* 22, 647–658. https://doi.org/10.1007/s11273-014-9360-8

le Hégarat-Mascle, S., Bloch, I., Vidal-Madjar, D., 1997. Application of Dempster-Shafer Evidence Theory to Unsupervised Classification in Multisource Remote Sensing. *IEEE Transactions on Geoscience and Remote Sensing* 35(4), 1018–1031. https://doi.org/10.1109/36.602544

Lu, D., Weng, Q., 2007. A survey of image classification methods and techniques for improving classification performance. *International Journal of Remote Sensing*, 28(5), 823–870. https://doi.org/10.1080/01431160600746456

Luber, H.H., 2002. Floristic Inventory of an Altamaha River Floodplain Area [Master's Thesis, University of Georgia]. https://getd.libs.uga.edu/pdfs/luber_holly_1_200208_ms.pdf

Naiman, R.J., Bechtold, J.S., Drake, D.C., Latterell, J.J., O'Keefe, T.C., Balian, E.V., 2005. Origins, Patterns, and Importance of Heterogeneity in Riparian Systems. In G.M. Lovett, M.G. Turner, C.G. Jones, K.C. Weathers (Eds.), *Ecosystem Function in Heterogeneous Landscapes* (1st ed., pp. 279–309). Springer Science + Business Media, Inc. https://doi.org/10.1007/0-387-24091-8_14

National Park Service (NPS), 2015. Lowland Forests. *Olympic National Park*. https://www.nps.gov/olym/learn/nature/lowland-forests.htm

National Park Service (NPS), 2020. Temperate Rain Forests. *Olympic National Park*. https://www.nps.gov/olym/learn/nature/temperate-rain-forests.htm

Open Topography, 2021. USGS 1/3 arc-second Digital Elevation Model.
https://doi.org/10.5069/G98K778D

R Core Team, 2023. R: A language and environment for statistical computing. R Foundation for
Statistical Computing. https://www.r-project.org/

Sabins Jr., F.F., Ellis, J.M., 2020. *Remote Sensing: Principles, Interpretation, and Applications*
(4th ed.). Waveland Press, Inc.

Samaritani, E., Shrestha, J., Fournier, B., Frossard, E., Gillet, F., Guenat, C., Niklaus, P.A.,
Pasquale, N., Tockner, K., Mitchell, E.A.D., Luster, J., 2011. Heterogeneity of soil carbon
pools and fluxes in a channelized and a restored floodplain section (Thur River,
Switzerland). *Hydrology and Earth System Sciences* 15(6), 1757–1769.
https://doi.org/10.5194/hess-15-1757-2011

Sambrook Smith, G.H., Best, J.L., Bristow, C.S., Petts, G.E., Jarvis, I. (Eds.), 2006. *Braided
Rivers: Process, Deposits, Ecology and Management* (Special Publication 36 of the IAS).
Blackwell Publishing Ltd. https://doi.org/10.1002/9781444304374

Schindler, S., O'Neill, F.H., Biró, M., Damm, C., Gasso, V., Kanka, R., van der Sluis, T., Krug,
A., Lauwaars, S.G., Sebesvari, Z., Pusch, M., Baranovsky, B., Ehlert, T., Neukirchen, B.,
Martin, J.R., Euller, K., Mauerhofer, V., Wrbka, T., 2016. Multifunctional floodplain
management and biodiversity effects: a knowledge synthesis for six European countries.
Biodiversity and Conservation 25, 1349–1382. https://doi.org/10.1007/s10531-016-1129-3

Schumm, S.A., 1985. Patterns of Alluvial Rivers. *Annual Review of Earth and Planetary
Sciences* 13, 5–27. https://doi.org/10.1146/annurev.ea.13.050185.000253

U.S. Environmental Protection Agency (EPA), 2013. Level III Ecoregions of the Conterminous
United States shapefile. U.S. EPA – National Health and Environmental Effects Research
Laboratory. https://www.epa.gov/eco-research/level-iii-and-iv-ecoregions-continental-
united-states

U.S. Geological Survey (USGS), 2016. McKenzie River Bare Earth Mosaic. http://prd-
tnm.s3.amazonaws.com/index.html?prefix=StagedProducts/Elevation/metadata/OR_McKen
zieRiver_2021_B21/OR_McKenzieRiver_1_2021/spatial_metadata/contractor_provided/

U.S. Geological Survey (USGS). (2018, November 27). NDVI, the Foundation for Remote
Sensing Phenology. https://www.usgs.gov/special-topics/remote-sensing-
phenology/science/ndvi-foundation-remote-sensing-phenology

U.S. Geological Survey (USGS), 2022a. Landsat Normalized Difference Vegetation Index. *Landsat Missions*. https://www.usgs.gov/landsat-missions/landsat-normalized-difference-vegetation-index

U.S. Geological Survey (USGS), 2022b. Normalized Difference Moisture Index. *Landsat Missions*. https://www.usgs.gov/landsat-missions/normalized-difference-moisture-index

U.S. Geological Survey (USGS), 2022c. StreamStats, ver 4.11.1. https://streamstats.usgs.gov/ss/

U.S. Geological Survey (USGS), 2023a. StreamStats ver 4.12.0. https://streamstats.usgs.gov/ss/

U.S. Geological Survey (USGS), 2023b. The National Map Download Client, ver 2.0. https://apps.nationalmap.gov/downloader/

Wada, T., Chikita, K.A., Kim, Y., Kudo, I., 2011. Glacial Effects on Discharge and Sediment Load in the Subarctic Tanana River Basin, Alaska. *Arctic, Antarctic, and Alpine Research* 43(4), 632–648. https://doi.org/10.1657/1938-4246-43.4.632

With, K.A. (2019). *Essentials of Landscape Ecology*. Oxford University Press. https://doi.org/10.1093/oso/9780198838388.001.0001

Wohl, E., Iskin, E.P., 2019. Patterns of Floodplain Spatial Heterogeneity in the Southern Rockies, USA. *Geophysical Research Letters* 46(11), 5864–5870. https://doi.org/10.1029/2019GL083140

4. CH 4: TRENDS & PROCESS[3]

Summary

I use the five landscape ecology metrics of aggregation index (AI), percentage of like adjacencies (PLADJ), interspersion and juxtaposition index (IJI), patch density (PD), and Shannon's evenness index (SHEI) to assess spatial heterogeneity at 15 floodplains in the continental United States. Assessments are based on floodplain patches delineated remotely using topography and vegetation. Floodplain reaches examined here represent diverse drainage areas, flow regimes, valley geometry, channel planforms, and biomes. I selected sites with minimal direct human alteration, such as upstream dams, widespread development, intensive grazing, intensive forestry, or extensive manmade levees. My objectives are to quantify floodplain spatial heterogeneity, evaluate whether statistically significant patterns are present, and interpret the statistical analyses with respect to the influence of channel lateral mobility and valley-floor space available. I develop a conceptual model of the influences on lateral mobility and space available, and then test specific hypotheses derived from this conceptual model. These natural floodplains have a median aggregation index of 58.8%, median interspersion and juxtaposition index of 74.9%, median patch density of 1241 patches/ha, median percentage of like adjacencies of 58.5%, and median Shannon's evenness index of 0.934 (n=15). In other words, natural floodplains have moderate aggregation of classes, high evenness and intermixing of classes, and a wide range of patch densities. Drainage area, floodplain width ratio (space available), and elevation, precipitation, total sinuosity, large wood volume, planform, and flow

---

regime (channel mobility) emerge as important variables to floodplain heterogeneity. More study is needed to determine how variables interact with each other to affect floodplain spatial heterogeneity, how river corridor restoration can boost heterogeneity, and the effects of climate change on floodplains.

4.1 Introduction

My primary objectives are to (i) quantify floodplain spatial heterogeneity for diverse natural floodplains in the United States using multiple heterogeneity metrics from landscape ecology, (ii) evaluate whether statistically significant patterns occur among these data and determine whether there are salient characteristics of river corridors that relate to multiple facets of heterogeneity, and (iii) interpret the statistical results in terms of the primary controls – channel lateral mobility and valley-floor space available – as well as the factors underlying mobility and space, such as flow regime and biota. I first review floodplain functions and the importance of floodplain spatial heterogeneity, then present the conceptual model and hypotheses.

Following Iskin and Wohl's (2023; In Review) methodologies, I define floodplain heterogeneity as the spatial variation of geomorphic and vegetation classes and patches across a floodplain. Classes represent distinct types of floodplain habitats that blend geomorphic features and vegetation communities. Geomorphic features identified in the field include active channels, secondary channels with limited or no surface hydrologic connectivity, accretionary bars, backswamps, and natural levees. Vegetation communities include old-growth and younger conifer forest and deciduous forest, mesic wetlands, grasses, xeric vegetation, and beaver meadows (willow carrs). This definition of floodplain heterogeneity can be applied to any floodplain; expands on the metric for floodplain heterogeneity from Graf (2006) and Wohl and

Iskin (2019); and is distinct from the metrics of floodplain connectivity (Ward et al., 2002), surface topographic complexity (Scown et al., 2015, 2016a, 2016b) and riparian vegetation (Aguiar et al., 2009) described in other studies.

4.1.1 Importance of Floodplain Heterogeneity

As summarized by Petsch et al. (2022), floodplains provide many ecosystem services including, but not limited to: soil formation, nutrient cycling, primary production, habitat provisioning, water regulation, erosion control, water purification, waste treatment, disease regulation, climate regulation, genetic resources, aesthetic, and cultural services. They store material and facilitate the internal and external exchange of surface water, hyporheic water, groundwater, solutes including dissolved carbon, nitrogen and phosphorous, sediment, and organic matter including coarse particulate organic matter and large wood (Appling et al., 2014; Hopkins et al., 2018; Wohl, 2021). Floodplains more effectively capture and biologically process organic matter when compared to laterally confined river reaches with small to no floodplain (Bellmore and Baxter, 2014; Wohl et al., 2018a) and store large wood, sometimes in unique ways compared to channels, such as long narrow logjams (Iskin and Wohl, 2021). They also serve as habitat for a diverse array of organisms, including microbes (Tockner et al., 2000; Benke, 2001; Jeffres et al., 2008; Zeug and Winemiller, 2008; Bellmore and Baxter, 2014; Doering et al., 2021) and are commonly more biodiverse than other landcover types (Tockner et al., 2008; Junk et al., 2010). Important floodplain functions are not limited to large floods, and exchange of water between the river and the floodplain can be similar for both large and small rivers (Scott et al., 2019), highlighting the importance of studies that incorporate multiple river sizes.

Floodplain heterogeneity both reflects and influences water and sediment connectivity. Fluxes and storage of water and sediment can modify floodplain configuration and alter connectivity, but these fluxes also respond to existing connectivity. Consequently, floodplain connectivity is dynamic in time, changing with the rising and falling limbs of inundating flows (Junk et al., 1989; Tockner et al., 2000), for example, as well as in response to channel movement and associated erosion and deposition (Amoros and Bornette, 2002), vegetation dynamics (Naiman et al., 2005; Larsen and Harvey, 2010), movement and storage of large wood (Wohl, 2021), modifications created by other biota (Larsen et al., 2021), and disturbances such as wildfire (Kleindl et al., 2015).

Floodplain heterogeneity has nuanced effects on floodplain forms and functions. Heterogeneity enhances diversity of hydrologic flow paths within the floodplain and thus diversity of water temperatures, water residence times, and associated biogeochemical reactions (Helton et al., 2014; Uno, 2016). Channel migration that creates heterogeneity also increases floodplain habitat diversity (Choné and Biron, 2016), including for foundational species such as the cottonwood (*Populus* sp.) (Stella, et al., 2011). Spatial heterogeneity in floodplain soils, particularly clay, results in heterogeneity of channel sinuosity and meander migration patterns (Güneralp and Rhoads, 2011a; Schwendel et al., 2015), as well as in preferential subsurface flow paths (Fuchs et al., 2009). Increased spatial heterogeneity of the entire river corridor, including floodplain presence, is associated with decreased catchment-wide sediment yield and sediment connectivity (Baartman et al., 2013). Floodplain heterogeneity affects the deposition and storage of pollutants because many contaminants travel adsorbed to sediment or are influenced by spatially diverse microbial transformations in patchy surface and subsurface environments (Lowell et al., 2009; Ciszewski and Grygar, 2016). Forested floodplain soil texture affects

carbon and nitrogen cycling (Appling et al., 2014) and floodplain heterogeneity is linked to heterogeneity of carbon storage (Samaritani et al., 2011; Lininger et al., 2018). Surface heterogeneity of vegetation is associated with near-surface soil nutrient heterogeneity (Naiman et al., 2005; Appling et al., 2014). Floodplain topographic heterogeneity influences inundation patterns and resulting vegetation establishment (Scott et al., 1996; Hughes, 1997; Friedman and Lee, 2002), as well as fish life cycles, aquatic communities, and food webs (Zeug and Winemiller, 2008; Bellmore et al., 2013; Stoffers et al., 2022; Uno et al., 2022). These previous studies highlight the importance and the effects of floodplain heterogeneity, but there is much work to be done in comparing heterogeneity across latitudes, elevations, and biomes and connecting heterogeneity to overarching floodplain processes.

This study builds directly off the development of a classification workflow in Ch 2 and 3, choice of metrics from landscape ecology, and investigation into floodplain heterogeneity around the continental United States. This work builds beyond the case study by quantifying floodplain spatial heterogeneity for 15 natural floodplains across North America that differ in relative channel mobility, flashiness of flood peaks, and biome to provide insights into the fluvial and ecological processes that create and maintain natural floodplain heterogeneity.

4.1.2 Conceptual Model

I seek to determine whether river corridor characteristics can predict levels of floodplain heterogeneity through a multivariate linear analysis and to infer processes that create and maintain floodplain heterogeneity. I start from the premise that the two primary controls of floodplain heterogeneity are the lateral space available for floodplain development in a river corridor and the lateral mobility of the channel. For the conceptual model in Figure 4.1, I assume that the space available for a river is governed primarily by processes acting at timespans of

millennia and longer (e.g., Wohl, 2015) and is thus static for the timespans of 10^1–10^2 years during which the floodplain features that I analyze are created and maintained. I use valley geometry to represent valley-floor space available for floodplain development and adjustment. I quantify drainage area (DrA) and the ratio of average floodplain width to average channel width (FP/CH) at the reach scale and use these as indicators of valley geometry because valley-floor width tends to increase with drainage area (e.g., Bhowmik, 1984; Beighley and Gummadi, 2011) but reach-scale variations in longitudinal trends are better captured by FP/CH for a reach (e.g., Wohl et al., 2017).

I expect flow regime, channel planform, and biota to influence lateral channel mobility. I categorize flow regime (Flow) as a proxy for the flashiness and relative erosional power of peak flows, under the assumption that snowmelt-dominated flow regimes are less flashy than rainfall-dominated regimes. Thirty-year normal precipitation (Precip) is a variable that can be easily quantified from publicly available data and that may influence flow regime and floodplain vegetation. Mean floodplain elevation (Elev) can be a proxy for elevational differences in climate and disturbance regime, particularly in high-relief watersheds (Sutfin and Wohl, 2019). Categorical planform (Plan) reflects relative lateral mobility, which I interpret to increase along a continuum from straight to meandering, anastomosing, and then braided channel planform (Schumm, 1985). Latitude (Lat) and elevation are likely to jointly distinguish ecoregions in the United States (Omernik, 1987; Barry et al., 2004) and median large wood volume (LWV) reflects a biotic influence on floodplain process and form (Figure 4.1). Methods used to determine values and categories for each predictor variable are described in the Methods section and provided for each site in Table 4.1.
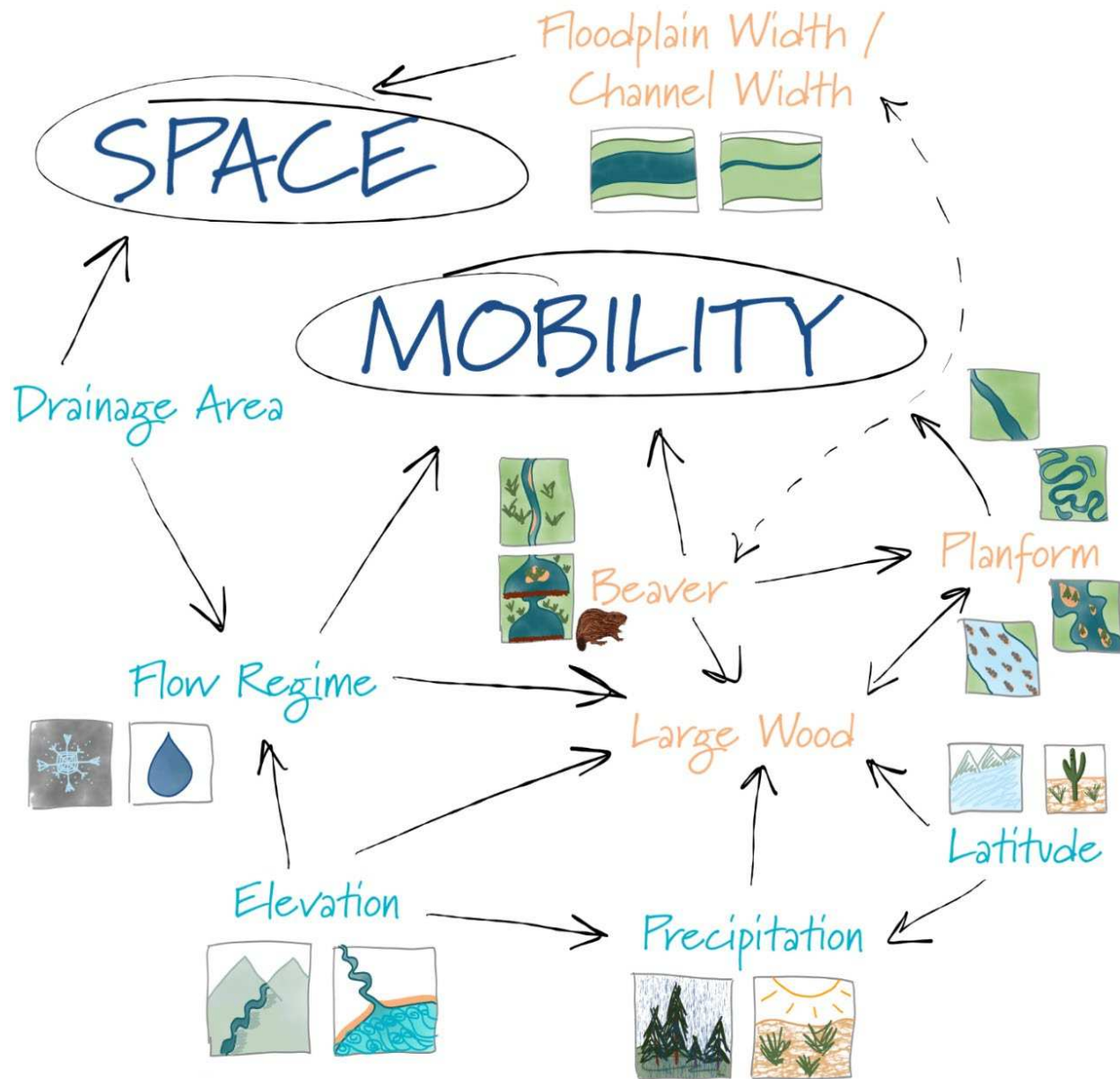
Figure 4.1. Main controls of floodplain spatial heterogeneity and the predictor variables used to quantify them. Main controls are shown in dark blue text and predictors are shown in turquoise and orange text. Turquoise predictors indicate to drainage basin-level values and categories, and orange predictors indicate study area-level values and categories. Solid arrows connect predictor variables to the main controls they represent and to other predictor variables that they influence or are influenced by, and double-sided arrows connect predictor variables the interact reciprocally with each other. The dashed arrow connecting Beaver and Floodplain Width/Channel Width represents the habitat preference of beaver for wider floodplains, but also the fact that their presence and dam building can increase the regularly flooded width of the valley floor (e.g., Westbrook et al., 2011). The inset tiles illustrate contrasting values or levels for each variable.

I relate the predictor variables in Figure 4.1 to five response variables that are commonly

used spatial patch- and class-based heterogeneity metrics from landscape ecology: aggregation

index (AI), percentage of like adjacencies (PLADJ), interspersion and juxtaposition index (IJI),

patch density (PD), and Shannon's evenness index (SHEI) (levels of each metric demonstrated Supplemental Figure 4.1). AI and PLADJ are both measures of the aggregation across a landscape based on class edge length (He et al., 2000; Hesselbarth et al., 2022), and going forward the term aggregation (AGG) will be used when I refer to AI and PLADJ together. Low values of AGG indicate that few pixels are adjacent to pixels of the same class (He et al., 2000; Hesselbarth et al., 2022). IJI is a measure of intermixing of class types at a patch level, or how spatially mixed patches of different classes are (McGarigal and Marks, 1995; Hesselbarth et al., 2022). PD is a measure of how broken up a landscape is, where a higher PD indicates a patchier landscape with more individual patches, regardless of class type (Hesselbarth et al., 2022). SHEI is a measure of diversity and distribution of class types across a landscape (Hesselbarth et al., 2022). A higher SHEI indicates that the landscape area is not dominated by one class type (McGarigal and Marks, 1995).

4.1.3 Hypotheses

I test five hypotheses regarding relationships between predictor and response variables using pairwise comparisons of medians and variances, and a multivariate linear analysis.

H1: AGG will increase and PD will decrease with increasing FP/CH. I based this hypothesis on the assumption that the turnover rate of a relatively broad floodplain will be longer (Mertes et al., 1996; Konrad, 2012) and individual patches will persist for longer and be subject to less frequent disturbance, thus merging into larger patches via vegetation establishment and encroachment.

H2: AGG, IJI, PD, and SHEI will increase with increasing LWV. This tests the inference that large wood accumulations can increase channel-floodplain connectivity (Jeffries et al., 2003;

Collins et al., 2012), increasing the size of patches, but can also affect vegetation establishment, store sediment, and armor channel banks (Daniels and Rhoads, 2003; Skalak and Pizzuto, 2010).

H3: For non-beaver sites, IJI, SHEI, and PD will increase and AGG will decrease with increasing channel mobility and migration (as reflected in the proxy of Plan). This hypothesis tests the assumption that new floodplain will be formed, vegetation succession will be reset, and sediment will be transported and deposited in new areas, thus dissecting large patches and therefore increasing the number of patches and class intermixing.

H4: IJI, SHEI, and PD will increase and AGG will decrease with increasing flow regime flashiness (as reflected in the category of Flow). This hypothesis tests the inference that the channel will be more mobile and the floodplain will be inundated more often with less time for large vegetation to establish (e.g., Everitt, 1968), increasing the number of small, interspersed patches and dissecting large patches.

H5: For beaver sites vs. non-beaver sites, IJI will decrease and AGG and PD will increase with the presence of beaver modification (as reflected in the proxy of Plan) because beaver organize the landscape in a specific way that accumulates wet and non-wet patches (Laurel and Wohl, 2019) while maintaining vegetation stands throughout the river corridor.

4.2 Study Area

This study examines 15 diverse river corridors from the continental United States (Figure 4.2). The sites are the Yukon River (YAK; floodplain area $= 2,380$ km^2) in the Yukon Flats National Wildlife Refuge in Alaska, the Hoh River (HWA; 10 km^2) and Sol Duc River (SDWA;

0.6 km^2) in Olympic National Park in Washington, Lookout Creek (LOR; 0.1 km^2) in HJ Andrews Experimental Forest in Oregon, the Swan River (SMT; 26 km^2) in the Swan River State Forest (including the Swan River National Wildlife Refuge) in Montana, Downs Fork (DFWY; 0.2 km^2) and Dinwoody Creek (DWY; 0.3 km^2) in the Fitzpatrick Wilderness in Wyoming, North St. Vrain Creek (NSV; 0.4 km^2) in Boulder County in Colorado, Rough and Tumbling Creek (RTCO; 0.1 km^2) in Park County in Colorado, East Plum Creek (EPC; 0.02 km^2) in Douglas County in Colorado, West Bijou Creek (WBJ; 1 km^2) in Arapahoe County in Colorado, Sand Creek (SOK; 0.1 km^2) in the Joseph H. Williams Tallgrass Prairie Preserve in Oklahoma, the Embarras River (EIL; 6 km^2) in the Chauncy Marsh Nature Preserve in Illinois, the Congaree River (CSC; 106 km^2) in Congaree National Park in South Carolina, and the Altamaha River (AGA; 37 km^2) in the Altamaha Wildlife Management Area in Georgia. Site information and data collected are presented in the next section.

I chose these sites to represent a range of drainage area (30–500,000 km^2), flow regime (snowmelt vs. rainfall), channel planform (straight, meandering, anastomosing, beaver, braided), and biome/latitude (31–66º). I emphasized the least human-altered floodplains and watersheds that I could identify. My intent was to minimize the effects of flow regulation, artificial levees, floodplain drainage and land cover changes, and channel engineering on floodplain process and form.
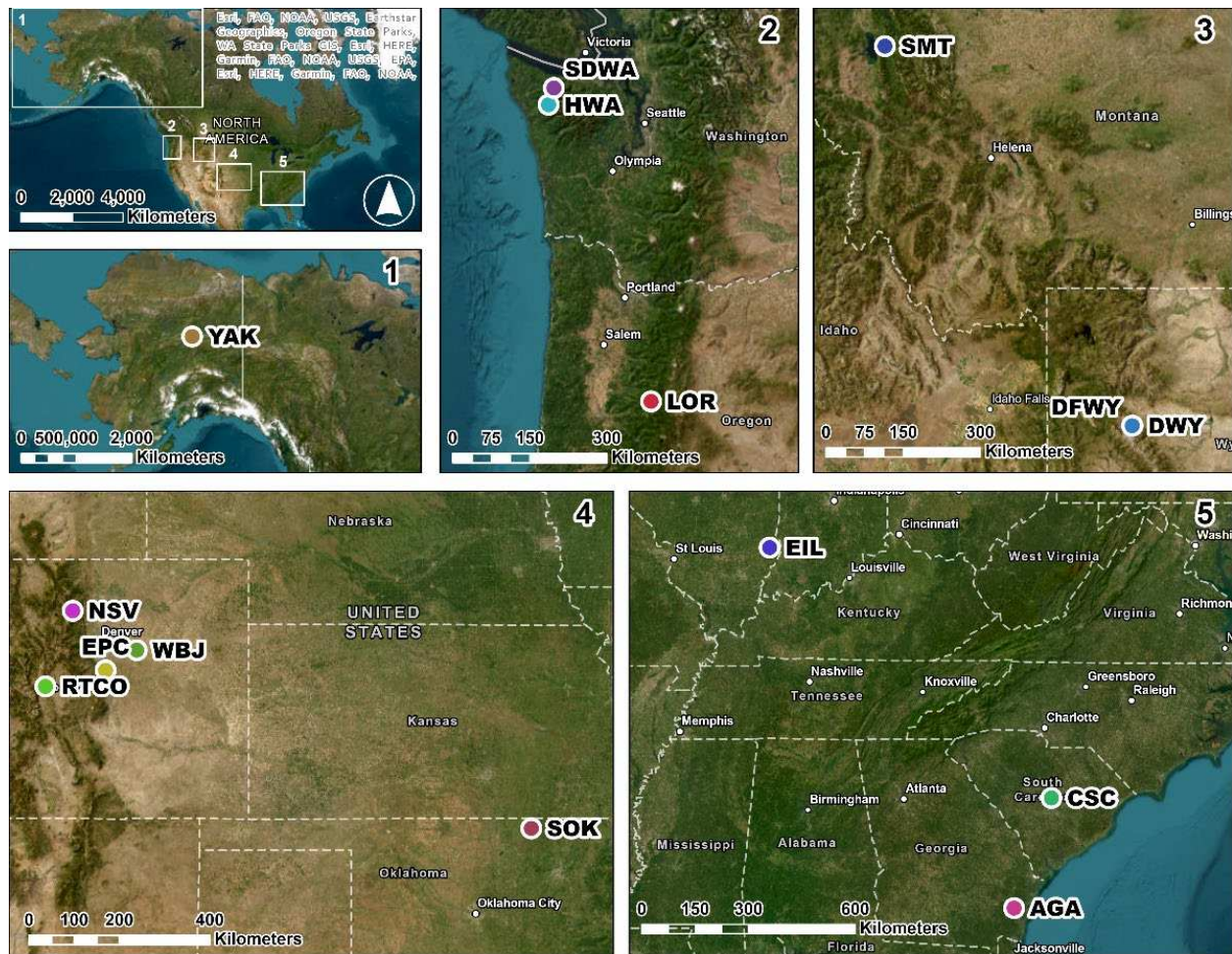
Figure 4.2. Floodplain sites used in this study, shown regionally and in more detail. Region 1 includes the Yukon River in the arctic (YAK); region 2 includes the Hoh River (HWA), Sol Duc River (SDWA), and Lookout Creek (LOR) in the Pacific Northwest; region 3 includes the Swan River (SMT), Downs Fork (DFWY), and Dinwoody Creek (DWY) in the Rocky Mountains; region 4 includes North St. Vrain Creek (NSV), Rough and Tumbling Creek (RTCO), East Plum Creek (EPC), West Bijou Creek (WBJ), and Sand Creek (SOK) in the Rocky Mountains and Great Plains; and region 5 includes Embarras River (EIL), Congaree River (CSC), and Altamaha River (AGA) in the (coastal) plains.

4.3 Methods

Following the methods from Ch 3, I present a full suite of sites with field data, classified floodplains, and values of heterogeneity. Field classifications for specific sites can be found in Tables 2.3 and 3.1, and Supplemental Table 4.1, and can be used to interpret the classified data (Iskin and Wohl, In Review). Field transect locations were spaced at approximately ten times the average channel width, and study reaches were chosen based on existence of a floodplain (river beads), access by car and foot, and in some cases by existence of published datasets. Patches

84

were defined in the field along the floodplain transects on the 3–10 m scale and with remote sensing on the 10 m scale. Classes are identified with an unsupervised remote sensing classification run with 10-band aerial imagery, high-resolution digital elevation models (DEMs), normalized difference vegetation index (NDVI), and normalized difference moisture index (NDMI) (Supplemental Table 4.3). Sentinel-2A data from 2022 only were used to create the multispectral mosaics in Google Earth Engine because the Sentinel processing baseline was updated in January 2022 (ESA, 2023). I used a timeframe of data from 1 May 2022 – 30 September 2022 to capture the entire summer growing period. I shortened this window for RTCO to exclude snow-covered periods and widened the window for CSC and AGA to reduce the impact of clouds in this humid region. I decreased the cloudy percentage as necessary to produce a clear mosaic (Supplemental Table 4.3). DEMs with higher spatial resolution than 10 m were used where available and when they covered the entire study site; 10 m DEMs were used otherwise (Supplemental Table 4.3).

Floodplains were delineated manually in ArcGIS Pro (Esri, 2022) using field transect data, DEMs, Sentinel imagery, and park boundaries (where applicable). For specifics on floodplain delineations of WBJ, EPC, SOK, and RTCO, see Ch 2, and for specifics for HWA, SDWA, LOR, and AGA, see Ch 3. A 10-m geodesic buffer was added to the floodplains to account for field and/or user error (Iskin and Wohl, 2023). Floodplains were generally drawn to exclude most of the human-impacted areas, but not all were excluded. No 10 m buffer was added to the DFWY and DWY floodplains because they are adjacent to each other and a buffer would have caused overlap. High elevation non-floodplain surfaces were removed from the SMT floodplain and agricultural areas were removed from the EIL floodplain using the *Erase* tool after the 10 m buffer was added. The YAK floodplain was obtained from Lininger et al. (2019)

and a 10 m buffer was added. The floodplain was then truncated to exclude the braided section upstream of the anastomosing section as there was an error in the Sentinel data in that region. Values and categories for each site are provided in Table 4.1. For this study, I assume that the metrics calculated from the classification are not very sensitive to the specific area that is being classified. For example, I assume that adding the 10 m buffer will not significantly affect the results.

4.3.1 Classification

Classification of the 15 study floodplains followed a similar workflow to Ch 3 and is detailed in Figure 4.3. The unsupervised classification was performed on 2022 Sentinel-2A mosaics, detrended highest resolution DEMs, and NDVI and NDMI rasters calculated from the Sentinel data (Supplemental Table 4.3). The inputs for the maximum number of classes for the tool to find were set to 50 (YAK; FPA > 2000 km^2), 30 (HWA, SMT, AGA, EIL, CSC; FPA > 5 km^2), 20 (WBJ, SDWA; FPA > 0.5 km^2), 10 (EPC, RTCO, NSV, LOR, DWY, DFWY; FPA < 0.5 km^2), and 5 (SOK). These values are subjective and were chosen to balance identifying more classes than were observed in the field without overclassifying the floodplains. The classifier delineated these maximum number classes for all sites expect EPC (set to 10, found 5) and RTCO (set to 10, found 9). The minimum size for a class was set to 4 pixels (each pixel is 10 m x 10 m in the appropriate Universal Transverse Mercator projections) and the sample interval was set to 2 pixels for all sites except YAK, as the tool could not classify the floodplain due to the large file size if set any lower than 6 pixels and 3 pixels.
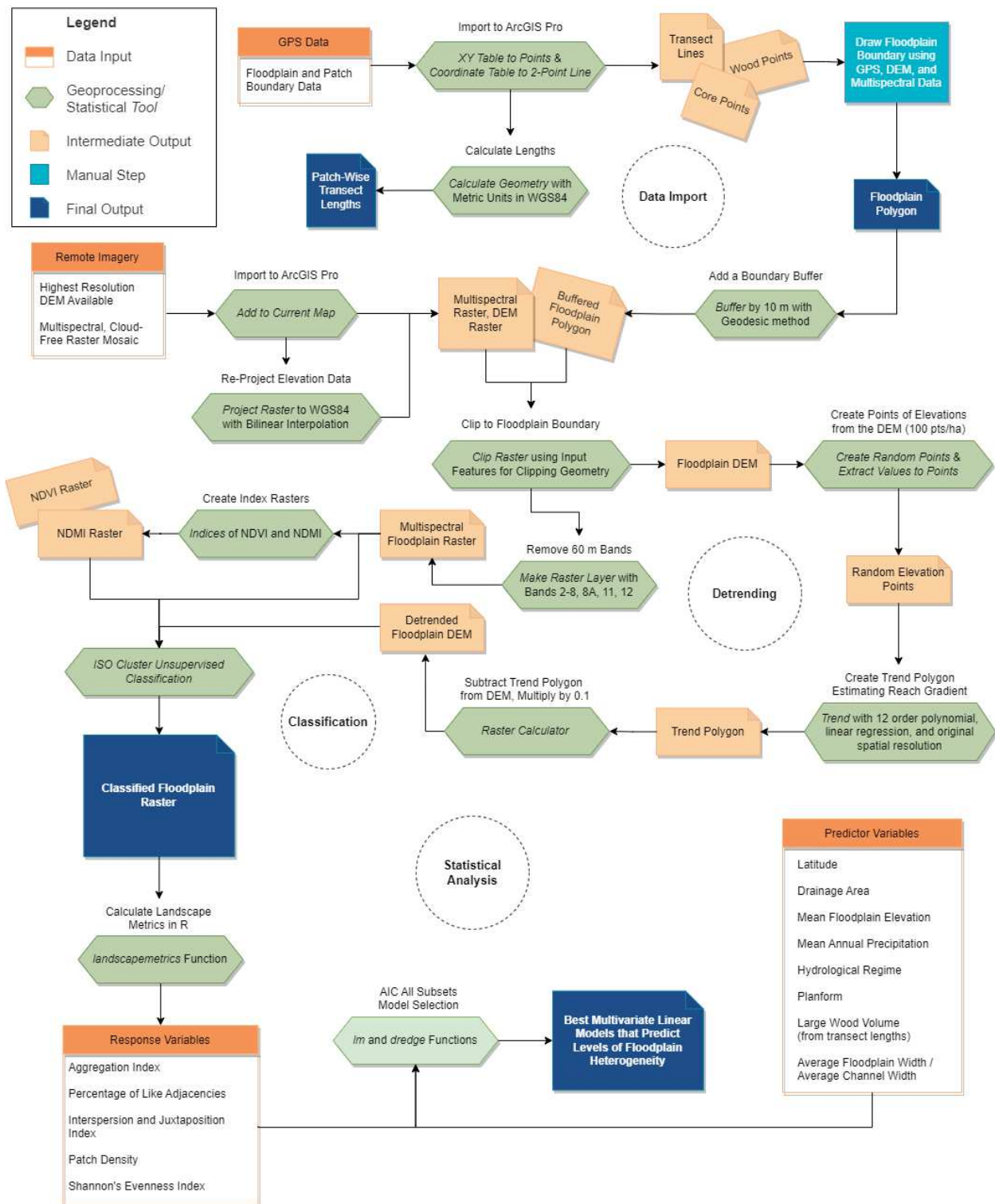
Figure 4.3. Analytical workflow completed in ArcGIS Pro and RStudio.

4.3.2 Statistical Analysis

For the statistical analysis, several values for each site were compiled: latitude (Lat) and longitude (Long), drainage area (DrA), floodplain area (FPA), floodplain perimeter (FPP), mean floodplain elevation (Elev), annual average precipitation (Precip), categorical flow regime (Flow), categorical planform (Plan), total sinuosity (TS), average transect large wood volume in (LWV), and average floodplain width per average channel width (FP/CH) (Table 4.1, 4.2). Although DWY and DFWY have somewhat overlapping drainage areas and floodplains, they were treated as independent sites in this analysis because they have distinct floodplain characteristics and originate from different upstream sources.

Table 4.1. Predictor variables and sources. Lat, Long, FPA, FPP, TS, and FP/CH are rounded to the nearest tenth; DrA and Precip are rounded to the nearest one; and Elev is rounded to the nearest ten.

River	Lat	Long	DrA	FPA	FPP	Elev	Precip	Flow	Plan	TS	FP/CH
Units	*DD*	*DD*	*km²*	*km²*	*km*	*m*	*mm*	*-*	*-*	*m/m*	*m/m*
WBJ	39.6	-104.3	653	1.1	6.5	1630	459	Rain	Braided	2.2	4.1
EPC	39.3	-104.9	192	0.02	0.6	1950	552	Snow	Straight	1.3	19.4
RTCO	39.1	-106.1	60	0.1	1.1	2950	591	Snow	Beaver	2.6	8.1
SOK	36.8	-96.4	31	0.1	2.2	300	994	Rain	Meandering	1.5	2.8
AGA	31.4	-81.6	36542	37.1	32.2	1	1233	Rain	Straight	1.2	19.3
HWA	47.8	-124	323	9.9	19	160	3984	Rain	Braided	4.1	7.0
SDWA	48	-123.9	101	0.6	6.1	420	3856	Rain	Meandering	1.5	7.0
LOR	44.2	-122.2	54	0.1	2.1	540	2341	Rain	Straight	1.3	3.2
YAK	65.9	-149.2	500329	2378.2	401.8	110	438	Snow	Anastomosing	13.3	7.5
SMT	47.9	-113.9	1540	26.2	65.2	960	1062	Snow	Anastomosing	4.8	12.5
CSC	33.8	-80.7	21918	106.1	53.8	30	1248	Rain	Meandering	2.0	59.2
EIL	38.9	-87.8	5496	6.2	21	130	1098	Rain	Meandering	2.2	25.9
DFWY	43.3	-109.6	62	0.2	2.2	2810	849	Snow	Anastomosing	5.6	17
DWY	43.3	-109.6	131	0.3	3.2	2810	834	Snow	Meandering	1.6	14.3
NSV	40.2	- 105.5	84	0.4	3.5	2540	935	Snow	Beaver	2.6	13.7
Scale		*Drainage Area*			*Study Reach*		*Drainage Area*	*Regional*		*Study Reach*	

DrA was obtained using StreamStats (USGS, 2023a) to delineate the contributing area upstream of the study reach, with the pour point specified as the downstream-most part of the study reach. The basin polygons were brought into ArcGIS Pro and the geodesic areas were calculated using *Calculate Geometry*. StreamStats is not available for interior Alaska or the state

of Wyoming, so the drainage basins for YAK, DFWY, and DWY were delineated in ArcGIS Pro using the *Watersheds (Ready to Use)* tool (Esri, 2023) with the default snap distance and finest data source resolution. Lat and Long were obtained from the pour points used to delineate the watersheds. FPA and FPP were obtained by calculating the geodesic areas and perimeters from the floodplain polygons. Elev was acquired from the DEM statistics.

Precip values were obtained from modeled average annual precipitation data for the coterminous U.S. (800 m resolution, 1991–2020 time period; PRISM, 2022), Alaska (800 m resolution, 1991–2020 time period; PRISM, 2018), and western Canada (2 km resolution, 1961–1990 time period; PRISM, 2002). The data were clipped to the respective drainage areas, and the mean values in millimeters were extracted from the raster statistics. Part of the YAK watershed is in Canada, so both the Alaska and western Canada PRISM data were used to calculate a mean precipitation value for the Yukon River. The *Mosaic to New Raster* tool was used to combine the Alaska and Canada rasters, specifying an 800 m cell size and that the Alaska cells should be kept in overlapping regions to preserve the detail of the smaller cells.

Flow was determined from visual inspection of 2021–2023 annual gage/discharge data for each site, and from nearby sites for ungaged streams (RTCO, SOK, SDWA) (USGS, 2023b). A snowmelt-dominated flow regime was assigned when the annual discharge had a few-months-long peak in the late spring/early summer, and a rainfall-dominated flow regime was assigned when the annual discharge had many short peaks in the year. There are no nearby gaging stations to WBJ, so it was assigned a rainfall-dominated flow regime because the drainage area is entirely on the plains and does not originate in the Rocky Mountains. There are also no nearby gaging stations to DWY and DFWY with a full year of data, so they were assigned snowmelt-dominated flow regimes because the drainage areas originate in the high elevations of the Wind River

Range. There is no nearby gaging station to NSV, so it was also assigned a snowmelt-dominated flow regime because the drainage area originates in the Rock Mountains.

Planform classifications reflect a continuum based on flow, sediment, and wood regimes (Schumm, 1985), but I chose one planform category for each site (straight, meandering, anastomosing, beaver, or braided) based on field experiences. I also calculated total sinuosity using base-flow imagery for each site available in Google Earth Pro as of March 2023 as a less subjective and numerical measure of planform characteristics. Both WBJ and HWA are transitioning (WBJ from braided to straight and HWA from braided to anastomosing), but I classified them both as braided for this analysis. Average FP/CH was calculated in ArcGIS Pro by measuring manually delineated floodplain widths and channel widths. Floodplain widths were measured perpendicular to the valley trend using the floodplain polygons. Channel widths were measured perpendicular to flow direction at the same locations as the floodplain widths using the Sentinel satellite imagery, DEMs, and ArcGIS Pro NAIP Hybrid base map where necessary. I excluded large anastomosing islands for YAK for channel widths, and included part of DFWY in the DWY measurements because it flows onto the DWY floodplain. The average bankfull channel width for NSV was calculated from field data because the beaver dams made discerning channels from imagery difficult.

LWV was calculated from field transect data from various sources that generally coincide with the delineated floodplains (Table 4.2) according to Van Wagner's method (1968). Large wood volume estimates should be considered minima for HWA because I could not access the channel or the river-left floodplain; SDWA and LOR because some jams on the transects were estimated with the box method (Livers et al., 2020); EPC because I encountered no wood on the three transects I walked; RTCO because the one transect did not include any of the beaver dams

present at the site; and AGA because the site was unexpectedly flooded during the field visit and

I could not access most of the floodplain.

Table 4.2. Floodplain large wood loads for the United States. These estimates include some instream wood at sites where the active channel was accessible by foot. Values are rounded to the nearest ten.

River	Median Transect Wood Load (m³/ha)	Range (m³/ha)	Number of Transects	Collected
West Bijou Creek	130	20–220	10	July and October 2020
East Plum Creek	0	No wood observed	3	September 2020
Rough and Tumbling Creek	0	No wood observed	1	August 2022
North St. Vrain Creek [1]	0	No wood observed	10	August 2010 and August 2018
Sand Creek	0	0–600	10	June 2021
Hoh River	2760	140–8820	7	July 2021
Sol Duc River	3900	800–18900	10	July 2021
Lookout Creek	4110	0–8660	10	July 2022
Altamaha River	10	0–140	4	October 2021
Embarrass River	1120	140–2220	4	March 2022
Swan River [2]	140	130–150	16	July 2017
Yukon River [3]	30	0–170	24 (patches)	June and July 2015
Downs Fork	30	10–50	6	July 2019
Dinwoody Creek	20	20–30	5	July 2019
Congaree River [4]	50	1–180	NA	October 2009

[1]Wohl and Cadol, 2011; Laurel and Wohl, 2019
[2]Wohl et al., 2018b
[3]Lininger et al., 2017 (Note: wood volumes do not include wood jams that were on the channel margins)
[4]Wohl et al., 2011

The classified floodplains and data from Table 4.1 were brought into R (R Core Team,

2023) and prepared for analysis and visualised using tools from the *tidyverse*, *raster*, *rasterVis*,

and *rgdal* packages (Wickham et al., 2019; Bivand et al., 2023; Hijmans, 2023; Lamigueiro and

Hijmans, 2023). Heterogeneity metrics were calculated using the *landscapemetrics* package

(Hesselbarth et al., 2019), the *coin* and *dunn.test* packages were used to compare medians

(Hothorn, 2008; Dinno, 2017), and the *car* package was used to compare variances (Fox and

Weisberg, 2019). The *tidymodels* package was used to perform the model fitting (Kuhn and

Wickham, 2020).

The Flow variable was ordered by flashiness (Snow < Rain) and the Plan variable was ordered by channel mobility (Straight < Meandering < Anastomosing < Beaver < Braided). The continuous predictor variables are compared to the heterogeneity metrics via correlation, and the planform and flow predictor variables are first compared to the heterogeneity metrics using boxplots and non-parametric comparisons of medians and variances. The nonparametric method of leave-one-out cross-validation (LOOCV) is then used to fit and choose multivariate models with the heterogeneity metrics as the response variables in turn. The LOOCV model selection is iterative and is ultimately based on choosing the model with the highest LOOCV R^2 value. These analyses include all 15 data points and none of the variables are transformed.

4.4 Results

The 15 classified floodplains from across the country are presented in Figure 4.4 and through a quantitative comparison of the heterogeneity metrics for each floodplain. Correlations and pairwise comparisons of heterogeneity between the levels of the categorical variables are provided, and the LOOCV multivariate models are presented. H1–H5 are discussed first with qualitative results and then with the model results. To summarize the results, floodplain heterogeneity is significantly related to river corridor characteristics and some heterogeneity metrics are also significantly related to each other.

4.4.1 Classification

The classified floodplains for all sites are provided in Figure 4.4. The classifications for HWA, SDWA, LOR, and AGA come from Ch 3, and the floodplain polygons used for WBJ, EPC, SOK, and RTCO come from Ch 2. Detail insets are provided for floodplains with an area $\geq$ 10 km^2. The YAK floodplain is the largest floodplain in this study (2,380 km^2) and spans nine DEM tiles from three different years (Supplemental Table 4.3).
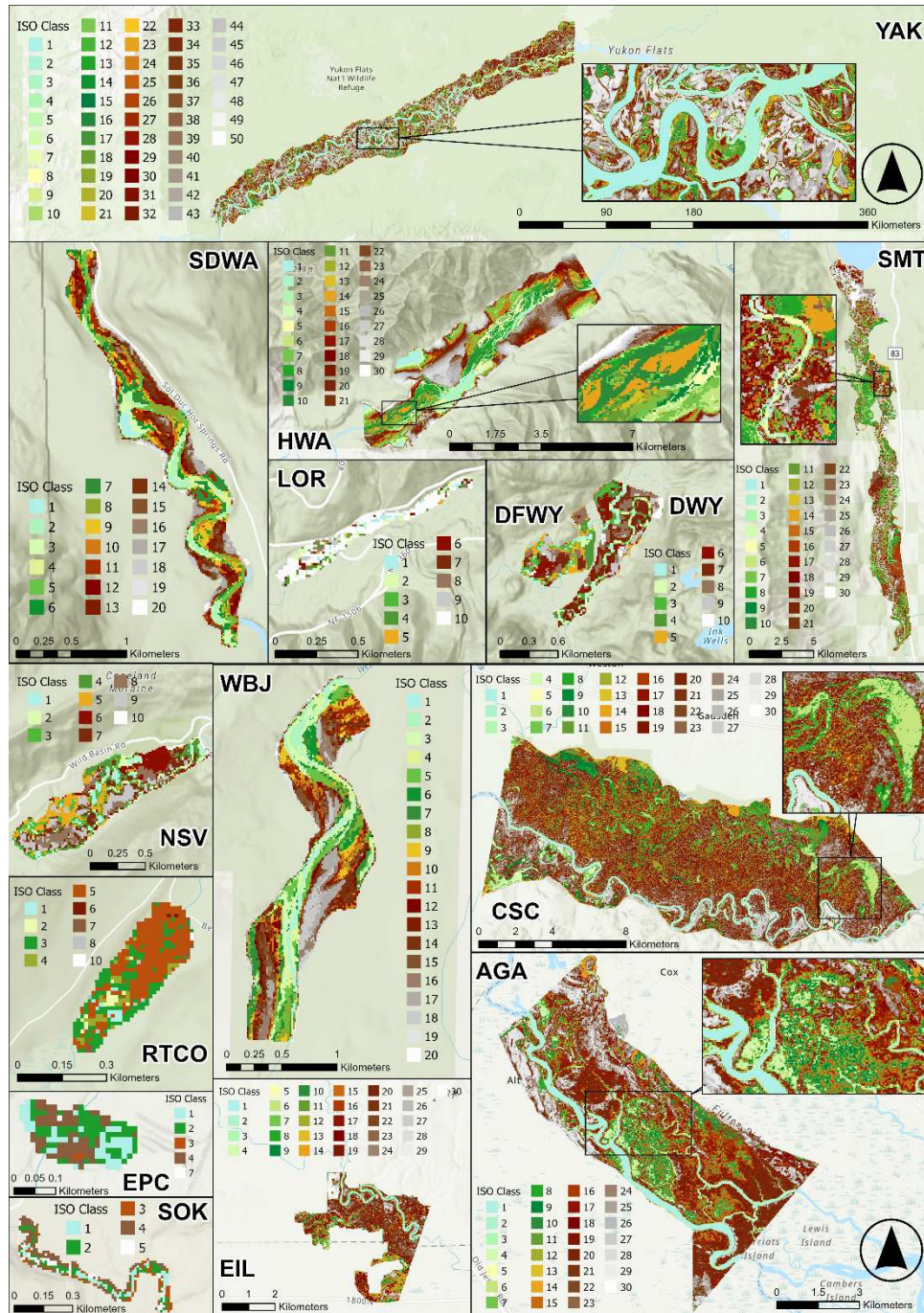
Figure 4.4. ISO unsupervised classification results for Regions 1–5: Yukon River, Alaska (YAK; with detail inset); Sol Duc River, Washington (SDWA); Hoh River, Washington (HWA; with detail inset); Swan River, Montana (SMT; with detail inset); Lookout Creek, Oregon (LOR); Downs Fork, Wyoming (DFWY); Dinwoody Creek, Wyoming (DWY); North St. Vrain Creek, Colorado (NSV); Rough and Tumbling Creek, Colorado (RTCO); West Bijou Creek, Colorado (WBJ); East Plum Creek, Colorado (EPC); Sand Creek, Oklahoma (SOK); Embarrass River, Illinois (EIL); Congaree River, South Carolina (CSC; with detail inset); and Altamaha River, Georgia (AGA; with detail inset). ISO classes are not equal to field classes.

4.4.2 Exploratory Statistics

First, I present the overall median values of floodplain heterogeneity and discuss relationships between the heterogeneity metrics. These floodplains have median AI of 58.8%, median IJI of 74.9%, median PD of 1241 patches/ha, median PLADJ of 58.5%, and median SHEI of 0.934 (Table 4.3). AI ranges from 46.9% for SOK to 75.7% at YAK. IJI ranges from 55.2% at EPC to 96.6% at SOK. PD ranges from 490 patches/100ha at YAK to 1870 patches/100ha at SDWA. PLADJ ranges from 48.6% at SOK to 75.6% at YAK. SHEI ranges from 0.554 at RTCO to 0.973 at WBJ and HWA. These results indicate that natural floodplains have moderate aggregation of classes, high evenness and intermixing of classes, and a wide range of patch densities.

Table 4.3. Calculated heterogeneity metrics for each site. Color scales represent red = 25%, yellow = 50%, and green = 75% of the metric's range, excluding PD. The PD color scale represents red = lowest value, yellow = 50th percentile, and green = highest value. AI, IJI, and PLADJ are rounded to the nearest tenth, PD is rounded to the nearest one, and SHEI is rounded to the nearest hundredth.

River	AI (%)	IJI (%)	PD (patches/100 ha)	PLADJ (%)	SHEI
WBJ	56.7	80.2	1328	55.4	0.973
EPC	60.6	55.2	1168	56.7	0.721
RTCO	65.8	55.8	1241	64.1	0.554
SOK	46.9	96.6	1823	48.6	0.972
AGA	58.8	73.3	1213	58.5	0.934
HWA	66.0	71.6	855	65.3	0.973
SDWA	50.8	79.9	1866	49.5	0.967
LOR	57.4	74.9	1698	58.6	0.639
YAK	75.7	73.4	491	75.6	0.966
SMT	50.8	78.9	1819	50.6	0.962
CSC	52.3	73.2	1578	52.1	0.922
EIL	55.7	71.7	1335	55.2	0.906
DFWY	69.5	78.3	832	67.0	0.927
DWY	60.2	79.3	1217	58.9	0.917
NSV	61.4	83.4	1148	60.1	0.957
Median	**58.8**	**74.9**	**1241**	**58.5**	**0.934**

Some of the heterogeneity metrics demonstrate high collinearity with each other, as shown in fitted linear models in Equations 4.1–4.3 and pairwise scatter plots in Supplemental

Figure 4.3 (bold values in the equations represent p-values < 0.05 for the models and individual predictors). The results show that PLADJ describes 97% of the variability in AI, indicating that perhaps only one of these metrics is necessary to capture the level of aggregation in a landscape. The opposite relationship between the AGG metrics and PD makes intuitive sense as one would expect an increase in the number of patches to decrease class aggregation (Eq. 4.1, 4.3). Because AI and PLADJ are highly correlated, AI will be the only aggregation metric discussed going forward.

$$AI = -\mathbf{0.018} \times \mathbf{PD} + \mathbf{83.00}; \text{ Multiple } R^2 = \mathbf{0.88} \qquad (4.1)$$

$$AI = \mathbf{1.04} \times \mathbf{PLADJ} - 1.54; \text{ Multiple } R^2 = \mathbf{0.97} \qquad (4.2)$$

$$PD = -\mathbf{49.97} \times \mathbf{PLADJ} + \mathbf{4226.34}; \text{ Multiple } R^2 = \mathbf{0.84} \qquad (4.3)$$

Correlation tables were calculated for all the predictor and response variables in this study. Correlations were calculated for n = 15 (Table 4.4) to look at numerical relationships. As Table 4.4 shows, there is some collinearity in the set of predictor variables, particularly Lat, Long, FPA, FPP, and TS. This intuitively makes sense as the variables are interconnected (Figure 4.1). Because of this, I removed Lat, Long, FPA, and FPP to get a final suite of predictor variables of DrA, Elev, Precip, TS, LWV, FP/CH, Flow, and Plan. I kept TS because it is the only numerical indicator of channel planform. The correlations show that FP/CH is weakly negatively correlated with AI, not supporting H1. LWV is weakly negatively correlated with AI and SHEI, and weakly positively correlated with PD, partially supporting H2. DrA is strongly positively correlated with AI, weakly positively correlated with SHEI, and strongly negatively correlated with PD. Precip is weakly positively correlated with PD and SHEI, and weakly negatively correlated with AI. TS follows the same trends as DrA, partially supporting H3. This

makes sense as these two predictor variables are strongly positively correlated. Elev is weakly

negatively correlated with SHEI, PD, and IJI, and weakly positively correlated with AI.

Table 4.4. Correlations between continuous variables with all sites (n = 15). Red indicates a correlation ≤ -0.75 and green represents a correlation ≥ 0.75.

	Lat	Long	DrA	FPA	FPP	Elev	Precip	TS	LWV	FP/CH	AI	IJI	PD
Lat													
Long	-0.94												
DrA	0.76	-0.59											
FPA	0.78	-0.62	1.00										
FPP	0.77	-0.57	0.99	0.99									
Elev	-0.12	-0.02	-0.29	-0.27	-0.34								
Precip	0.15	-0.28	-0.23	-0.23	-0.22	-0.43							
TS	0.84	-0.68	0.89	0.90	0.91	-0.11	-0.19						
LWV	0.23	-0.38	-0.17	-0.16	-0.18	-0.38	0.87	-0.19					
FP/CH	-0.41	0.60	-0.10	-0.10	-0.03	-0.17	-0.17	-0.15	-0.29				
AI	0.52	-0.51	0.58	0.58	0.51	0.32	-0.18	0.68	-0.17	-0.17			
IJI	0.01	0.02	-0.05	-0.05	-0.04	-0.21	0.10	-0.02	0.03	-0.21	-0.43		
PD	-0.42	0.35	-0.57	-0.56	-0.51	-0.23	0.23	-0.64	0.31	0.05	-0.94	0.34	
SHEI	0.18	0.00	0.18	0.17	0.23	-0.34	0.13	0.25	-0.15	0.09	-0.17	0.68	-0.07

Comparing median heterogeneity values among the categorical variables of Plan (Figure

4.6) and Flow (Figure 4.7), there are no significant differences in medians (Wilcoxon Rank Sum,

Wilcoxon Rank Sum with ties, and Kruskal-Wallis Rank Sum test p-values all > 0.05). There are

also no significant differences in heterogeneity variances by Flow (Levene's test p-values >

0.05), but there are significant differences in variances for SHEI by Plan (Levene's test p-values

< 0.05).
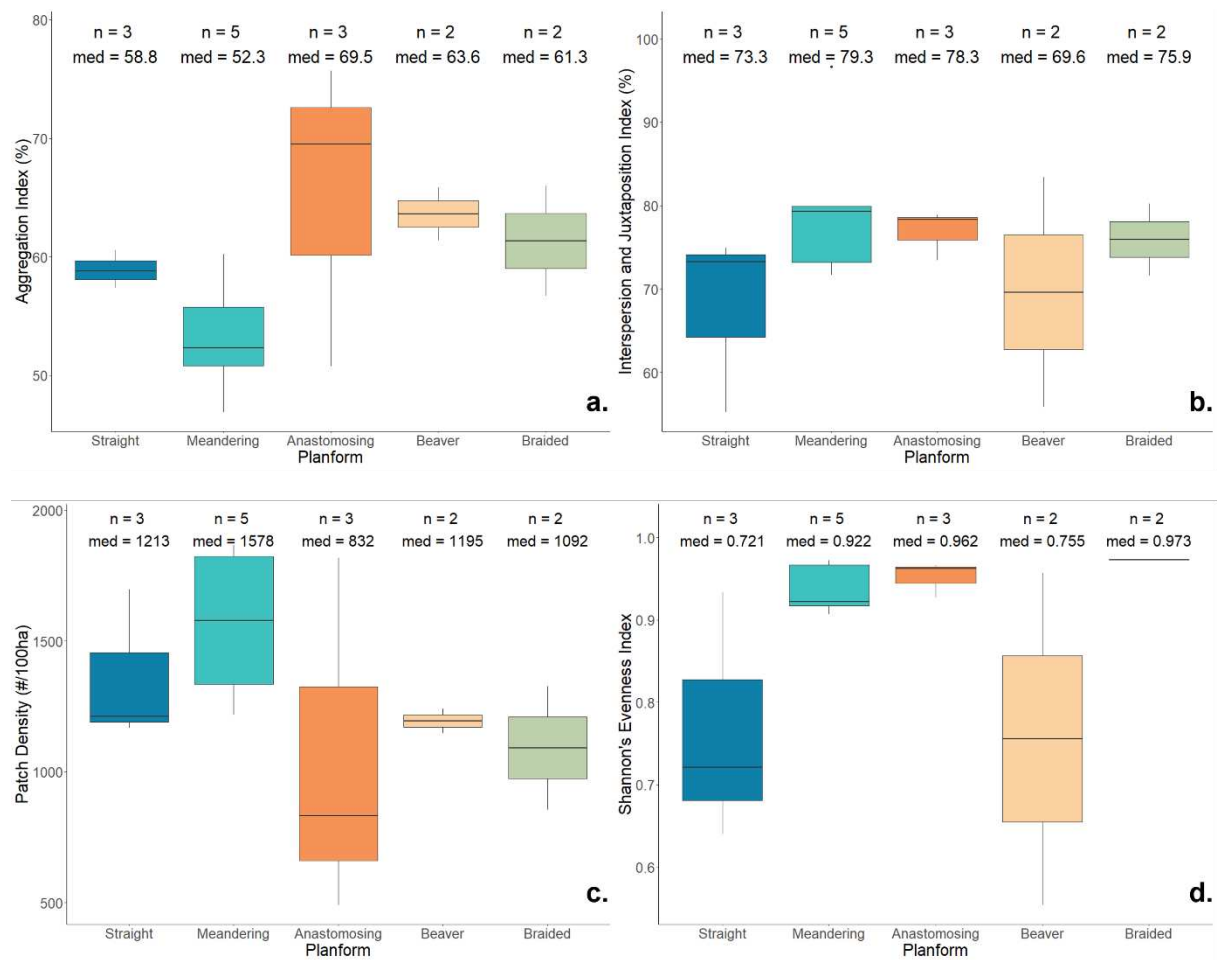
Figure 4.6. Pairwise comparisons of heterogeneity metrics by reach-scale channel planform for a) AI, b) IJI, c) PD, and d) SHEI. There are no statistical differences in medians.
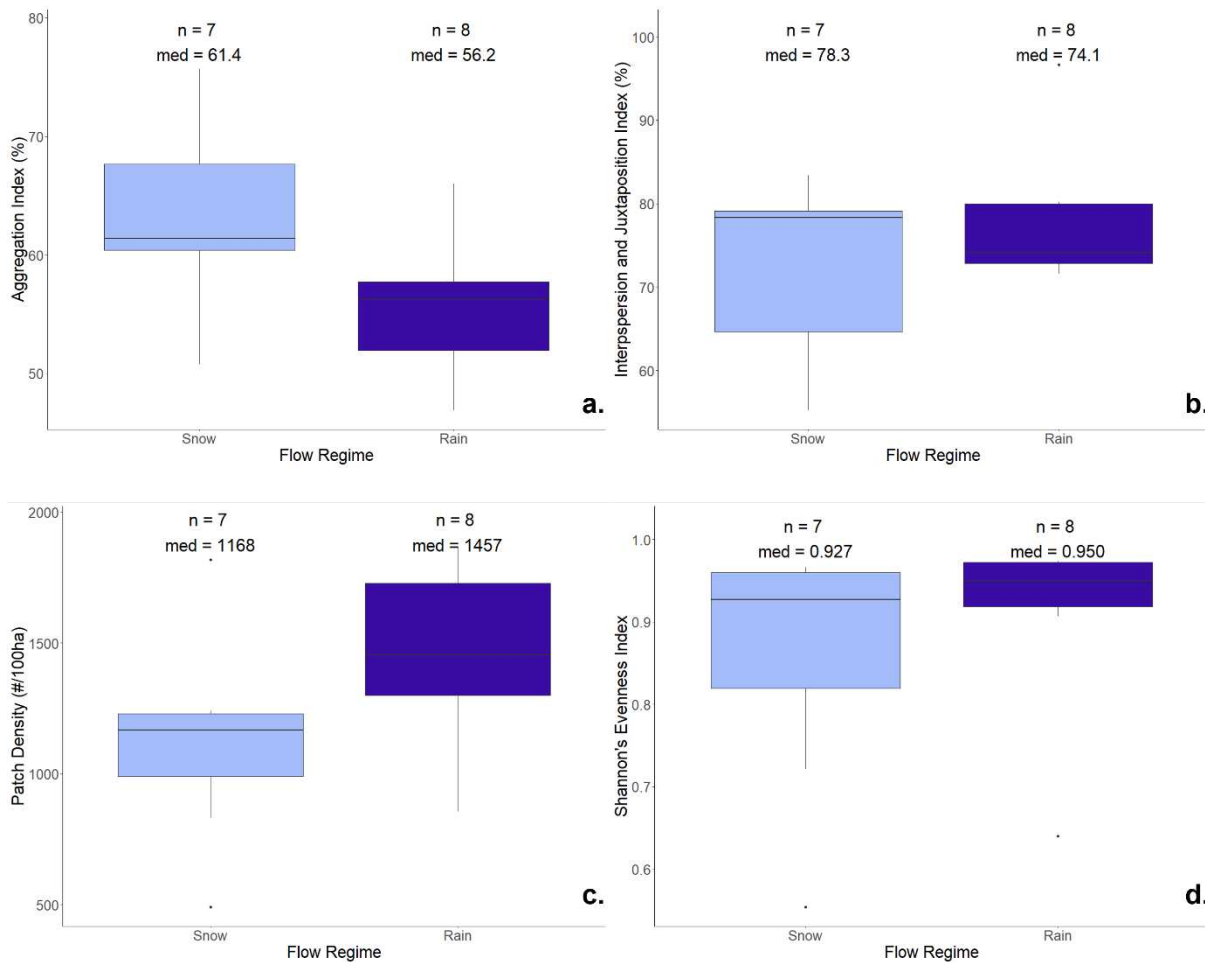
Figure 4.7. Pairwise comparisons of heterogeneity metrics by watershed-scale flow regime for a) AI, b) IJI, c) PD, and d) SHEI. There are no statistical differences in medians.

Although there are no significant differences in medians, I can draw qualitative inferences in relation to the conceptual model-based hypotheses (H3–H5). H3 proposed that IJI, SHEI and PD would increase with increasing channel mobility (not including beaver-modified planforms). Figure 4.6b shows that straight planforms (least mobile) generally have lower IJI than the other planform types, supporting H3. Figure 4.6c shows that meandering planforms have greater PD than straight planforms, but that anastomosing and braided planforms (most mobile) have lower PD than all the others, partially supporting H3. Figure 4.6d shows that median SHEI increases from least mobile to most mobile planforms, supporting H3. H3 also proposed that AGG would decrease with channel mobility. From Figure 4.6a, meandering planforms have the

lowest AI and straight, anastomosing, and braided planforms have similar and higher AI. This only partially supports H3, as straight planforms have higher AI than meandering, but anastomosing and braided planforms also have greater AI than meandering. Overall, H3 is primarily supported by the data, but inclusion of more sites in each planform category would strengthen future analyses.

Similar to H3, H4 proposed that IJI, SHEI and PD would increase and AGG would decrease with increasing flow regime flashiness. Figures 4.7b,d show that median IJI and SHEI are similar for snowmelt (less flashy) and rainfall (flashier) flow regimes, not supporting H4. Figure 4.7c, however, shows increasing PD with increasing flashiness of the flow regime, supporting H4. Figure 4.7a shows that AI decreases with increasing flashiness, supporting H4. Overall, I conclude that H4 is partially supported by the data.

H5 proposed that AGG and PD would be higher and IJI would be lower for beaver-modified planforms vs. non-beaver planforms. Figure 4.6a shows that beaver planforms have higher AI than straight and anastomosing planforms, partially supporting H5. Figure 4.6c shows that beaver planforms have lower PD than meandering planforms, not supporting H5. Figure 4.6b shows no discrimination between IJI for different planform types, not supporting H5. Overall, I conclude that H5 is not supported by the data.

4.4.3 Multivariate Models

Multiple attempts using standard methods for multivariate linear analysis led to overfitting and little applicability beyond my dataset of 15 sites. Instead, I used a non-parametric method of model fitting that guards against overfitting and can provide insights into important predictors of floodplain heterogeneity. The final LOOCV models are presented in Table 4.5. Boxplots of the estimates for each predictor variable for each model are given in Supplemental

99

Figures 4.4–4.7. Predictor values are considered "important" (as opposed to statistically significant) if the interquartile range of the boxplots does not include zero and the range of the boxplots are reasonably narrow.

The results show that 45% of the variability in AI can be explained by the full model: the combination of DrA, Elev, Precip, TS, LWV, FP/CH, Plan, and Flow. DrA, Elev, FP/CH, Plan and Flow are important in this model, with smaller drainage areas, higher elevations, and greater floodplain width ratios corresponding to larger AI values, supporting H1. Straight planforms have higher AI than anastomosing, beaver, and braided planforms, partially supporting H3. Rainfall dominated flow regimes have higher AI than snowmelt dominated ones, not supporting H4. LWV can explain 77% of the variability in IJI. The combination of DrA, TS, LWV, and Plan can explain 48% of the variability in PD. All of these predictor variables are important in this model, with larger drainage areas, higher large wood volumes, and lower total sinuosity corresponding to larger PD values, supporting H2. Straight planforms have lower PD than anastomosing and braided planforms, supporting H3. Lastly, Precip can explain 59% of the variability in SHEI and is important in this model, with greater annual average precipitation over the drainage area corresponding with an increase in SHEI. Table 4.6 summarizes support of hypotheses 1–5 from the qualitative and quantitative results.

Table 4.5. Leave-one-out cross-validation multivariate models and R^2 values.

Response Variable	Predictor Variables	LOOCV R^2
AI	DrA + Elev + Precip + TS + LWV + FP/CH + Plan + Flow	0.45
IJI	LWV	0.77
PD	DrA + TS + LWV + Plan	0.48
SHEI	Precip	0.59

Table 4.6. Summary of support for study hypotheses

Hypothesis	Result
H1: ↑ in AGG, ↓ in PD with ↑ in FP/CH	Partially Supported
H2: ↑ in AGG, IJI, PD, SHEI with ↑ LWV	Supported
H3: ↑ in IJI, PD, SHEI, ↓ in AGG with ↑ mobility	Supported
H4: ↑ in IJI, PD, SHEI, ↓ in AGG with ↑ flashiness	Partially Supported
H5: ↑ in AGG and PD, ↓ in IJI for beaver planforms	Not Supported

4.5 Discussion

Although a sample size of 15 is small in the realm of statistics, these were hard-won data points from three years of field work and both the qualitative and LOOCV analyses provide a launching point for future study. More work could be done to (i) identify a more robust way to choose the maximum number of classes in the unsupervised classification workflow, as it is known that these metrics are sensitive to the number of classes used (Huang et al., 2006), and (ii) test whether the delineated floodplain area significantly affects the metrics. Additionally, even with Blend mosaicking, the boundaries between the YAK DEM tiles from 2016 and 2017 are visible in the final classification. Ways to reduce discrepancies in the satellite data could be further investigated as well. That said, the results from the classification workflow are straightforward and are discussed at length in Ch 2 and 3, so the following discussion addresses both the qualitative results from the boxplot comparisons and quantitative results from the LOOCV model fitting. Qualitatively, H2 and H3 are supported, H1 and H4 are partially supported, and H5 is not supported by the results. Quantitatively, river corridor characteristics can explain 45-77% of the variability in floodplain heterogeneity. These results can provide insights into the fluvial processes that create and maintain floodplain heterogeneity. An important caveat on this discussion is that some variables potentially relevant to channel lateral mobility and thus floodplain spatial heterogeneity, such as discharge, sediment load in the

channel (Constantine et al., 2014), or floodplain stratigraphy (Güneralp and Rhoads, 2011b), were not quantified in this study.

The main controls of floodplain spatial heterogeneity are the space a river has available and the mobility of the channel across its floodplain (Figure 4.1). The predictor variables were chosen specifically to capture different fluvial processes that relate to and affect space and mobility. Determining the specific controls of floodplain heterogeneity within channel mobility and space available is complex, especially with a small sample size. The non-statistically significant boxplot comparisons show that there may be differences in heterogeneity between planform and flow regime types. The low sample sizes at the individual levels of the categorical variables are probably obscuring potential differences in heterogeneity between channel planforms and flow regimes. This could be investigated by including additional sites from each of the levels of Plan and Flow. I will not discuss pairwise comparisons in a process-based framework due to the lack of statistical significance. The main takeaways from the exploratory analysis are the general trends seen across sites of moderate aggregation, high interspersion and evenness, and varying patch density. Future work could focus on establishing thresholds for these metrics, such as between planform types of natural floodplains and for natural vs. degraded floodplains.

Shifting focus to the quantitative results, I find that DrA, Elev, Precip, TS, LWV, FP/CH, Plan, Flow all influence floodplain heterogeneity. This important finding supports the idea that heterogeneity is complex and reflects the influence of many fluvial processes. Additionally, no model is the same (Table 4.5), indicating that the metrics are capturing difference facets of floodplains heterogeneity and that it may be important to consider all four metrics when assessing a floodplain's heterogeneity across space and through time.

I infer that channel mobility in the form of planform and total sinuosity influences floodplain heterogeneity, and that there is (1) a difference in aggregation between straight and all other planforms, (2) a difference in patch density between straight and the most mobile planforms (anastomosing and braided), and (3) that patch density decreases with increasing total sinuosity. This is an interesting result as we would expect increasing channel mobility (straight < meandering < anastomosing < braided) to be positively related to increasing total sinuosity (Hong and Davies, 1979), but we see the opposite trend with patch density, a pattern that remains to be explained. Channel planform reflects differences in rates and styles of lateral mobility and associated patchiness of the floodplain. Meandering channels, for example, move in predictable directions, with meander migration toward the outside of each bend and episodic cutoffs. Braided channels are more likely to experience avulsion (e.g., Ashmore, 2009) rather than gradual lateral migration and to create a three-dimensional mosaic of floodplain topography and stratigraphy rather than the meander-scroll topography and fining upward stratigraphy characteristic of meandering rivers (Miall, 1977). Previous studies suggest that channel planform integrates the effects of flow regime, sediment dynamics, large wood load, and floodplain vegetation, so it makes sense that channel planform is an important factor influencing reach-scale floodplain heterogeneity in this analysis. To return to the conceptual model, channel planform reflects differences in lateral mobility and space available in that braided, anastomosing, and meandering channels require a greater minimum floodplain width to develop when compared to straight channels. Future study could investigate the relationships between categorical planform, total sinuosity, and patch density. An additional predictor that may help illuminate these connections could be rate of change through time to examine the magnitude and direction of heterogeneity in relation to channel mobility.

I also infer that space available in the form of drainage area and floodplain width ratio exerts an influence on floodplain heterogeneity, and that (1) aggregation decreases with increasing drainage area, (2) aggregation increases with floodplain width ratio, and (3) patch density increases with drainage area. Once again, this is an interesting result as drainage area and floodplain width ratio exhibit opposite trends in relation to aggregation. This supports previous studies that show that reach-scale variations in valley-floor width and floodplain area can create substantial variations in the relationship between drainage area and floodplain width (e.g., Wohl et al., 2017). Greater drainage areas are more likely to have large flood magnitudes and therefore increasing disturbance of at least the channel-proximal portions of the floodplain, leading intuitively to the relationship with increased patch density. Wider floodplains are more likely to have portions farther from the contemporary active channel that have long turnover times (Konrad, 2012) and may experience homogenization through vegetation succession and prolonged vertical accretion, as reflected in greater aggregation for greater floodplain width ratios. These results suggest that healthy river beads are very important to floodplain heterogeneity (Wohl et al., 2018a).

The variables of average annual precipitation, mean floodplain elevation, and categorical flow regime were all chosen to constrain discharge characteristics. The results show that (1) aggregation increases with elevation, (2) aggregation is higher for rainfall dominated flow regimes, and (3) Shannon's evenness increases with precipitation. I expect increasing elevation to correspond with greater likelihood of snowmelt-dominated flow regimes and therefore less flashy systems and less floodplain disturbance due to colder winters. I see this reflected in aggregation increasing with elevation but not with higher aggregation for rainfall vs. snowmelt. This suggests that elevation may not be an effective proxy for snowmelt vs rainfall dominated

flow regimes, and that the relationship between aggregation and elevation could more strongly

reflect other vegetation dynamics rather than fluvial disturbances caused by different flow

regimes. Lower aggregation for snowmelt systems could be due to the shorter growing season

and reduced time for vegetation succession each year, resulting in less aggregated areas of

vegetation. Evenness increasing with precipitation could reflect more evenly distributed

resources for vegetation through higher groundwater levels across the floodplain (Zeng et al.,

2019). Clearly, the relationships between elevation, precipitation, and flow regime need more

study. Future study could use other proxies for flow regime, such as annual mean and range of

temperature paired with precipitation and snow water equivalent, or direct measurements of flow

regime such as mean annual flow, maximum annual flow, and base flow.

Large wood volume exerts an important influence on floodplain heterogeneity and is

related to heterogeneity by (1) explaining 77% of the variability in interspersion and

juxtaposition and (2) increasing patch density with large wood volume. It makes intuitive sense

that large wood would increase patch density as wood can increase channel bifurcation and

avulsion, island formation, planform complexity, and patchiness of floodplain forests (Collins et

al., 2012). The primary effects of large wood in river corridors can be complex, however, as

large wood can also reduce near-bank velocity and shear stress and reduce channel mobility

(Daniels and Rhoads, 2003). Increasing the spatial detail of the large wood metric may shed light

on the effects of large wood on floodplains, especially as large wood was once living trees and

wood volumes reflect complex interactions between climate, habitat, and channel dynamics

(Benda and Sias, 2003), shown simply in the strong positive relationship between precipitation

and large wood volume (Table 4.4). This dataset only includes wood volume per area from a

limited number of transects and does not include the spatial distribution or concentration (e.g.,

jams) of the wood on the floodplain. Wood loads can be dynamic in space and time (Wohl, 2013; Iroumé et al., 2015; Villanueva et al., 2016; Tonon et al., 2017; Wohl et al., 2019) and the distribution of wood in a channel or floodplain can change substantially over 1–2 years (Wohl and Iskin, 2022). This highlights the need for more detailed study of large wood on floodplains to determine its effect on fluvial processes as related to floodplain heterogeneity. Isolating the category of large wood and including characteristics such as percentage of wood load in jams vs individual pieces, average distance between floodplain jams, average piece diameter, average piece length, and piece decay and/or burn class may allow for a more detailed understanding of the relationship between large wood and floodplain heterogeneity.

4.6 Conclusion

The results show that different facets of floodplain heterogeneity can be quantified with metrics from landscape ecology and that the patterns across the United States are varied and related to complex and dynamic fluvial processes. Although floodplain heterogeneity is a complex concept, there are some emergent trends from the LOOCV model results that are easily interpretable, even with a sample size of 15. Qualitatively, I find that space available (measured by drainage area and floodplain width ratio) and channel mobility (measured by channel planform and flow regime) are related to floodplain heterogeneity, and that natural floodplains in the United States have moderate aggregation, high interspersion and evenness, and a range of patch densities. Quantitatively, I find that drainage area, elevation, total sinuosity, floodplain width ratio, large wood volume, planform, and flow regime all influence floodplain heterogeneity and can explain 45-77% of the variability in aggregation, interspersion, patch density, and evenness.

These findings can inform how river corridors can be managed in a way to protect the processes that create and maintain floodplain heterogeneity, and how floodplains might change due to climate change. River corridor management and restoration can benefit from knowing the main controls of floodplain heterogeneity. Although management and restoration cannot target drainage area, elevation or precipitation, they can target aspects related to natural flow, sediment, and wood regimes that affect sinuosity, floodplain width ratio, large wood volume, planform, and flow regime. Climate change is predicted to affect all the controls of floodplain heterogeneity, especially species distribution across latitude and elevation (Gray and Hamann, 2013) and habitat refugia (Michalak et al., 2018). The predicted effects of climate change are complex, and the results of this study highlight the need for additional investigation into how climate change will specifically affect floodplains and functional heterogeneity that sustain river ecosystems.

For natural corridors, I highlight the fact that it is difficult to isolate individual characteristics from each other (such as flow regime and elevation), because they commonly have dependent effects and are controlled by currently unidentified thresholds (e.g., does large wood volume influence planform, reflect planform, or both?). The results presented here represent the beginning of cross-site investigations into floodplain heterogeneity, and the story that will unfold is bound to be interesting. Future research should focus on natural sites where it is possible to keep all/most of the characteristics consistent except for the variable of interest and compare floodplain heterogeneity related to that specific variable. For example, the Dinwoody Creek and Downs Fork sites in Wyoming occur adjacent to each other, so they have similar latitudes, elevations, precipitation, and flow regimes. The main distinguishing factor for these sites is that Dinwoody Creek has a straight planform, whereas Downs Fork has a history of

glacier-outburst floods, creating an anastomosing planform. Searching for regions with sites like this would be an effective way to investigate the effects of specific controls on floodplain spatial heterogeneity.

4.7 References

Aguiar, F.C., Ferreira, M.T.A., Segurado, P., 2009. Structural and functional responses of riparian vegetation to human disturbance: performance and spatial scale-dependence. *Fundamental and Applied Limnology* 175(3), 249–267. https://doi.org/10.1127/1863-9135/2009/0175-0249

Appling, A.P., Bernhardt, E.S., Stanford, J.A., 2014. Floodplain biogeochemical mosaics: A multidimensional view of alluvial soils. *Journal of Geophysical Research: Biogeosciences* 119(8), 1538–1553. https://doi.org/10.1002/2013JG002543

Ashmore, P., 2009. Intensity and characteristic length of braided channel patterns. *Canadian Journal of Civil Engineering* 36(10), 1656–1666. https://doi.org/10.1139/L09-088

Baartman, J.E.M., Masselink, R., Keesstra, S.D., Temme, A.J.A.M., 2013. Linking landscape morphological complexity and sediment connectivity. *Earth Surface Processes and Landforms* 38(12), 1457–1471. https://doi.org/10.1002/esp.3434

Barry, R., Chorley, R., Barry, R. G., Chorley, T. late R., 2004. Atmosphere, Weather and Climate (8th ed.). Routledge. https://doi.org/10.4324/9780203428238

Beighley, R.E., Gummadi, V., 2011. Developing channel and floodplain dimensions with limited data: a case study in the Amazon Basin. *Earth Surface Processes and Landforms* 36(8), 1059–1071. https://doi.org/10.1002/esp.2132

Bellmore, J.R., Baxter, C.V., 2014. Effects of Geomorphic Process Domains on River Ecosystems: A Comparison of Floodplain and Confined Valley Segments. *River Research and Applications* 30(5), 617–630. https://doi.org/10.1002/rra.2672

Bellmore, J.R., Baxter, C.V., Martens, K., Connolly, P.J., 2013. The floodplain food web mosaic: A study of its importance to salmon and steelhead with implications for their recovery. *Ecological Applications* 23(1), 189–207. https://doi.org/10.1890/12-0806.1

Benda L.E., Sias, J.C., 2003. A quantitative framework for evaluating the mass balance of in-stream organic debris. *Forest Ecology and Management* 172, 1-16. https://doi.org/10.1016/S0378-1127(01)00576-X

Benke, A.C., 2001. Importance of flood regime to invertebrate habitat in an unregulated river – floodplain ecosystem. *Journal of the North American Benthological Society* 20(2), 225–240. https://doi.org/10.2307/1468318

Bhowmik, N.G., 1984. Hydraulic geometry of floodplains. *Journal of Hydrology* 68(1–4), 369–374, 377–401. https://doi.org/10.1016/0022-1694(84)90221-X

Bivand, R., Keitt, T., Rowlingson, B., 2023. rgdal: Bindings for the "Geospatial" Data Abstraction Library, ver 1.6-4. https://cran.r-project.org/package=rgdal

Choné, G., Biron, P.M., 2016. Assessing the Relationship Between River Mobility and Habitat. *River Research and Applications* 32(4), 528–539. https://doi.org/10.1002/rra.2896

Ciszewski, D., Grygar, T.M., 2016. A Review of Flood-Related Storage and Remobilization of Heavy Metal Pollutants in River Systems. *Water, Air, & Soil Pollution* 227, 239. https://doi.org/10.1007/s11270-016-2934-8

Collins, B.D., Montgomery, D.R., Fetherston, K.L., Abbe, T.B., 2012. The floodplain large-wood cycle hypothesis: A mechanism for the physical and biotic structuring of temperate forested alluvial valleys in the North Pacific coastal ecoregion. *Geomorphology* 139–140, 460–470. https://doi.org/10.1016/j.geomorph.2011.11.011

Constantine, J.A., Dunne, T., Ahmed, J., Legleiter, C., Lazarus, E.D., 2014. Sediment supply as a driver of river meandering and floodplain evolution in the Amazon Basin. *Nature Geoscience* 7, 899–903. https://doi.org/10.1038/ngeo2282

Daniels, M.D., Rhoads, B.L., 2003. Influence of a large woody debris obstruction on three-dimensional flow structure in a meander bend. *Geomorphology* 51(1–3), 159–173. https://doi.org/10.1016/S0169-555X(02)00334-3

Dinno, A., 2017. dunn.test: Dunn's Test of Multiple Comparisons Using Rank Sums, ver 1.3.5. https://CRAN.R-project.org/package=dunn.test

Doering, M., Freimann, R., Antenen, N., Roschi, A., Robinson, C.T., Rezzonico, F., Smits, T.H.M., Tonolla, D., 2021. Microbial communities in floodplain ecosystems in relation to altered flow regimes and experimental flooding. *Science of the Total Environment* 788, 147497. https://doi.org/10.1016/j.scitotenv.2021.147497

Esri, 2023. Watershed (Ready To Use). *ArcGIS Pro 3.0 Help: Hydrology toolset*. https://pro.arcgis.com/en/pro-app/latest/tool-reference/ready-to-use/watershed.htm (accessed 2.11.23).

Esri, 2022. ArcGIS Pro. https://www.esri.com/en-us/arcgis/products/arcgis-pro/overview

European Space Agency (ESA), 2023. Processing Baseline. *Sentinel Online*. https://sentinels.copernicus.eu/web/sentinel/technical-guides/sentinel-2-msi/processing-baseline (accessed 1.18.23).

Everitt, B.L., 1968. Use of the cottonwood in an investigation of the recent history of a flood plain. *American Journal of Science* 266(6), 417–439. https://doi.org/10.2475/ajs.266.6.417

Fox, J., Weisberg, S., 2019. An {R} Companion to Applied Regression, Third. ed. Sage, Thousand Oaks, CA. https://socialsciences.mcmaster.ca/jfox/Books/Companion/

Friedman, J.M., Lee, V.J., 2002. Extreme floods, channel change, and riparian forests along ephemeral streams. *Ecological Monographs* 72(3), 409–425. https://doi.org/10.1890/0012-9615(2002)072[0409:EFCCAR]2.0.CO;2

Graf, W.L., 2006. Downstream hydrologic and geomorphic effects of large dams on American rivers. *Geomorphology* 79(3–4), 336–360. https://doi.org/10.1016/j.geomorph.2006.06.022

Gray, L.K., Hamann, A., 2013. Tracking suitable habitat for tree populations under climate change in western North America. *Climatic Change* 117, 289–303. https://doi.org/10.1007/s10584-012-0548-8

Güneralp, İ., Rhoads, B.L., 2011a. Influence of floodplain erosional heterogeneity on planform complexity of meandering rivers. *Geophysical Research Letters* 38(14), L14401. https://doi.org/10.1029/2011GL048134

He, H.S., Dezonia, B.E., Mladenoff, D.J., 2000. An aggregation index (AI) to quantify spatial patterns of landscapes. *Landscape Ecology* 15, 591–601. https://doi.org/10.1023/A:1008102521322

Helton, A.M., Poole, G.C., Payn, R.A., Izurieta, C., Stanford, J.A., 2014. Relative influences of the river channel, floodplain surface, and alluvial aquifer on simulated hydrologic residence time in a montane river floodplain. *Geomorphology* 205, 17–26. https://doi.org/10.1016/j.geomorph.2012.01.004

Hesselbarth, M.H.K., Sciaini, M., Nowosad, J., Hanss, S., Graham, L.J., Hollister, J., With, K.A., 2022. Package "landscapemetrics" Refernce Manual. https://cran.r-project.org/web/packages/landscapemetrics/

Hesselbarth, M.H.K., Sciaini, M., With, K.A., Wiegand, K., Nowosad, J., 2019. landscapemetrics: an open-source R tool to calculate landscape metrics. *Ecography* 42(10), 1648–1657. https://doi.org/10.1111/ecog.04617

Hijmans, R.J., 2023. raster: Geographic Data Analysis and Modeling, ver 3.6–14. https://cran.r-project.org/package=raster

Hong, L.B., Davies, T.R.H., 1979. A study of stream braiding. *Geological Society of America Bulletin Part II* 90, 1839-1859.

Hopkins, K.G., Noe, G.B., Franco, F., Pindilli, E.J., Gordon, S., Metes, M.J., Claggett, P.R., Gellis, A.C., Hupp, C.R., Hogan, D.M., 2018. A method to quantify and value floodplain sediment and nutrient retention ecosystem services. *Journal of Environmental Management* 220, 65–76. https://doi.org/10.1016/j.jenvman.2018.05.013

Hothorn, T., Hornik, K., van de Wiel, M.A., Zeileis, A., 2008. Implementing a class of permutation tests: The coin package. *Journal of Statistical Software* 28(8), 1–23. https://doi.org/10.18637/jss.v028.i08

Huang, C., Geiger, E.L., Kupfer, J.A., 2006. Sensitivity of landscape metrics to classification scheme. *International Journal of Remote Sensing* 27(14), 2927–2948. https://doi.org/10.1080/01431160600554330

Hughes, F.M.R., 1997. Floodplain biogeomorphology. *Progress in Physical Geography: Earth and Environment* 21(4), 501–529. https://doi.org/10.1177/030913339702100402

Iroumé, A., Mao, L., Andreoli, A., Ulloa, H., Ardiles, M.P., 2015. Large wood mobility processes in low-order Chilean river channels. *Geomorphology* 228, 681–693. https://doi.org/10.1016/j.geomorph.2014.10.025.

Iskin, E.P., Wohl, E., 2023. Quantifying floodplain heterogeneity with field observation, remote sensing, and landscape ecology: Methods and metrics. *River Research and Applications*, 1–19. https://doi.org/10.1002/rra.4109

Iskin, E.P., Wohl, E., In Review. Sensitivity Analysis of Spatial and Spectral Resolution in Quantifying Floodplain Heterogeneity. *Journal of Hydrology*.

Iskin, E.P., Wohl, E., 2021. Wildfire and the patterns of floodplain large wood on the Merced River, Yosemite National Park, California, USA. *Geomorphology* 389, 107805. https://doi.org/10.1016/j.geomorph.2021.107805

Jeffres, C.A., Opperman, J.J., Moyle, P.B., 2008. Ephemeral floodplain habitats provide best growth conditions for juvenile Chinook salmon in a California river. *Environmental Biology of Fishes* 83, 449–458. https://doi.org/10.1007/s10641-008-9367-1

Jeffries, R., Darby, S.E., Sear, D.A., 2003. The influence of vegetation and organic debris on flood-plain sediment dynamics: case study of a low-order stream in the New Forest, England. *Geomorphology* 51(1–3), 61–80. https://doi.org/10.1016/S0169-555X(02)00325-2

Kleindl, W.J., Rains, M.C., Marshall, L.A., Hauer, F.R., 2015. Fire and flood expand the floodplain shifting habitat mosaic concept. *Freshwater Science* 34(4), 1366–1382. https://doi.org/10.1086/684016

Konrad, C.P., 2012. Reoccupation of floodplains by rivers and its relation to the age structure of floodplain vegetation. *Journal of Geophysical Research: Biogeosciences* 117(G4). https://doi.org/10.1029/2011JG001906

Kuhn, M., Wickham, H., 2020. Tidymodels: a collection of packages for modeling and machine learning using tidyverse principles. https://www.tidymodels.org

Lamigueiro, O.P., Hijmans, R., 2023. rasterVis, ver 0.51.5. https://oscarperpinan.github.io/rastervis/

Larsen, A., Larsen, J.R., Lane, S.N., 2021. Dam builders and their works: Beaver influences on the structure and function of river corridor hydrology, geomorphology, biogeochemistry and ecosystems. *Earth-Science Reviews* 218, 103623. https://doi.org/10.1016/j.earscirev.2021.103623

Larsen, L.G., Harvey, J.W., 2010. How vegetation and sediment transport feedbacks drive landscape change in the Everglades and wetlands worldwide. *American Naturalist* 176(3), E66–E79. https://doi.org/10.1086/655215

Laurel, D., Wohl, E., 2019. The persistence of beaver-induced geomorphic heterogeneity and organic carbon stock in river corridors. *Earth Surface Processes and Landforms* 44(1), 342–353. https://doi.org/10.1002/esp.4486

Lininger, K.B., Wohl, E., Rose, J.R., 2018. Geomorphic Controls on Floodplain Soil Organic Carbon in the Yukon Flats, Interior Alaska, From Reach to River Basin Scales. *Water Resources Research* 54(3), 1934–1951. https://doi.org/10.1002/2017WR022042

Lininger, K.B., Wohl, E., Rose, J.R., Leisz, S.J., 2019. Significant Floodplain Soil Organic Carbon Storage Along a Large High-Latitude River and its Tributaries. *Geophysical Research Letters* 46(4), 2121–2129. https://doi.org/10.1029/2018GL080996

Lininger, K.B., Wohl, E., Sutfin, N.A., Rose, J.R., 2017. Floodplain downed wood volumes: a comparison across three biomes. *Earth Surface Processes and Landforms* 42(8), 1248–1261. https://doi.org/10.1002/esp.4072

Livers, B., Lininger, K.B., Kramer, N., Sendrowski, A., 2020. Porosity problems: Comparing and reviewing methods for estimating porosity and volume of wood jams in the field. *Earth Surface Processes and Landforms* 45(13), 3336–3353. https://doi.org/10.1002/esp.4969

Lowell, J.L., Gordon, N., Engstrom, D., Stanford, J.A., Holben, W.E., Gannon, J.E., 2009. Habitat Heterogeneity and Associated Microbial Community Structure in a Small-Scale Floodplain Hyporheic Flow Path. *Microbial Ecology* 58, 611–620. https://doi.org/10.1007/s00248-009-9525-9

McGarigal, K., Marks, B.J., 1995. FRAGSTATS: Spatial Pattern Analysis Program for Quantifying Landscape Structure, U.S. Forest Service General Technical Report PNW-GTR-351. Portland. https://doi.org/10.2737/PNW-GTR-351

Mertes, L.A.K., Dunne, T., Martinelli, L.A., 1996. Channel-floodplain geomorphology along the Solimões-Amazon River, Brazil. *Geological Society of America Bulletin* 108(9), 1089–1107. https://doi.org/10.1130/0016-7606(1996)108<1089:CFGATS>2.3.CO;2

Miall, A.D., 1997. A review of the braided-river depositional environment. *Earth-Science Reviews* 13(1), 1–62. https://doi.org/10.1016/0012-8252(77)90055-1

Michalak, J.L., Lawler, J.J., Roberts, D.R., Carroll, C., 2018. Distribution and protection of climate refugia in North America. *Conservation Biology* 32(6), 1414–1428. https://doi.org/10.1111/cobi.13130

Naiman, R.J., Bechtold, J.S., Drake, D.C., Latterell, J.J., O'Keefe, T.C., Balian, E. v., 2005. Origins, Patterns, and Importance of Heterogeneity in Riparian Systems, in: Lovett, G.M., Turner, M.G., Jones, C.G., Weathers, K.C. (Eds.), *Ecosystem Function in Heterogeneous Landscapes*. Springer Science + Business Media, Inc., New York, pp. 279–309. https://doi.org/10.1007/0-387-24091-8_14

Omernik, J.M., 1987. Ecoregions of the conterminous United States. Map (scale 1:7,500,000). Annals of the Association of American Geographers 77, 118-125.

Petsch, D.K., Cioneck, V.d., Thomaz, S.M., dos Santos, N.C.L., 2022. Ecosystem services provided by river-floodplain ecosystem. *Hydrobiologia*. https://doi.org/10.1007/s10750-022-04916-7

PRISM Climate Group (PRISM), 2022. United States Average Total Precipitation, 1991-2020 (800m; ASCII Grid). *Oregon State University*. https://prism.oregonstate.edu/normals/ (accessed 3.24.23).

PRISM Climate Group (PRISM), 2018. Alaska Average Annual Precipitation, 1981-2010 (800m; ASCII Grid). *Oregon State University*. https://prism.oregonstate.edu/projects/alaska.php (accessed 3.24.23).

PRISM Climate Group (PRISM), 2002. Western Canada Average Annual Precipitation, 1961-1990 (2km; ASCII Grid). *Oregon State University*. https://prism.oregonstate.edu/projects/canw.php (accessed 3.26.23).

R Core Team, 2023. R: A language and environment for statistical computing. https://www.r-project.org/

Samaritani, E., Shrestha, J., Fournier, B., Frossard, E., Gillet, F., Guenat, C., Niklaus, P.A., Pasquale, N., Tockner, K., Mitchell, E.A.D., Luster, J., 2011. Heterogeneity of soil carbon pools and fluxes in a channelized and a restored floodplain section (Thur River, Switzerland). *Hydrology and Earth System Sciences* 15(6), 1757–1769. https://doi.org/10.5194/hess-15-1757-2011

Scamardo, J., Nichols, M., Rittenour, T., Wohl, E., In Review. Drivers of Geomorphic Heterogeneity in Unconfined Non-Perennial River Corridors. *Journal of Geophysical Research: Earth Surface.*

Schumm, S.A., 1985. Patterns of Alluvial Rivers. *Annual Review of Earth and Planetary Sciences* 13, 5–27. https://doi.org/10.1146/annurev.ea.13.050185.000253

Schwendel, A.C., Nicholas, A.P., Aalto, R.E., Sambrook Smith, G.H., Buckley, S., 2015. Interaction between meander dynamics and floodplain heterogeneity in a large tropical sand-bed river: The Rio Beni, Bolivian Amazon. *Earth Surface Processes and Landforms* 40(15), 2026–2040. https://doi.org/10.1002/esp.3777

Scott, D.T., Gomez-Velez, J.D., Jones, C.N., Harvey, J.W., 2019. Floodplain inundation spectrum across the United States. *Nature Communications* 10, 5194. https://doi.org/10.1038/s41467-019-13184-4

Scott, M.L., Friedman, J.M., Auble, G.T., 1996. Fluvial process and the establishment of bottomland trees. *Geomorphology* 14(4), 327–339. https://doi.org/10.1016/0169-555X(95)00046-8

Scott, D.N., Wohl, E.E., 2018. Natural and Anthropogenic Controls on Wood Loads in River Corridors of the Rocky, Cascade, and Olympic Mountains, USA. *Water Resources Research*, 54(10), 7893–7909. https://doi.org/10.1029/2018WR022754

Scown, M.W., Thoms, M.C., de Jager, N.R., 2016a. Measuring spatial patterns in floodplains: A step towards understanding the complexity of floodplain ecosystems, in: Gilvear, D.J., Greenwood, M.T., Thoms, M.C., Wood, P.J. (Eds.), *River Science: Research and Management for the 21st Century*. John Wiley & Sons, Ltd, Hoboken, pp. 103–131. https://doi.org/10.1002/9781118643525.ch6

Scown, M.W., Thoms, M.C., de Jager, N.R., 2016b. An index of floodplain surface complexity. *Hydrology and Earth System Sciences* 20(1), 431–441. https://doi.org/10.5194/hess-20-431-2016

Scown, M.W., Thoms, M.C., de Jager, N.R., 2015. Measuring floodplain spatial patterns using continuous surface metrics at multiple scales. *Geomorphology* 245, 87–101. https://doi.org/10.1016/j.geomorph.2015.05.026

Skalak, K., Pizzuto, J., 2010. The distribution and residence time of suspended sediment stored within the channel margins of a gravel-bed bedrock river. *Earth Surface Processes and Landforms* 35(4), 435–446. https://doi.org/10.1002/esp.1926

Stella, J.C., Hayden, M.K., Battles, J.J., Piégay, H., Dufour, S., Fremier, A.K., 2011. The Role of Abandoned Channels as Refugia for Sustaining Pioneer Riparian Forest Ecosystems. *Ecosystems* 14, 776–790. https://doi.org/10.1007/s10021-011-9446-6

Stoffers, T., Buijse, A.D., Verreth, J.A.J., Nagelkerke, L.A.J., 2022. Environmental requirements and heterogeneity of rheophilic fish nursery habitats in European lowland rivers: Current insights and future challenges. *Fish and Fisheries* 23(1), 162–182. https://doi.org/10.1111/faf.12606

Sutfin, N. A., Wohl, E., 2019. Elevational differences in hydrogeomorphic disturbance regime influence sediment residence times within mountain river corridors., *Nature Communications* 10, 2221. https://doi.org/10.1038/s41467-019-09864-w

Tockner, K., Malard, F., Ward, J.V., 2000. An extension of the flood pulse concept. *Hydrological Processes* Special Issue: Linking Hydrology and Ecology 14(16–17), 2861–2883. https://doi.org/10.1002/1099-1085(200011/12)14:16/17<2861::AID-HYP124>3.0.CO;2-F

Uno, H., 2016. Stream thermal heterogeneity prolongs aquatic-terrestrial subsidy and enhances riparian spider growth. *Ecology* 97(10), 2547–2553. https://doi.org/10.1002/ecy.1552

Uno, H., Yokoi, M., Fukushima, K., Kanno, Y., Kishida, O., Mamiya, W., Sakai, R., Utsumi, S., 2022. Spatially variable hydrological and biological processes shape diverse post-flood aquatic communities. *Freshwater Biology* 67(3), 549–563. https://doi.org/10.1111/fwb.13862

U.S. Geological Survey (USGS), 2023a. StreamStats. https://streamstats.usgs.gov/ss/

U.S. Geological Survey (USGS), 2023b. National Water Dashboard. https://dashboard.waterdata.usgs.gov/app/nwd

van Wagner, C.E., 1968. The Line Intersect Method In Forests Fuel Sampling. *Forest Science* 14(1), 20–26.

Ruiz-Villanueva, V., Piégay, H., Gaertner, V., Perret, F., Stoffel, M., 2016. Wood density and moisture sorption and its influence on large wood mobility in rivers. *CATENA* 140, 182–194. https://doi.org/10.1016/j.catena.2016.02.001.

Tonon, A., Iroumé, A., Picco, L., Oss-Cazzador, D., Lenzi, M.A., 2017. Temporal variations of large wood abundance and mobility in the Blanco River affected by the Chaitén volcanic eruption, southern Chile. *CATENA* 156, 149–160. https://doi.org/10.1016/j.catena.2017.03.025

Ward, J. v., Malard, F., Tockner, K., 2002. Landscape ecology: A framework for integrating pattern and process in river corridors. *Landscape Ecology* 17, 35–45. https://doi.org/10.1023/A:1015277626224

Westbrook, C.J., Cooper, D.J., Baker, B.W., 2011. Beaver assisted river valley formation. *River Research and Applications* 27(2), 247–256. https://doi.org/10.1002/rra.1359

Wickham, H., Averick, M., Bryan, J., Chang, W., McGowan, L.D., François, R., Grolemund, G., Hayes, A., Henry, L., Hester, J., Kuhn, M., Pedersen, T.L., Miller, E., Bache, S.M., Müller, K., Ooms, J., Robinson, D., Seidel, D.P., Spinu, V., Takahashi, K., Vaughan, D., Wilke, C., Woo, K., Yutani, H., 2019. Welcome to the tidyverse. *Journal of Open Source Software* 4(43), 1686. https://doi.org/10.21105/joss.01686

Wohl, E., 2021. An Integrative Conceptualization of Floodplain Storage. *Reviews of Geophysics* 59(2), e2020RG000724. https://doi.org/10.1029/2020rg000724

Wohl, E., 2015. Particle dynamics: The continuum of bedrock to alluvial river segments. Geomorphology 241, 192–208. https://doi.org/10.1016/j.geomorph.2015.04.014

Wohl, E., 2013. Floodplains and wood. *Earth-Science Reviews* 123, 194–212. https://doi.org/10.1016/j.earscirev.2013.04.009

Wohl, E., Cadol, D., 2011. Neighborhood matters: Patterns and controls on wood distribution in old-growth forest streams of the Colorado Front Range, USA. *Geomorphology* 125(1), 132–146. https://doi.org/10.1016/j.geomorph.2010.09.008

Wohl, E., Iskin, E.P., 2022. The Transience of Channel-Spanning Logjams in Mountain Streams. *Water Resources Research* 58(5), e2021WR031556. https://doi.org/10.1029/2021WR031556

Wohl, E., Iskin, E.P., 2019. Patterns of Floodplain Spatial Heterogeneity in the Southern Rockies, USA. *Geophysical Research Letters* 46(11), 5864–5870. https://doi.org/10.1029/2019GL083140

Wohl, E., Kramer, N., Ruiz-Villanueva, V., Scott, D.N., Comiti, F., Gurnell, A.M., Piégay, H., Lininger, K.B., Jaeger, K.L., Walters, D.M., Fausch, K.D., 2019. The Natural Wood Regime in Rivers. *BioScience* 69(4), 259–273. https://doi.org/10.1093/biosci/biz013

Wohl, E., Lininger, K.B., Scott, D.N., 2018a. River beads as a conceptual framework for building carbon storage and resilience to extreme climate events into river management. *Biogeochemistry* 141, 365–383. https://doi.org/10.1007/s10533-017-0397-7

Wohl, E., Polvi, L.E., Cadol, D., 2011. Wood distribution along streams draining old-growth floodplain forests in Congaree National Park, South Carolina, USA. *Geomorphology* 126(1–2), 108–120. https://doi.org/10.1016/j.geomorph.2010.10.035

Wohl, E., Rathburn, S., Chignell, S., Garrett, K., Laurel, D., Livers, B., Patton, A., Records, R., Richards, M., Schook, D.M., Sutfin, N.A., Wegener, P., 2017. Mapping longitudinal stream connectivity in the North St. Vrain Creek watershed of Colorado. *Geomorphology* 277, 171–181. https://doi.org/10.1016/j.geomorph.2016.05.004

Wohl, E., Scott, D.N., Lininger, K.B., 2018. Spatial Distribution of Channel and Floodplain Large Wood in Forested River Corridors of the Northern Rockies. *Water Resources Research* 54(10), 7879–7892. https://doi.org/10.1029/2018WR022750

Wyżga, B., Zawiejska, J., 2005. Wood storage in a wide mountain river: case study of the Czarny Dunajec, Polish Carpathians. *Earth Surface Processes and Landforms*, 30(12), 1475–1494. https://doi.org/10.1002/esp.1204

Zeng, Y., Zhao, C., Li, J., Li, Y., Lu, G., Liu, T., 2019. Effect of groundwater depth on riparian plant diversity along riverside-desert gradients in the Tarim River. *Journal of Plant Ecology* 12, 564-573. https://doi.org/10.1093/jpe/rty048

Zeug, S.C., Winemiller, K.O., 2008. Relationships between hydrology, spatial heterogeneity, and fish recruitment dynamics in a temperate floodplain river. *River Research and Applications* 24(1), 90–102. https://doi.org/10.1002/rra.1061

5. CH 5: CONCLUSION

Through this dissertation research, I have come to my own conceptualization of rivers and our responsibility to them. Rivers comprise entire ecosystems that are intimately connected to the surrounding land (floodplains and hillslopes), the ground (hyporheic and groundwater), and the atmosphere (gas exchange). They are hydrological, geological, and ecological systems that are integral to our natural environments. The world as we know it today is the way it is because of rivers. Without rivers, there would be no fertile land, deltas, or beaches from ancient sediment deposition. There would be significantly less biodiversity from the loss of river and floodplain functions and species native to rivers in general and endemic to specific rivers. We classify rivers in different ways (planforms, bedforms, beads and strings, stream order), but the processes that underly the forms are what truly drive fluvial dynamics. Local river form reflects local processes, and rivers naturally change in time and space; a straight reach can begin to meander, a cascading reach can become a step-pool reach, and so on. Rivers are not static or homogeneous in any sense; I am not sure there is true stationarity in any real river system.

Climate, geology, topography, flow regime, sediment regime, and large wood regime are the main controlling factors of river systems, and changes in one or more of these factors will cause rivers to shift to reach new energy equilibria. With this in mind, humans have negatively impacted almost every aspect of many rivers around the world – we have altered climate with industry and automobiles; we have altered topography by draining, leveling, and building on floodplains and building dams; we have altered flow regimes by building dams, diversions, and paving surfaces in every population center; we have altered sediment regimes by building dams, dredging reservoirs, and mining sand and gravel; and we have altered wood regimes by logging

and removing wood from floodplains and rivers. When the rivers adjust to these changes in external forces, we react to reduce the adjustment; i.e., when a river begins to cut into a bank because the reach is sediment starved, we reinforce banks with concrete and riprap, forcing the river to adjust in another way. It is our understanding of fluvial processes and the innate connectivity of rivers that will guide us in river restoration. Without a true understanding of rivers as landscape integrators, we will only continue to "restore" rivers by fixing symptoms of form and not curing the processes.

These ideas are important in the context of floodplains as well. Floodplains are biomes that only exist next to rivers, and they depend on the natural dynamic of overbank flows to be maintained. Biota all over the world depend on these cycles (Uno et al., 2022), without which they might perish. Emergent trends from this study are that classification from remotely sensed data can be a great way to expand the breadth of study sites, especially in areas that are difficult to access on foot, and that pairing field data with classification results can increase the interpretability of the classifications. My results show that natural floodplains have many, interconnected facets of heterogeneity, just a few of which are aggregation, intermixing, patch density, and evenness. These floodplains have moderate to high levels of most of the metrics, indicating that natural floodplains have generally high spatial heterogeneity that is related to many river corridor characteristics, including variables that can be influenced by management and restoration (large wood volume, planform, and flow regime). Knowing this, we cannot wait any longer to protect the naturally functioning heterogeneous floodplains we have left, and to come up with creative ways to restore the processes to degraded floodplains that create and maintain this heterogeneity.

5.1 Future Directions

Future directions building from this research include increasing the breadth and depth of the dataset. Increasing breadth includes (1) expanding the dataset in the United States, such as including streams from the Southwest and Northeast, (2) expanding the dataset globally to include natural rivers where sufficient elevation data are available, and (3) adding degraded sites to compare heterogeneity between impacted and natural floodplains. Adding sites that have been altered by human use might facilitate the delineation of metric thresholds for natural sites and provide more detail into natural vs. altered levels of heterogeneity. Increasing depth includes (1) increasing the sample size at the individual levels of the categorical variables to better discern statistically significant trends, (2) adding one or more predictor variables that relate to dominant disturbance regime, such as wildfire, mass movements, glacial outburst floods, etc., (3) using other statistical methods, such as regression trees, that can use a predictor variable more than once to tease out emergent trends among the predictor variables, and (4) comparing metrics through time – within a growing season, between seasons, between years, and after major disturbance.

The ultimate goal of this dissertation is to inform ways that management and restoration practices can enhance floodplain functions that create and maintain heterogeneity. My results only begin to narrow the aspects that influence heterogeneity, but I can say that no one measure of heterogeneity can capture the variability seen in the four metrics used extensively in this study. From my results, I recommend that practitioners focus on measuring large wood characteristics and investigating historical planforms and sinuosity values as they relate to fluvial processes relevant to a specific site and consider measuring and monitoring interspersion and patch density, as they are the most readily understandable and interpretable metrics. My hope is

that this work is just the beginning of a body of work that investigates the relationship between floodplain heterogeneity, connectivity, and fluvial processes, with the goal of protecting, improving, and restoring our river systems.

5.2 Reference

Uno, H., Yokoi, M., Fukushima, K., Kanno, Y., Kishida, O., Mamiya, W., Sakai, R., Utsumi, S., 2022. Spatially variable hydrological and biological processes shape diverse post-flood aquatic communities. *Freshwater Biology* 67(3), 549–563. https://doi.org/10.1111/fwb.13862

APPENDICES

Appendix I: CH 2 Supplemental Material

Google Earth Engine Code:
https://code.earthengine.google.com/e802adc8540bd51fae1922fda062af29
https://code.earthengine.google.com/a47a47aad63d9856cd2faab37a8699ee

Supplemental Table 2.1. Study area characteristics, where the "Study Reach" is the floodplain where field data were collected, and "Drainage Basin" is the basin delineated in StreamStats at the downstream-most part of the study reach.

	Characteristic	East Plum Creek	West Bijou Creek	Sand Creek	Rough and Tumbling Creek	Source
Study Reach	Level II Ecoregion of study reach	South Central Semi-Arid Prairies	South Central Semi-Arid Prairies	South Central Semi-Arid Prairies	Western Cordillera	EPA, 2013
	Level III Ecoregion of study reach	Southwestern Tablelands	Southwestern Tablelands	Flint Hills	Southern Rockies	
	Underlying lithology of study reach	Modern and older gravels and alluviums and eolian deposits (eastern edge); underlain by Cretaceous Fox Hills Sandstone	Modern gravels and alluviums (older just beyond study reach) and eolian deposits; underlain by Cretaceous Fox Hills Sandstone	Pennsylvanian Ada Formation with shale, sandstone, limestone, and conglomerate	Evaporitic facies of Pennsylvanian Minturn and Belden Formations, siltstone and shale	Horton, 2017; Horton et al., 2017; USGS, 2022a
	Floodplain area (ha)	2.1	109	5.5	5.6	
	Number of Random Points (100 pts/ha)	200	11,000	600	600	Field delineation
	Dates field data collected	9/29/2020	7/9/2020 and 10/29/2020	6/16/2021 to 6/18/2021	8/15/2022	
Drainage Basin	Drainage area upstream of study reach (km^2)	192	653	31.4	59.8	
	Mean basin annual precipitation (mm)	569.5	457.2	990.9	608.1	USGS, 2021, 2022b
	Mean basin elevation (m)	2255	1861	347	3376	
	Mean basin slope from 10-m DEM	17%	7%	5%	24%	
Site Characteristics	Channel planform	Straight to braided		Straight to meandering	Multithread	
	Flow regime	Rainfall dominated			Snowmelt dominated	Field observation
	Dominant vegetation	Shortgrass prairie and open woodland		Tallgrass prairie and woodland	Beaver-modified meadow	
	Confinement	Unconfined				
	Soil Type	Sandy wet alluvial land	Sandy alluvial land	Verdigris silt loam, 0–1% slopes, occasionally to frequently flooded	Not available	NRCS, 2022a

Supplemental Table 2.2. Inputs used for raster classification in ArcGIS Pro.

River	Number of Classes	Minimum Class Size (pixels)	Sample Interval	Actual Number of Classes Found
West Bijou Creek, CO	20	4	2	20
East Plum Creek, CO	5	4	2	4
Sand Creek, OK	10	4	2	10
Rough and Tumbling Creek, CO	10	4	2	10

Appendix II: CH 3 Supplemental Material

Google Earth Engine Code:
https://code.earthengine.google.com/cd34cb787996d650676198999cf0e381
https://code.earthengine.google.com/0167529f885e330859082b7a0e796c9b

Supplemental Table 3.1. Study area characteristics, where the "Study Reach" is the floodplain where field data were collected, and "Drainage Basin" is the basin delineated in StreamStats at the downstream-most part of the study reach.

	Characteristic	Lookout Creek	Hoh River	Sol Duc River	Altamaha River [2]	Source
Study Reach	Level II Ecoregion of study reach	Western Cordillera	Marine West Coast Forest and Western Cordillera	Marine West Coast Forest and Western Cordillera	Mississippi Alluvial and Southeast USA Coastal Plains	EPA, 2013
	Level III Ecoregion of study reach	Cascades	Coast Range and North Cascades	Coast Range and North Cascades	Southern Coastal Plain	
	Underlying lithology of study reach	Undifferentiated tuffaceous sedimentary rocks, tuffs, and basalt with basalt and basaltic-andesite; Landslide and debris-flow deposits with coarse-detrital	Mesozoic-Tertiary marine rocks, undivided with graywacke, slate, and argillite	Younger glacial drift with fine- and coarse-detrital; Alluvium with silt and sand; and Mesozoic-Tertiary marine rocks, undivided with graywacke, slate, and argillite	Stream alluvium; Holocene Shoreline Complex – marsh and lagoonal facies; and Pamlico shoreline complex – marsh and lagoonal facies all with fine-detrital	Horton, 2017; Horton et al., 2017; USGS, 2022a
	Floodplain area (ha)	6.9	987.8	58.1	3,705.3	
	Number of random points (100 pts/ha)	700	99,000	5,800	371,000	Field delineation
	Dates field data collected	7/6/2022 to 7/13/2022	7/7/2021 to 7/18/2021	7/6/2021 to 7/17/2021	10/19/2021	
Drainage Basin	Drainage area upstream of study reach (km^2)	53.6	323	101	36,500	
	Mean basin annual precipitation (mm)	2,263.1	4,343.4	2,590.8	1,229.4 [3]	USGS, 2022b, 2023a
	Mean basin elevation (m)	1,033	978	975	132	
	Mean basin slope from 30-m DEM	37% [1]	56%	52%	5% [4]	
	Channel planform	Straight to Anastomosing	Braided to Anastomosing	Meandering to Straight	Meandering to Straight	
Site Characteristics	Flow regime	Rain and snow	Rain and snow	Rain and snow	Rainfall dominated	Field observation
	Dominant vegetation	Conifer forest	Conifer rainforest	Conifer forest	Swamp forest	
	Confinement	Confined	Unconfined	Confined	Unconfined	
	Soil Type	Jimbo-Greenpeter-Manlywham complex, 0–15% slopes; Aschoff-Kinney complex, 40–85% slopes, south-facing; and Saturn clay loam, 0–5% slopes	Isomesic valley bottom floodplain, river channel, and alluvial terraces, 0–15% slopes	Mesic valley bottom floodplain, river channel, and alluvial terraces, 0–15% slopes; Colluvial debris aprons, 15–60% slopes	Swamp, 0–2% slopes; Galestown fine sand, 0–2% slopes; Satilla silt loam, 0–1% slopes; Bladen loam and clay loam, 0–2% slopes; Meggett loam, frequently flooded, 0–2% slopes	NRCS, 2022a, 2022b, 2023

[1]Source topographic data not indicated in StreamStats, converted from slope degrees to slope percent; [2]The drainage basin for the Altamaha River includes 2.4 km of the study reach and excludes 11.2 km of the study reach (downstream) due to limitations in StreamStats and proximity to coastline (an exclusion area); [3]Basin average mean annual precipitation for 1971–2000 from PRISM; [4]From 10-m DEM

Supplemental Table 3.2. Extracted Data and Interpretation for Classification 2 at the Altamaha River, Georgia

ISO Class	Average Detrended Elevation	Average NDVI	Average NDMI	Number of Points	Nearest Field Class (3 m)	Interpretation
1	-1.0	-0.05	0.05	-	-	
2	-0.8	0.06	0.09	-	-	Active channel, tributaries, side channels, and/or standing water
3	-0.5	0.19	0.13	-	-	
4	0.2	0.28	0.09	-	-	Active floodplain with inundated areas and areas of exposed sediment, varying vegetation health/density, evergreen and deciduous trees, bamboo, palmettos, moss, vines, leaf litter, holly, and maples
5	-0.2	0.35	0.16	-	-	
6	0.1	0.34	0.12	-	-	
7	-0.3	0.29	0.17	-	-	
8	1.0	0.41	0.12	-	-	Structures, roads, other manmade surfaces, and/or active floodplain with similar spectral properties
9	0.1	0.38	0.15	-	-	Active floodplain with inundated areas and areas of exposed sediment, varying vegetation health/density, evergreen and deciduous trees, bamboo, palmettos, moss, vines, leaf litter, holly, and maples
10	-0.6	0.39	0.16	-	-	
11	0.2	0.41	0.16	-	-	
12	-0.1	0.41	0.18	-	-	
13	0.1	0.45	0.20	-	-	
14	-0.9	0.45	0.20	-	-	
15	0.2	0.44	0.18	-	-	
16	-0.3	0.44	0.19	-	-	
17	-0.1	0.46	0.21	-	-	
18	-0.5	0.49	0.23	-	-	
19	0.3	0.47	0.20	-	-	
20	0.0	0.49	0.22	-	-	
21	0.2	0.51	0.23	-	-	
22	-0.1	0.51	0.25	-	-	
23	-0.6	0.53	0.26	-	-	
24	1.1	0.51	0.24	Class: 4	Class: 1	Structures, roads, other manmade surfaces, and/or active floodplain with similar spectral properties
25	0.1	0.54	0.26	Class: 4	Class: 1	Active floodplain with inundated areas and areas of exposed sediment, varying vegetation health/density, evergreen and deciduous trees, bamboo, palmettos, moss, vines, leaf litter, holly, and maples
26	3.2	0.50	0.23	Class: 24	Class: 5, 6	Structures, roads, other manmade surfaces, and/or active floodplain with similar spectral properties
27	-0.1	0.56	0.28	Class: 6	Class: 0, 1, 2, 4	Active floodplain with inundated areas and areas of exposed sediment, varying vegetation health/density, evergreen and deciduous trees, bamboo, palmettos, moss, vines, leaf litter, holly, and maples
28	0.7	0.56	0.27	Class: 3	Class: 1, 2	
29	0.3	0.59	0.29	Class: 8	Class: 2, 3	
30	5.5	0.47	0.18	-	-	Structures, roads, other manmade surfaces, and/or active floodplain with similar spectral properties

Note: Red elevation indicates ≥ 1 m and above the active floodplain, yellow NDVI indicates [0.2, 0.5] and sparse/unhealthy vegetation and/or shrubs/grassland, and brown NDVI indicates < 0.1 and unhealthy vegetation or bare soil, sediment, or snow. General NDVI thresholds from USGS (2018).

Supplemental Table 3.3. Extracted Data and Interpretation for Classification 2 at the Hoh River, Washington

ISO Class	Average Detrended Elevation	Average NDVI	Average NDMI	Number of Points	Nearest Soil Textures (10 m)	Nearest Soil Moistures (10 m)	Nearest Field Class (3 m)	Interpretation
1	-35.3	0.41	0.23	-	-	-	-	Active floodplain with channel features, wetlands, younger forest and groundcover, and varying vegetation health/density
2	-16.6	0.03	0.01	-	-	-	-	Bare sediment, water, and/or sparsely vegetated midchannel islands in and around the active channel
3	-27.9	0.38	0.20	-	-	-	-	Active floodplain with channel features, wetlands, younger forest and groundcover, and varying vegetation health/density
4	-18.8	0.44	0.24	Class: 4 Cores: 1	Sandy Loam 0–30 cm	-	Class: 4, 5, 10, 11 Cores: 5	
5	-13.9	0.61	0.32	Class: 18 Cores: 22	Loamy Sand 0–5 cm Sandy Loam 0–60 cm	Saturated 0–15 cm Moist 0–60 cm	Class: 2, 4, 6, 9, 12 Cores: 9, 12	
6	-12.8	0.41	0.22	Class: 5 Cores: 6	Loamy Sand 0–10 cm Sandy Loam 0–30 cm	Dry 0–10 cm Saturated 0–15 cm	Class: 1, 2, 4, 8 Cores: 1, 5, 9	
7	-9.0	0.39	0.21	Class: 23 Cores: 4	Loamy Sand 0–10 cm	Dry 0–10 cm	Class: 1, 2, 6, 8 Class: 1	Old growth forest floor/inactive floodplain with varying vegetation health/density and nurse logs; mosses, fern, alder, conifer, maple
8	-12.0	0.05	0.03	-	-	-	-	Bare sediment, water, and/or sparsely vegetated midchannel islands in and around the active channel
9	-10.6	0.56	0.29	Class: 14 Cores: 62	Sand 0–5 cm Loam 0–60 cm Loamy Sand 0–10 and 30–90 cm Sandy Loam 0–90 cm	Saturated 0–55 cm Moist 0–90 cm	Class: 1, 2, 4, 6, 8, 10 Cores: 1, 2, 3, 4, 6, 10, 11	Active floodplain with channel features, wetlands, younger forest and groundcover, and varying vegetation health/density
10	-8.7	0.05	0.02	Cores: 2	Loamy Sand 0–10 cm	Dry 0–10 cm	Cores: 1	Bare sediment, water, and/or sparsely vegetated midchannel islands in and around the active channel
11	-6.8	0.54	0.28	Class: 7 Cores: 9	Loamy Sand 0–90 cm Sandy Loam 0–90 cm	Moist 0–90 cm Saturated 30–90 cm	Class: 2, 7, 8 Cores: 2, 7	Old growth forest floor/inactive floodplain with varying vegetation health/density and nurse logs; mosses, fern, alder, conifer, maple
12	-5.5	0.39	0.21	Class: 9	-	-	Class: 8	
13	-3.6	0.49	0.25	Class: 4 Cores: 25	Sand 0-5 cm Loamy Sand 0–90 cm	Moist 0–90 cm Saturated 0–5 and 30–90 cm	Class: 4, 8, Road Cores: 6, 7, 8	

					Sandy Loam 0–90 cm			
14	-5.0	0.03	0.02	Cores: 6	Loamy Sand 0–90 cm	Moist 0–60 cm Saturated 30–90 cm	Cores: 7	Bare sediment, water, and/or sparsely vegetated midchannel islands in and around the active channel
15	-2.0	0.39	0.21	Class: 16	-	-	Class: 8, Road	Old growth forest floor/inactive floodplain with varying vegetation health/density and nurse logs; mosses, fern, alder, conifer, maple
16	-0.2	0.52	0.28	Class: 5 Cores: 20	Loam 0–35 cm Sandy Loam 0–90 cm	Moist 0–90 cm	Class: 8 Cores: 8, 12	
17	1.2	0.40	0.22	Class: 3	-	-	Class: 8	
18	1.4	0.06	0.03	-	-	-	-	Bare sediment, water, and/or sparsely vegetated midchannel islands in and around the active channel
19	3.9	0.39	0.21	Class: 8	-	-	Class: 1, 8, 9	Old growth forest floor/inactive floodplain with varying vegetation health/density and nurse logs; mosses, fern, alder, conifer, maple
20	3.6	0.51	0.25	Class: 5	-	-	Class: 1, 8	
21	6.6	0.38	0.21	Class: 4	-	-	Class: 8, 9	
22	7.0	0.49	0.25	Class: 5	-	-	Class: 3, 4, 5	Uplands and inactive floodplain with varying vegetation health/density
23	9.6	0.40	0.22	Class: 1	-	-	Class: 8	
24	11.2	0.55	0.29	Class: 7	-	-	Class: 3, 4	
25	12.6	0.40	0.21	Class: 2	-	-	Class: 3, Road	
26	16.0	0.40	0.21	Class: 6	-	-	Class: 6, 8, Road	
27	20.8	0.42	0.22	-	-	-	-	
28	28.6	0.40	0.21	-	-	-	-	
29	43.1	0.42	0.23	-	-	-	-	
30	70.6	0.41	0.23	-	-	-	-	

Note: Red elevation indicates ≥ 5 m and above the active floodplain, green NDVI indicates [0.6, 0.9] and healthy/dense vegetation, yellow NDVI indicates [0.2, 0.5] and sparse/unhealthy vegetation and/or shrubs/grassland, and brown NDVI indicates < 0.1 and unhealthy vegetation or bare soil, sediment, or snow. General NDVI thresholds from USGS (2018).

Supplemental Table 3.4. Extracted Data and Interpretation for Classification 2 at the Sol Duc River, Washington

ISO Class	Average Detrended Elevation	Average NDVI	Average NDMI	Number of Points	Nearest Soil Textures (10 m)	Nearest Soil Moistures (10 m)	Nearest Field Class (3 m)	Interpretation
1	-21.7	0.50	0.28	-	-	-	-	Active floodplain with side channels, overflow surfaces, varying vegetation health/density, and nurse logs, and/or vegetation overhanging channel; mosses, alder, maple, leafy groundcover, fern, conifer, grasses
2	-14.8	0.17	0.10	Class: 2 Cores: 2	Sandy Loam 0–30 cm	Moist 0–30 cm	Class: 3, 4 Cores: 4	Active channel
3	-12.7	0.46	0.26	Class: 1	-	-	Class: 6	Active floodplain with side channels, overflow surfaces, varying vegetation health/density, and nurse logs, and/or vegetation overhanging channel; mosses, alder, maple, leafy groundcover, fern, conifer, grasses
4	-9.9	0.28	0.15	Class: 6 Cores: 8	Sandy Loam 0–45 cm	Moist 0–45 cm	Class: 3, 8 Cores: 4, 9	
5	-7.0	0.20	0.12	Class: 3 Cores: 2	Loamy Sand 0–5 cm	Saturated 0–5 cm	Class: 3, 8 Cores: 3	
6	-6.3	0.42	0.22	Class: 16	-	-	Class: 1, 3, 4, 5, 6, 8, 10	
7	-4.3	0.54	0.27	Class: 7	-	-	Class: 6, 8, 10	
8	-2.9	0.19	0.10	Class: 11	-	-	Class: 1, 2, 3, 4	Active channel
9	-3.5	0.42	0.22	Class: 17 Cores: 13	Sand 0–30 cm Loamy Sand 0–35 cm Sandy Loam 0–55 cm	Moist 0–45 cm Saturated 0–55 cm	Class: 1, 3, 4, 5, 7, 8, 9 Cores: 4, 5, 6, 9	Active floodplain with side channels, overflow surfaces, varying vegetation health/density, and nurse logs, and/or vegetation overhanging channel; mosses, alder, maple, leafy groundcover, fern, conifer, grasses
10	-1.1	0.40	0.22	Class: 25 Cores: 13	Loamy Sand 0–30, 60–90 cm Sand 30–60 cm Sandy Loam 0–90 cm	Moist 0–90 cm	Class: 1, 3, 4, 5, 7, 8 Class: 5, 7, 8	
11	-0.7	0.50	0.28	Class: 10 Cores: 11	Sandy Loam 0–85 cm	Moist 0–85 cm	Class: 5, 7, 8 Cores: 7, 8	
12	1.3	0.40	0.23	Class: 5 Cores: 6	Sandy Loam 0–90 cm	Moist 0–90 cm	Class: 7, 8 Cores: 8	
13	2.6	0.47	0.26	Class: 10 Cores: 10	Loamy Sand 0–30, 60–90 cm Sand 30–60 cm Sandy Loam 0–90 cm	Moist 0–90 cm	Class: 1, 7, 8 Cores: 5, 7, 8	
14	4.6	0.42	0.24	Class: 13 Cores: 3	Sandy Loam 0–30 cm	Moist 0–30 cm	Class: 1, 2, 8 Cores: 7	
15	7.9	0.44	0.26	Class: 8 Cores: 1	Sandy Loam 0–10 cm	Moist 0–10 cm	Class: 1, 7, 8 Cores: 1	
16	4.7	0.55	0.30	Class: 4	-	-	Class: 1, 8	
17	11.8	0.46	0.27	Class: 4	-	-	Class: 1	Higher elevation surfaces and/or uplands, including vertical cliffs above the channel and conifer forest
18	18.8	0.48	0.27	-	-	-	-	
19	34.1	0.43	0.25	-	-	-	-	
20	53.4	0.45	0.27	-	-	-	-	

Note: Red elevation indicates ≥ 5 m and above the active floodplain and yellow NDVI indicates [0.2, 0.5] and sparse/unhealthy vegetation and/or shrubs/grassland. General NDVI thresholds from USGS (2018).

Supplemental Table 3.5. Extracted Data and Interpretation for Classification 2 at Lookout Creek, Oregon

ISO Class	Average Detrended Elevation	Average NDVI	Average NDMI	Number of Points	Nearest Soil Textures (10 m)	Nearest Soil Moistures (10 m)	Nearest Field Class (3 m)	Interpretation
1	-1.8	0.54	0.27	Class: 3 Cores: 7	Loam 0–5 cm Sandy Loam 0–60 cm	Dry 0–25 cm Moist 0–60 cm	Class: 5, 9 Cores: 5, 6, 9	Active channel and floodplain with midchannel island, boulder bars, backwater channels, side channels and varying vegetation health/density; fir, viny maple, fern, cedar, alders, horsetail, grasses, beaver chew
2	-2.9	0.45	0.23	Class: 4 Cores: 9	Sandy Loam 0–20 cm Sandy Clay Loam 0–30 cm Loam 0–60 cm	Saturated 0–20 cm Moist 0–60 cm	Class: 1, 3, 5 Cores: 3, 5, 11	
3	-2.0	0.52	0.25	Class: 1 Cores: 2	Sandy Loam 0–16 cm	Moist 0–16 cm	Class: 6 Cores: 12	
4	-0.5	0.44	0.22	Class: 8 Class: 2	Loam 0–8 cm	Dry 0–7 cm Moist 0–8 cm	Class: 1, 7, 9, 10 Class: 7	
5	-0.5	0.50	0.25	Class: 1	-	-	Class: 1	
6	1.2	0.47	0.22	-	-	-	-	
7	0.4	0.52	0.25	-	-	-	-	
8	0.9	0.46	0.23	Class: 2 Cores: 1	Loam 0–7 cm	Loam 0–7 cm	Class: 1, 2 Cores: 7	
9	7.2	0.41	0.21	Cores: 2	Sandy Loam 0–60 cm	Moist 0–60 cm	Cores: 9	Bridge, road, steep banks and/or boundaries next to channel and floodplain
10	0.1	0.51	0.25	Class: 40 Cores: 18	Loam 0–9 cm Sandy Loam 0–60 cm	Saturated 0–30 cm Moist 0–60 cm	Class: 1, 2, 3, 4, 5, 6, 9, 10, 11, 12, 13 Cores: 4, 5, 7, 9, 11, 12	Active channel and floodplain with midchannel island, boulder bars, backwater channels, side channels and varying vegetation health/density; fir, viny maple, fern, cedar, alders, horsetail, grasses, beaver chew

Note: Red elevation indicates ≥ 5 m and above the active floodplain and yellow NDVI indicates [0.2, 0.5] and sparse/unhealthy vegetation and/or shrubs/grassland. General NDVI thresholds from USGS (2018)

Appendix III: CH 4 Supplemental Material

Google Earth Engine code:
https://code.earthengine.google.com/0167529f885e330859082b7a0e796c9b
https://code.earthengine.google.com/a9ab1223e0d40b3aa0b781afeaa69fa9
https://code.earthengine.google.com/e04628ad8e8f6e095e47d04b52790183
https://code.earthengine.google.com/da9c215b3b589df5073471eaf9f1ae22
https://code.earthengine.google.com/81295533ab5babc0a1ac4b1847e1b1ca
https://code.earthengine.google.com/03b6beb2bc20da178a672f9fcbaa273d
https://code.earthengine.google.com/b8249d631f020570e37a4b5456069823

Supplemental Table 4.1. Field class descriptions

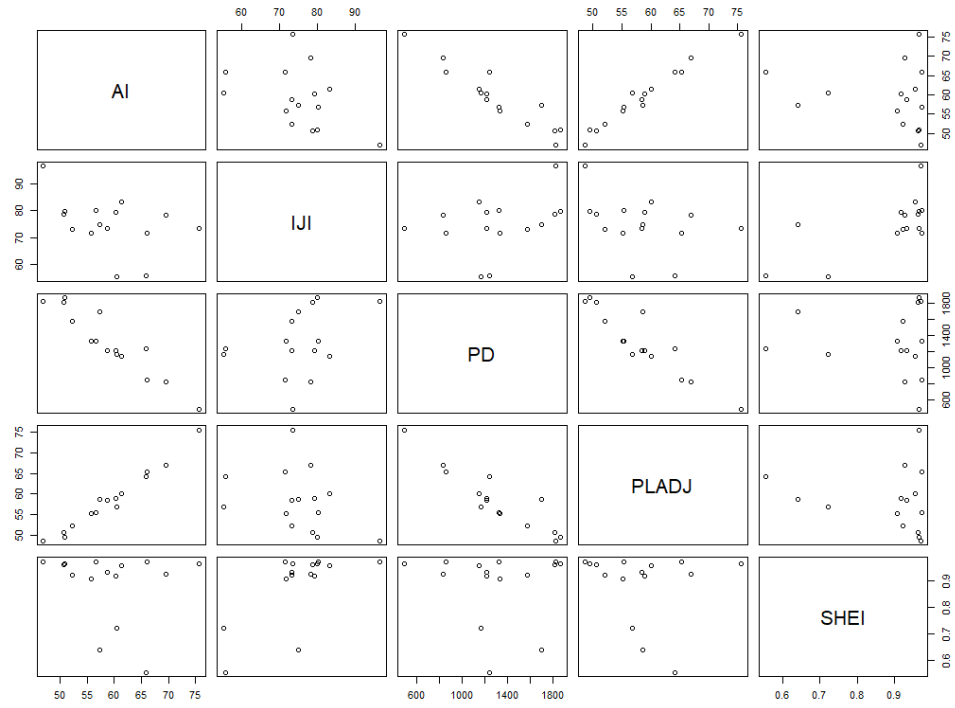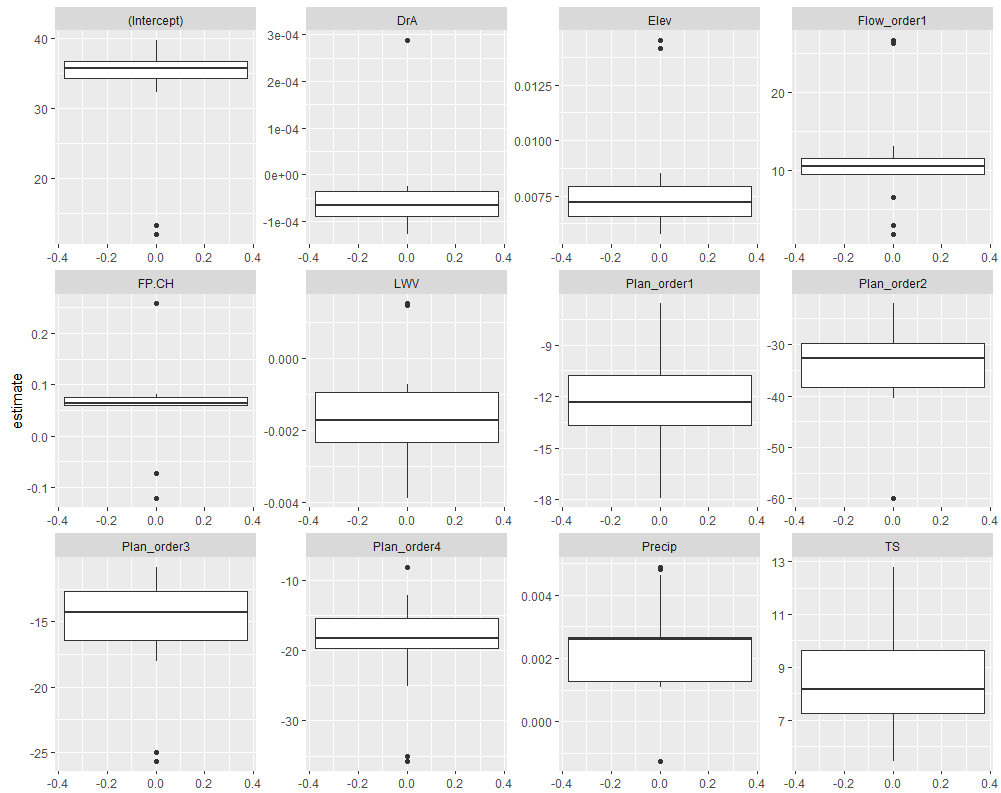| River	Class No.	Description
Embarrass River, IL	1	Bottomland forest with 2 m HWMs, mature forest, standing water, wood accumulations, abandoned channels, all deciduous trees
	2	Higher surface, now farmed, grasses
	3	Active channel, sandy banks, incised 4–5 m
	4	Overflow surface, 1–2 m undulating topography, a lot of wood, 30–40 cm DBH
	5	Overflow surface, 1 m above Class 4, older trees, 70 cm DBH, denser ground cover
	6	Flowing secondary channel, incised 6 m
	7	Higher surface, vegetation flow fabric present, small trees
	8	Overflow surface, (fewer) wood accumulations, 10–30 cm DBH, 2 m higher than Class 7, some standing water, linear features
	9	Tall grass, brambles/thicket, woody shrubs, small trees, standing shallow water
	10	Standing water, 40 cm–4 m away, abandoned meander?, slow current
	11	Beaver pond, a lot of beaver chew, standing water
	12	Dry upland, dense undergrowth, 20 cm DBH, briars
	13	Cattail marsh
	14	Standing water, abundant saplings, 10–40 cm DBH, not much ground cover
Swan River, MT	1	Active channel
	2	Head high grasses, scalloped riverbank, gradual grassy bank into river, hawthorn and mock orange trees, willow, bedrock exposure, beaver chew, siltation on vegetation 25 cm off the ground
	3	Boundary patch, grasses interspersed, leafy ground cover, big leaf willows, 10–20 cm DBH birch and hawthorn, dense leafy trees
	4	Marshy, lily pads, horsetail, marsh grass, standing water, possible meander scar
	5	Boundary patch, dense thorny bushes/trees, willow
	6	Alderleaf buckthorn, 50–150 cm tall, very dense, "understory" grass
	7	Young, up to 15 cm DBH poplar, 150 cm tall alderleaf buckthorn; wet, horsetail, mossy logs, large leafy plants (Western skunk cabbage), plentiful downed wood, evidence of channelized flow, poplar/birch are multistem, high/dry areas, ponded areas, marsh grass
	8	Very dense willow, grasses and other trees interspersed, siltation on vegetation 1 m off the ground, dense grass
	9	Forest floor at floodplain elevation
	10	Flooded forest, no standing water, many channels under conifers and bushes
	11	Active side channel with overflow banks on both sides, lots of wood, 1 m HWMs
	12	Large beaver meadow/pond, ample grass, lily pads, standing water, beaver lodge, lots of chew, similar to Class 4 but much larger and beaver modified, mosses and sundews, many channels, some deep
	13	Young conifers, 2 m high ferns, dense ground cover
		Note: HWMs stands for high water marks. DBH stands for diameter at breast height, measured mostly by eye. Species identification was not exact and not field guide was used.

134
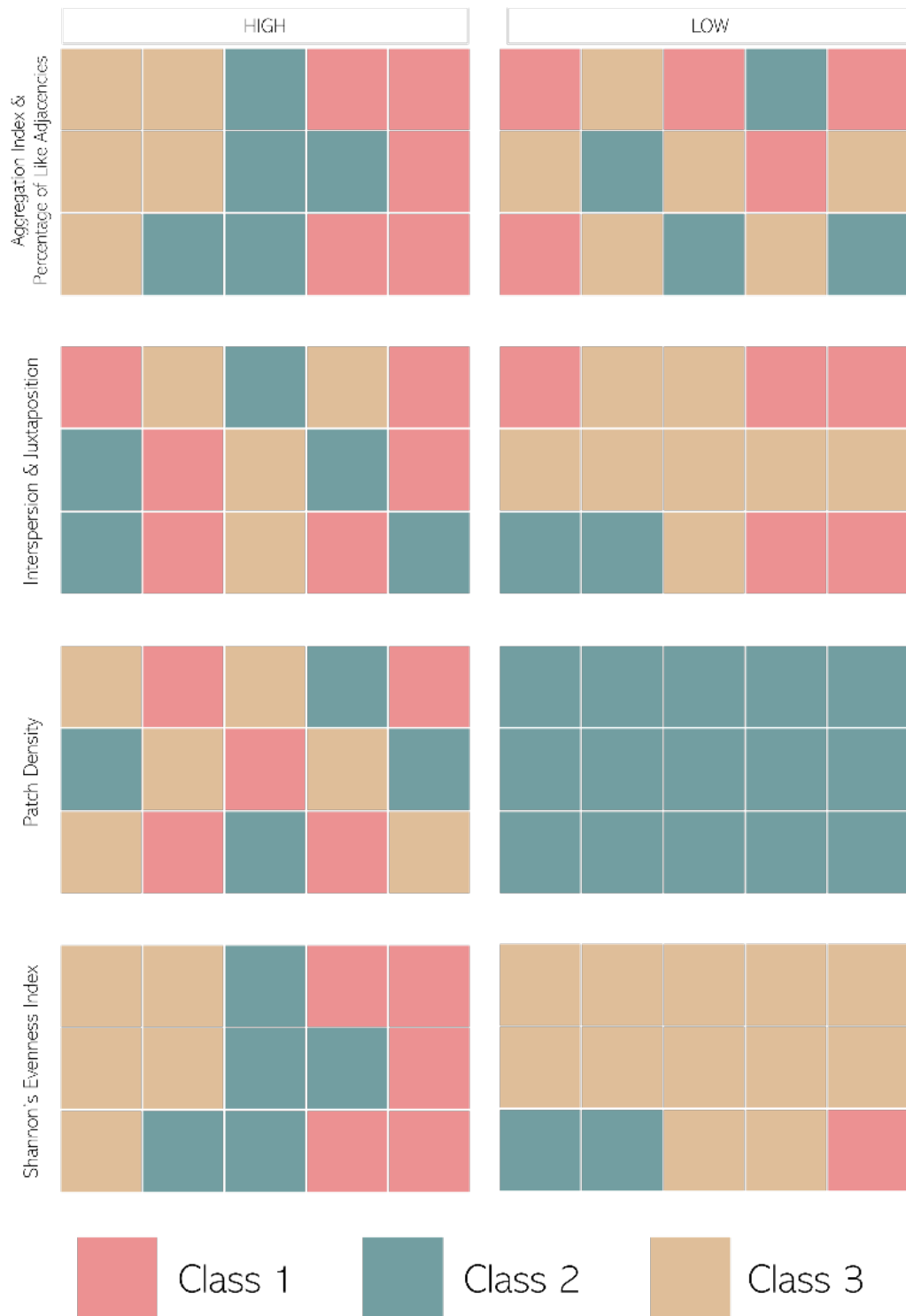
Supplemental Figure 4.1. Visual representation of rook's case highs and lows of heterogeneity metrics, based on information from He et al. (2000) and Hesselbarth et al. (2022). Individual squares represent individual pixels in a landscape raster. Aggregation index (AI) and percentage of like adjacencies (PLADJ) have high values when pixels of the same class occur next to each other; interspersion and juxtaposition index has a low value when certain classes only occur next to each other (e.g. Class 1 and Class 2 only occurring next to Class 3); patch density (PD) has a high value when there are many patches across the landscape; and Shannon's evenness index (SHEI) has a high value when each class covers the same proportion of area across the landscape.

*Supplemental Table 4.3. Classification input data and sources*

Data	Details	Resolution	Tools Used	References
GPS Locations	Transect location, patch boundaries, and large wood locations	± 3 m	Garmin GPSMAP 66ST	-
Watershed Characteristics	Drainage basin shapefiles downloaded on 9/13/21 (WBJ), 11/1/22 (HWA, SDWA, LOR), 1/19/23 (AGA), 2/12/23 (EIL, SMT, CSC, EPC, RTCO, SOK), and 3/24/23 (NSV) Drainage basins delineated for areas without StreamStats (DFWY, DWY, YAK) 30-yr normal precipitation values from 1981–2010 for YAK and 1991–2020 for all other sites on 3/24/23	Varies depending data used by StreamStats and ArcGIS Pro 800 m spatial, 0.001 mm depth for precipitation data	StreamStats ArcGIS Pro PRISM Climate Data	Esri, 2022; USGS, 2023a; PRISM, 2002, 2018, 2022
Digital Elevation Models	WBJ: LD33481653, LD33481644, LD33481650, LD33481647, LD33451647, LD33451644 DEMs published 10/17/2018 EPC: 13SED510350 published 7/1/2014 RTCO: CWCB_PARK_0408 published 4/10/2020 NSV: 2020 DRCOG W0454N4452, W0454N4450, W0453N4452, W0453N4450 published 5/14/2020 SMT: NCALM Preliminary Bare Earth DEM without bathymetric correction SOK: Oklahoma Bare Earth DEM mosaic 8/1/2016 HWA: 2013 DEM 4, 5 SDWA: 2014 DEM 47, 57 LOR: McKenzie River 2016 DEM mosaic AGA: 3DEP Tile N32W082 7/25/2022 CSC: 3DEP Tile N34W081 5/4/2022 DFWY and DWY: 3DEP Tile N44W110 6/15/2021 EIL: 3DEP Tile N39W088 12/5/2022 YAK*: 3DEP Tiles N66W145 2/2/2018, N66W149 11/5/2018, N66W150 9/30/2016, N67W145 1/302018, N67W146 1/29/2018, N67W147 12/28/2017, N67W148 12/27/2017, N67W149 1/5/2016, N67W150 4/3/2017	0.91 m (HWA and LOR) 1 m (WBJ, EPC, RTCO, NSV, SOK, SMT) 3 m (SDWA) 10 m (AGA, SOK, EIL, CSC, DFWY, DWY, YAK) 32-bit radiometric (All)	Colorado Hazard Mapping & Risk MAP Portal OKMaps Portal WA DNR Lidar Portal The National Map	Allison and Martinez, 2013; Gleason and McWethy, 2014; USGS, 2016, 2023b; Open Topography, 2021; Division of Geology and Earth Resources, 2022; CWCB, 2023; NCALM, 2023; Oklahoma Office of Geographic Information, 2023;
Aerial Imagery	From GEE Image Collection "COPERNICUS/S2_SR" WBJ, EPC, NSV, SOK, HWA, SDWA, LOR, EIL, SMT, DFWY, DWY: 2% cloud-free mosaics from 5/1/2022–9/30/2022 AGA, CSC: 0.5% cloud-free mosaics from 4/1/2022–9/30/2022 RTCO: 2% cloud-free mosaic from 6/1/2022–9/30/2022 YAK*: 1% cloud-free mosaic from 5/1/2022–9/30/2022	10 m: Bands 2, 3, 4, 8 20 m: Bands 5, 6, 7, 8a, 11, 12 12-bit radiometric 5-day temporal	Google Earth Engine	Gorelick et al., 2017; Sabins Jr. and Ellis, 2020; ESA, 2021; Google Developers, 2022

*YAK DEM and Sentinel tiles were mosaicked using the "Blend" Mosaic Operator to try to reduce the impact of the boundaries between tiles from different years. All other DEM tiles were mosaicked, if necessary, using the default Mosaic Operator in ArcGIS Pro.
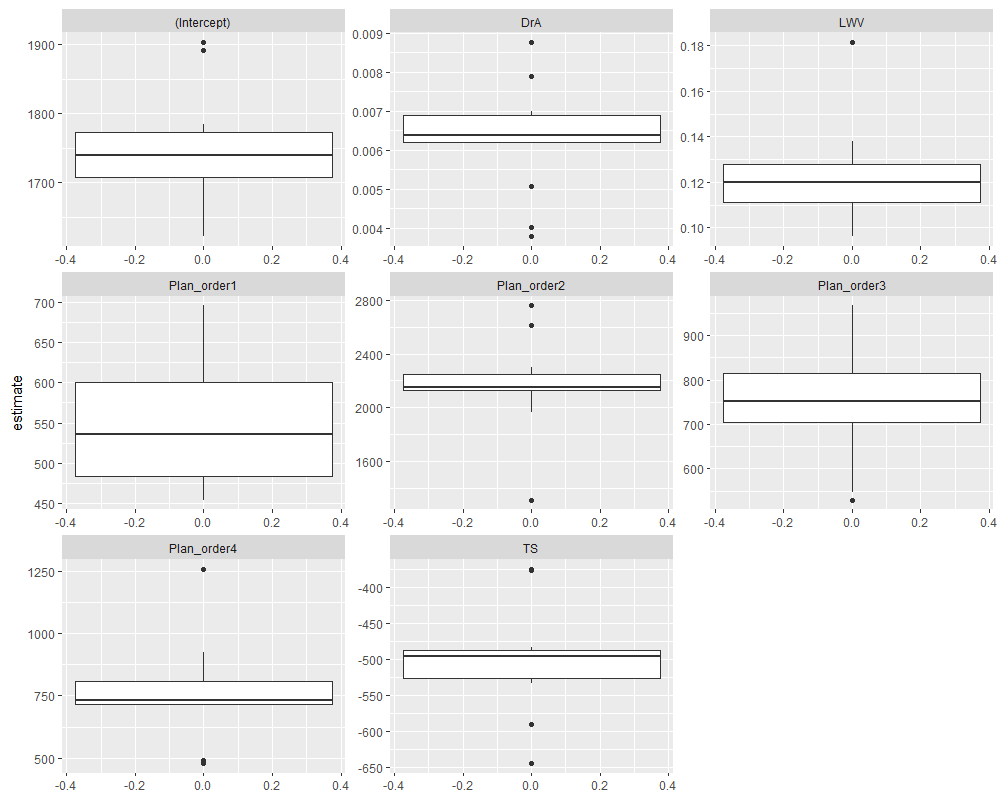
Supplemental Figure 4.3. Pairwise scatter plots of heterogeneity metrics.
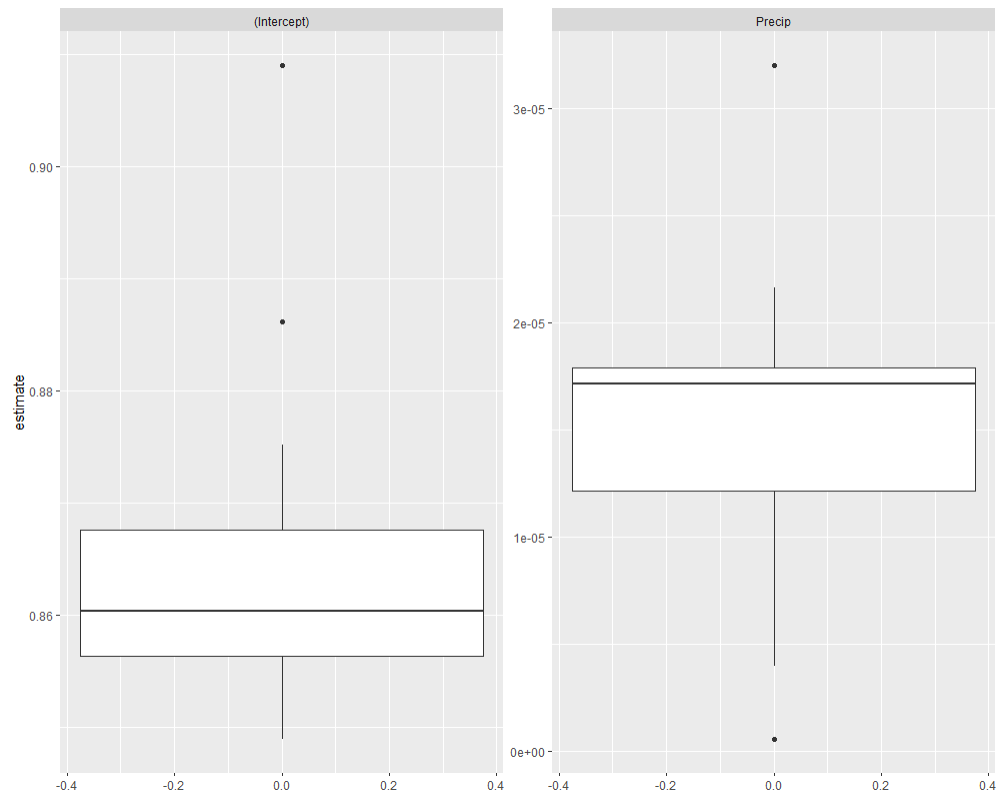

Supplemental Figure 4.4. AI LOOCV model estimates.

137
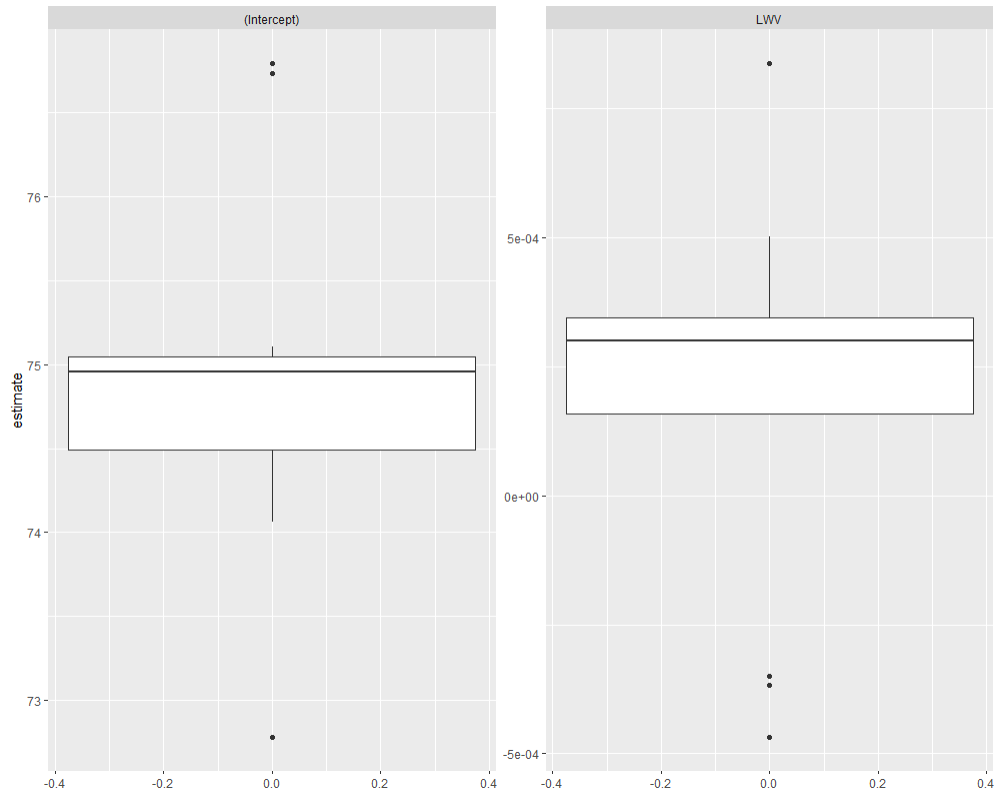
Supplemental Figure 4.5. IJI LOOCV model estimates.

Supplemental Figure 4.6. PD LOOCV model estimates.

138

Supplemental Figure 4.7. SHEI LOOCV model estimates.

Appendix IV: References for all Supplemental Sections

Allison, S., Martinez, D., 2013. Hoh River LiDAR-Delivery 2 Technical Data Report. https://pugetsoundlidar.ess.washington.edu/lidardata/proj_reports/Hoh_River_LiDAR_131104_Final_Report.pdf

Colorado Water Conservation Board (CWCB), 2023. Colorado Hazard Mapping & Risk MAP Portal. https://coloradohazardmapping.com/

Division of Geology and Earth Resources, 2022. Washington Lidar Portal. *Washington State Department of Natural Resources*. https://lidarportal.dnr.wa.gov/

Esri, 2022. ArcGIS Pro. https://www.esri.com/en-us/arcgis/products/arcgis-pro/overview

European Space Agency (ESA), 2021. Level-2A. *Sentinel Online*. https://sentinel.esa.int/web/sentinel/user-guides/sentinel-2-msi/product-types/level-2a (accessed 11.18.21).

Gleason, A., McWethy, G., 2014. Lidar Project Quality Assurance Report.

Google Developers, 2022. Sentinel-2 MSI: MultiSpectral Instrument, Level-2A. *Earth Engine Data Catalog*. https://developers.google.com/earth-engine/datasets/catalog/COPERNICUS_S2_SR#bands (accessed 11.27.22).

Gorelick, N., Hancher, M., Dixon, M., Ilyushchenko, S., Thau, D., Moore, R., 2017. Google Earth Engine: Planetary-scale geospatial analysis for everyone. *Remote Sensing of the Environment* 202, 18–27. https://doi.org/10.1016/j.rse.2017.06.031

He, H.S., Dezonia, B.E., Mladenoff, D.J., 2000. An aggregation index (AI) to quantify spatial patterns of landscapes. *Landscape Ecology* 15, 591–601. https://doi.org/10.1023/A:1008102521322

Hesselbarth, M.H.K., Sciaini, M., Nowosad, J., Hanss, S., Graham, L.J., Hollister, J., With, K.A., 2022. Package "landscapemetrics" Refernce Manual. https://cran.r-project.org/web/packages/landscapemetrics/index.html

Horton, J.D., 2017. The State Geologic Map Compilation (SGMC) geodatabase of the conterminous United States (ver. 1.1, August 2017): U.S. Geological Survey data release, https://doi.org/10.5066/F7WH2N65

Horton, J.D., San Juan, C.A., and Stoeser, D.B, 2017, The State Geologic Map Compilation (SGMC) geodatabase of the conterminous United States (ver. 1.1, August 2017): U.S. Geological Survey Data Series 1052, 46 p., https://doi.org/10.3133/ds1052

National Center for Airborne Laser Mapping (NCALM), 2023. Preliminary Swan River Green Lidar DEM (1 m).

Oklahoma Office of Geographic Information, 2023. OKMaps. https://okmaps.org/ogi/search.aspx

Open Topography, 2021. USGS 1/3 arc-second Digital Elevation Model. https://doi.org/10.5069/G98K778D

PRISM Climate Group (PRISM), 2022. United States Average Total Precipitation, 1991-2020 (800m; ASCII Grid). *Oregon State University.* https://prism.oregonstate.edu/normals/ (accessed 3.24.23).

PRISM Climate Group (PRISM), 2018. Alaska Average Annual Precipitation, 1981-2010 (800m; ASCII Grid). *Oregon State University.* https://prism.oregonstate.edu/projects/alaska.php (accessed 3.24.23).

PRISM Climate Group (PRISM), 2002. Western Canada Average Annual Precipitation, 1961-1990 (2km; ASCII Grid). *Oregon State University.* https://prism.oregonstate.edu/projects/canw.php (accessed 3.26.23).

Sabins Jr., F.F., Ellis, J.M., 2020. *Remote Sensing: Principles, Interpretation, and Applications*, 4th ed. Waveland Press, Inc., Long Grove. https://www.waveland.com/browse.php?t=421

U.S. Environmental Protection Agency (EPA), 2013. Level III Ecoregions of the Conterminous United States shapefile.

U.S. Environmental Protection Agency. (2013). Level III Ecoregions of the Conterminous United States shapefile. *U.S. EPA – National Health and Environmental Effects Research Laboratory*. https://www.epa.gov/eco-research/level-iii-and-iv-ecoregions-continental-united-states

U.S. Geological Survey (USGS), 2016. McKenzie River Bare Earth Mosaic. http://prd-tnm.s3.amazonaws.com/index.html?prefix=StagedProducts/Elevation/metadata/OR_McKenzieRiver_2021_B21/OR_McKenzieRiver_1_2021/spatial_metadata/contractor_provided/

U.S. Geological Survey, 2018. NDVI, the Foundation for Remote Sensing Phenology. https://www.usgs.gov/special-topics/remote-sensing-phenology/science/ndvi-foundation-remote-sensing-phenology

U.S. Geological Survey (USGS), 2022a. The National Geologic Map Database MapView. https://ngmdb.usgs.gov/mapview/

U.S. Geological Survey (USGS), 2023b. The National Map Download Client.
https://apps.nationalmap.gov/downloader/

U.S. Geological Survey (USGS), 2021. StreamStats. https://streamstats.usgs.gov/ss/

U.S. Geological Survey (USGS), 2022b. StreamStats. https://streamstats.usgs.gov/ss/

U.S. Geological Survey (USGS), 2023a. StreamStats. https://streamstats.usgs.gov/ss/

USDA Natural Resources Conservation Service (NRCS), 2022a. Web Soil Survey.
https://websoilsurvey.sc.egov.usda.gov/App/WebSoilSurvey.aspx

USDA Natural Resources Conservation Service (NRCS), 2022b. Olympic National Park Alluvial
Units (unofficial/unpublished).

USDA Natural Resources Conservation Service (NRCS), 2023. Web Soil Survey.
https://websoilsurvey.sc.egov.usda.gov/App/WebSoilSurvey.aspx